ISSN 1512-1127

საქართველოს გეოფიზიკური საზოგადოების ჟურნალი

სერია ა. დედამიწის ფიზიკა

JOURNAL OF THE GEORGIAN GEOPHYSICAL SOCIETY

Issue A. Physics of Solid Earth

ტომი 16ა 2013

vol. 16A 2013

ISSN 1512-1127

საქართველოს გეოფიზიკური საზოგადოების ჟურნალი

სერია ა. დედამიწის ფიზიკა

ივ. ჯავახიშვილის სახელობის თბილისის სახელმწიფო უნივერსიტეტის მ. ნოდიას გეოფიზიკის ინსტიტუტის 80 წლისადმი მიძღვნილი სამეცნიერო კონფერენციის შრომები
სტატიების ფერადი ვერსიები წარმოდგენილია კომპაქტ დისკზე

JOURNAL
OF THE GEORGIAN GEOPHYSICAL SOCIETY

Issue A. Physics of Solid Earth

Reports, presented on the Scientific Conference "80 years of the M. Nodia Institute of Geophysics"
Color versions of papers are presented on the compact disk

ტომი 16ა 2013
vol. 16A 2013

საქართველოს გეოფიზიკური საზოგადოების შრომები

სერია ა. დედამიწის ფიზიკა

სარედაქციო კოლეგია
კ. ზ. ქართველიშვილი (მთ. რედაქტორი), ვ. აბაშიძე, ბ. ბალავაძე, ა. გველესიანი (მთ. რედაქტორის მოადგილე), გ. გუგუნავა, კ. ეფტაქსიასი (საბერძნეთი), თ. ჭელიძე, ვ. ჩიჭინაძე, გ. ჯაში, ი. გეგენი (საფრანგეთი), ი. ჩშაუ (გერმანია), თ. მაჭარაშვილი, ვ. სტაროსტენკო (უკრაინა), ჯ. ქირია, ლ. დარახველიძე (მდივანი)
მისამართი:
საქართველო, 0160, თბილისი, ალექსიძის ქ. 1,
მ. ნოდიას გეოფიზიკის ინსტიტუტი
ტელ.: 33-28-67; 94-35-91; Fax; (99532 332867);
ჟურნალის შინაარსი:
ჟურნალი (ა) მოიცავს მყარი დედამიწის ფიზიკის ყველა მიმართულებას. გამოქვეყნებულ იქნება: კვლევითი წერილები, მიმოხილვები, მოკლე ინფორმაციები, დისკუსიები, წიგნების მიმოხილვები, განცხადებები.
გამოქვეყნების განრიგი და ხელმოწერა
სერია (ა) გამოიცემა წელიწადში ერთხელ.
ხელმოწერის ფასია (უცხოელი ხელმომწერისათვის) 50 დოლარი, საქართველოში – 10 ლარი, ხელმოწერის მოთხოვნა უნდა გაიგზავნოს რედაქციის მისამართით.

ЖУРНАЛ ГРУЗИНСКОГО ГЕОФИЗИЧЕСКОГО ОБЩЕСТВА

серия А. Физика Твердой Земли

Редакционная коллегия:
К. З. Картвелишвили (гл. редактор), В.Г. Абашидзе, Б.К. Балавадзе, Гвелесиани (зам. гл. редактора), Г.Е. Гугунава, К. Эфтаксиас (Греция), Т.Л. Челидзе, В.К. Чичинадзе, Г.Г. Джаши, И. Геген (Франция), И. Чшау (Германия), Т. Мачарашвили, В. Старостенко (Украина), Дж. Кириа, Л. Дарахвелидзе
Адрес:
Грузия, 0160, Тбилиси, ул. Алексидзе, 1.
Институт геофизики им. М. З. Нодия
Тел: 33-28-67; 94-35-91; Fax: (99532) 332867;
Содержание журнала:
Журнал (А) Грузинского геофизического общества охватывает все направления физики твердой Земли. В журнале будут опубликованы научные статьи, обозрения, краткие информации, дискуссии, обозрения книг, объявления.
Порядок издания и условия подписи:
Том серии (А) издается по одному номеру в год.
Подписная цена 50 долларов США, включая стоимость пересылки.
Заявка о подписке высылается в адрес редакции.

JOURNAL OF THE GEORGIAN GEOPHYSICAL SOCIETY

Issue A. Physics of Solid Earth

Editorial board:
K. Kartvelishvili (Editor-in-Chief), V. Abashidze, B. Balavadze, T. Chelidze, V. Chichinadze, K. Eftaxias (Greece), A. Gvelesiani (Vice-Editor-in-Chief), G. Gugunava, G. Jashi, Y. Gueguen (France), I. Zschau (Germany), T. Matcharashvili, V. Ctarostenko (Ukraine), J. Kiria, L. Darakhvelidze
Address:
M. Nodia Institute of Geophysics, 1 Alexidze Str., 0160 Tbilisi, Georgia
Tel.: 33-28-67; 94-35-91; Fax: (99532) 332867;
Scope of the Journal:
The Journal (A) is devoted to all branches of the Physics of Solid Earth. Types of contributions are: research papers, reviews, short communications, discussions, book reviews, announcements.
Publication schedule and subscription information:
One volume issue (A) per year is scheduled to be published.
The subscription price is 50 $, including postage.
Subscription orders should be sent to editor's address.

Journal of Georgian Geophysical Society,
Issue (A), Physics of Solid Earth, v. 16a, 2013, pp. 3-10

Acoustic pulses generated by landslide activation: laboratory modeling

Nodar Varamashvili, Tamaz Chelidze, Zurab Chelidze
M. Nodia Institute of Geophysics of Ivane Javakhishvili Tbilisi State University,
1, Alexidze Str., 0160 Tbilisi, Georgia

Abstract

The prevention of loss to life and property due to natural calamities is viewed very seriously in many countries of the world. There are many uncertainties in the forecasting of when a movement in a landslide will occur. Acoustic emission (AE) is a natural phenomenon that occurs when a solid subjected to stress experiences non-elastic deformation – fracturing or stick-slip. Acoustic emissions carry information about location, intensity and mechanisms of deformation occurring in a material. The aim of our research is modeling, registration and monitoring of landslide motion by recording acoustic emissions. Registering the acoustic pulses, which occur during the preparation and movement of the landslide is realized by acoustic sensor. One of the goals of our experiment is optimization of equipment to use them in the field and work for development of a landslides' acoustic early warning system.

Introduction

For many countries around the world landslides are one the most severe of all natural disasters, with large humanitarian and economic losses. The earth surface is not static but dynamic system and landforms change over time as a result of weathering and surface processes (i.e., erosion, sediment transport and deposition). The fast mass-movement has a potential to cause significant harm to population and civil engineering projects. Landslides are important natural geomorphic agents that shape mountainous areas and redistribute sediment (Sidle And Ochiai, 2006). Large-scale experiments and field observations show that the landslide may reveal a slow steady slip, episodic stick-slip or sudden acceleration.

Problem description

Landslides are sources of considerable hazards for human life, economy and infrastructure in mountainous areas, such as Georgia. This is why understanding of properties, statistics, and dynamics of this process in order to reveal its physical nature, to predict landslides or to decrease mass movement risk is an important scientific and practical problem.

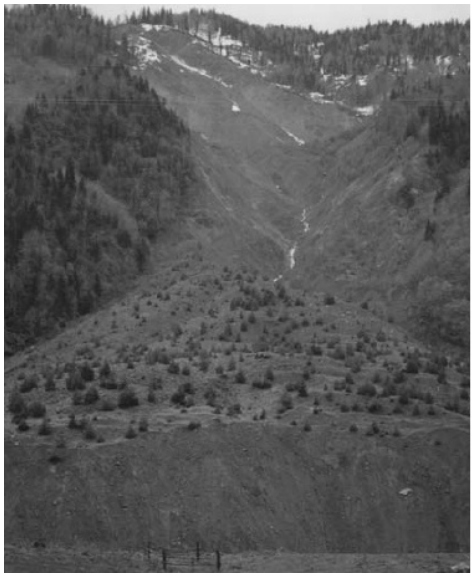

Fig.1.Landslide of 1988 (the photo taken in 2003), Mountain Adzharia, Valley of Skhalta River, Georgia

Fig.2.Built-up and cultivated landslide of approximately 100 years of age, Mountain Adzharia, Valley of Skhalta River, Georgia

Landslides occur in hills/mountains in response to a wide variety of terrain conditions and triggering processes like heavy rainstorms, earthquakes, floods and unsafe developmental activities. With growing population, urbanization and human interventions in terms of developmental activities over unstable slopes, landslides pose increasing risk to human lives, buildings, structures, infra-structures and environment (Anderson and Holcombe, 2013). Changing climatic conditions manifested in the form of global warming, glacial melting, erratic and uneven rains, extreme temperature conditions etc. are also extending these risks to even unexpected areas. Large scale deforestation along with faulty management has led to increased vulnerability to landslides.

For example, as a result of heavy rain the soil slid in several places in Vaziani-Gombori-Telavi (Georgia) motor-way in the zone of 2011 landslide. The damaged area of the road is sliding every day and the asphalt is moving towards the ravine (Fig.3).

Fig.3. Landslide on Vaziani-Gombori-Telavi (Georgia) motor-way

Acoustic emissions (AE) is a natural phenomenon that occurs when a solid is subjected to large enough stress. This external stress, causes fracturing or stick-slip on various scale and a sudden

release of sound waves resulting in acoustic/microseismic activity, which can be detected by transducers.AE are transient, high-frequency, elastic waves‘ bursts generated by the rapid release of stored elastic energy. In brittle materials like rocks, crack formation and crack propagation generate AE. In granular materials, frictional sliding and rolling are sources of AE. Another source of AE in the nature is the breaking of roots.

Acoustic emissions carry information about location, intensity, and deformation mechanisms occurring in a material. It is a non-invasive method and gives real-time information on what is happening during deformation. In rock mechanics, AE monitoring has been successfully used to identify various stages of the failure process, such as crack initiation, crack growth, and crack propagation prior to global failure.

Traditional methods of monitoring slope movements have included surface surveying and sub-surface instrumentation techniques. However, many of these methods lack the sensitivity to detect deformation at low pre-failure strain rates. Over 40 years research has been conducted on the use of AE to monitor soil movements. Interesting work has been carried by Chelidze et al., (2012) out. The most notable contributions in terms of field of AE monitoring were provided by Koerner *et al.* (1981) and Dixon *et al.* (2003).

Detecting AE generated by a developing shear surface within a slope is not an easy task. As AE propagates through soil, it suffers from a loss of signal amplitude: attenuation is high in soil because it is a particulate (granular) medium and energy is lost as AE travels across boundaries from one particle to another. The use of a waveguide to provide a path of low attenuation from the source of the AE (within a soil slope) to the sensor (usually situated above ground surface) has become a standard practice in AE research. The presence of a waveguide, typically a metal pipe inserted within an unstable slope, also greatly increases the monitoring ability of the AE sensor.

Dixon *et al.* (1996) outlined two generic types of waveguides; passive and active. A passive waveguide does not introduce additional sources of AE, and thus all detected AE is assumed to originate from the surrounding soil slope. In comparison, the active waveguide uses an annulus of high AE-responsive backfill material around the waveguide. As the slope deforms the waveguide, AE is assumed to originate from the backfill only.

Kousteni (2002) showed that gravel emitted higher levels of AE than sand.

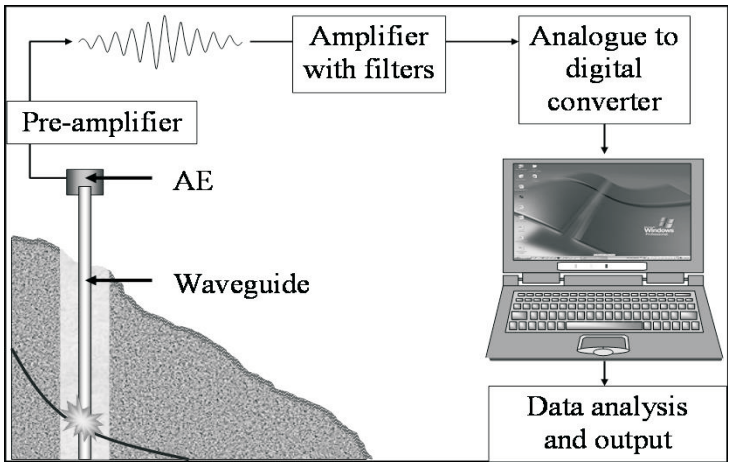

Fig. 4. Components of an AE monitoring system (Dixon et al., 2003)

Figure 4 shows a schematic representation of a typical AE instrumentation system. AE originating from the deformation of a backfill within the active waveguide propagates along a steel

waveguide to a piezoelectric sensor secured to the top of the metal waveguide. The AE signal is then amplified by a preamplifier and an amplifier to enable the signal to travel down the lengths of cable without being subsequently affected by background or electrical noise. Finally the AE is converted to a digital signal for subsequent analysis and manipulation using real time data acquisition software.

Experimental setup

The goal of our study is registration and monitoring of landslide slow motion (creep) by recording the acoustic emission. For this goal we developed the special equipment (Fig.3). Plastic barrel is filled with a soil from the landslide, the in the center of which is a cylinder filled with small stones. The cylinder diameter is approximately 15 cm and a mean diameter of stones about 7 mm. In the center of gravel parcel thick-wall stainless steel tube is placed, through which acoustic pulses arisen in the gravel are transmitted to the acoustic sensor. The deformation of the experimental set up is done with the help of a mechanical jack.

Fig.5. Landslide creep modeling and accompanying AE registration

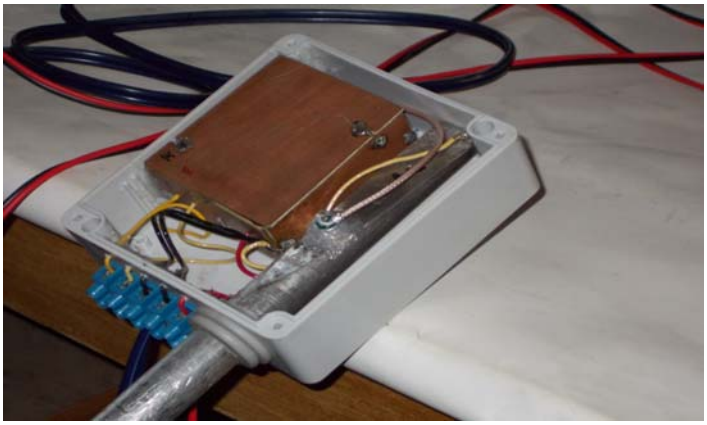

Fig.6. Acoustic sensors

The goal of acoustic monitoring is to record acoustic signals generated by preliminary displacement of geologic formations before activation of the fast phase of landslides.

The similar technique based on the recording of the acoustics generated by displacement in the gravel coating around acoustic sensor was earlier developed by Loughborough University team, but it demands drilling of relatively deep borehole down to the sliding surface. This procedure is quite expensive. Our objective was to develop a cost-effective version of the mentioned method. The idea is to use two sensitive acoustic probes grounded on different depths, one on the depth of several meters and other close to the day surface. The former probe is the basic and the role of latter one is to distinguish signals of surface origin, which in this case are considered as noise.

The probes are constructed from thick-wall stainless steel tube (Fig.6) containing acoustic sensor. The length can be chosen according to the depth of investigation by screwing additional sections to the tube containing basic sensor. The length of these sections is 1.5 m; the maximal depth of probe is of the order of 4 m.

The diameter of the tubes is 20 mm and the thickness of the walls is 2 mm. In order to transfer surface acoustic wave without significant loss the contact of sections is performed with maximal accuracy. This ensures strong contact between sections and minimizes acoustic energy losses.

The upper part of the basic probe is manufactured as a cylinder rod with an inclined cut. The precise finish of the cut surface guarantees good contact of acoustic sensor with probe tube. Investigation of various types of acoustic sensors in laboratory led to conclusion that for the frequency range of interest, i.e. frequencies generated by displacements in the gravel coating (5-25 KHz) the best solution is the capacity capsule-microphone, glued with his sensitive membrane side to the surface of the upper end of the probe.

Electronic module consists of low-noise amplifier, buffer amplifiers of output for signal wavetrains and precision peak-integrator and DC voltage output for recording in the data logger. The integrator fixes in its memory the maximal value of obtained signal and after this the signal decays by the rate 5% per minute. Fixing on data logger the readings with the sampling rate 1 per minute allow obtaining the necessary information on the variation of acoustic noise in the time domain. This method allows saving the power, what is important in field conditions. There are two outputs for fixing signal in two different ways. Signal output 1 allows obtaining acoustic waveform recording by application of high quality ADC. It is also possible to record acoustic signals in the real-time regime, when signal from the output 1 is transferred to the USB recording oscilloscope with the input ADC module capable to record acoustic signals up to the frequency 100 KHz. The signal from output 2 can be recorded simultaneously by another channel of the same USB oscilloscope with input set to DC regime.

Registration of acoustic pulses occurring at small shifting of the landslide soil was produced by the acoustic sensor, which was attached to the USB oscilloscope (Fig.7), with which after using special processing software information is sent to computer.

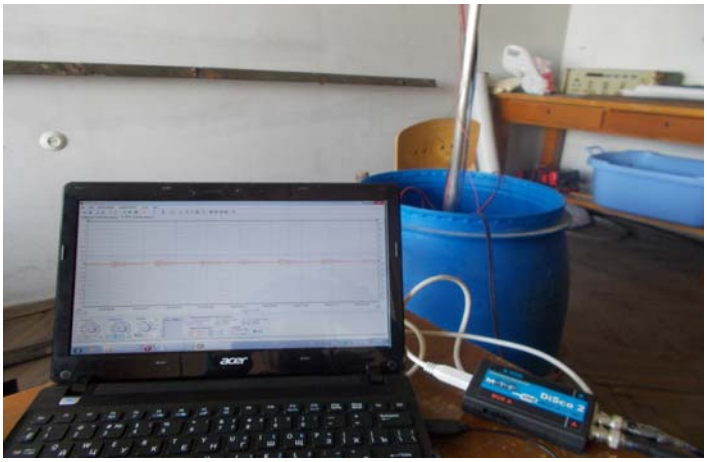

Fig.7. Registration of acoustic pulses using USB oscilloscope

Results analysis

Experimental equipment is described above (Fig.5). The deformation of the experimental equipment is done with the help of a mechanical jack which was compressing the soil or producing shear deformation.

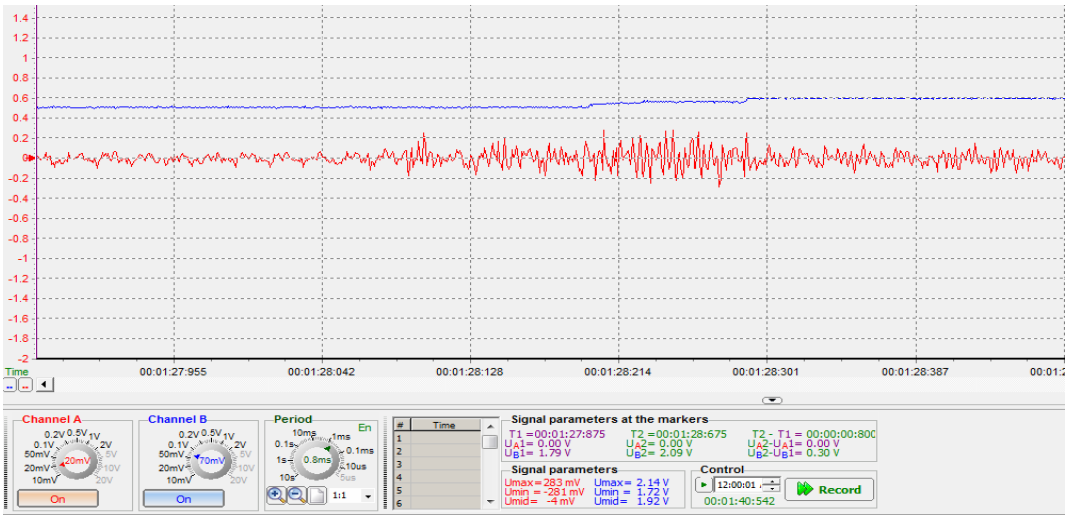

Fig.8. Records of acoustic signal level and waveform using USB oscilloscope; x-axis is time in sec, y-axis is the acoustic signal intensity in volts

Continuous recording waveform and DC voltage was done using USB oscilloscope. One of the record fragments is shown on Fig.8. The signal arising in the compression and shear deformation was negligible. For the registration of each small shift in-depth processing of the data file (~10^5 data in the second) is required and/or increasing the density of the gravel. The increase in density would make occurrence and detection of acoustic pulses in each small shift more efficient. Figure 6 shows the case when quick release of tension from the experimental setup was made. Every step of stress relief can be detected on the record at Fig 6 (arrows indicate 3 most distinguished case).

One of the goals of our experiment was optimization of equipment to use them in the field in a landslide area. Therefore, in some experiments we used data logger for the registration the data. Data logger can record only the DC voltage with a recording frequency of 1 Hz. Our guess is that in this direction, it is possible to develop early warning acoustic system for revealing landslide incipient slipping.

Refereces

[1] Anderson, M. G. and Holcombe, E. Community-Based Landslide Risk Reduction, The World Bank, Washington, DC, 2013

[2] Chelidze, T., Varamashvili, N. and Chelidze, Z., Acoustic early warning telemetric system of catastrophic debris flows in mountainous areas, Journal of the Georgian Geophysical Society, Issue A, vol.15A, 2012, 35-42

[3] Dixon, N. Kavanagh, J. and Hill, R. Monitoring landslide activity and hazard by acoustic emission. Journal of the Geological Society of China, Vol.39, No. 4, 1996, .437-464

[4] Dixon, N., Hill, R. and Kavanagh, J. Acoustic emission monitoring of slope instability: Development of an active wave guide system. Institution of Civil Engineers Geotechnical Engineering Journal, 156, 2, 2003, 83-95

[5] Koerner, R.M. McCabe,W. M. and Lord, A. E., Acoustic emission behavior and monitoring of soils. Proceedings of the First Synopsis on Acoustic Emission in Soils, 1981, 93-141

[6] Kousteni, A., Investigation of Acoustic Emission Waveguide Systems for Detecting Slope Instability. PhD Thesis, The Nottingham Trent University, 2002

[7] Sidle, R.C. and Ochiai H., Landslides-Processes, Prediction, and Land Use, AGU, Washington, DC, 2006

[8] Spriggs, M. and Dixon, N. The Instrumentation of Landslides Using Acoustic Emission, Geotechnical News, September, 2005, 27-31.

მეწყრის გააქტიურების დროს გენერირებული აკუსტიკური ემისია: ლაბორატორიული მოდელირება

ნოდარ ვარამაშვილი, თამაზ ჭელიძე, ზურაბ ჭელიძე

რეზიუმე

სტიქიური უბედურებების შედეგად მსხვერპლისა და ზარალის თავიდან ასაცილებლად პრევენციული ზომები სერიოზულად განიხილება მსოფლიოს ბევრ ქვეყანაში. არსებობს ბევრი გაურკვევლობა მეწყრის დასრიალების დროის პროგნოზირებაში. აკუსტიკური ემისია არის ბუნებრივი მოვლენაა, რომელიც ხდება, როდესაც მყარი სხეული იმყოფება დაძაბულობის ქვეშ. აკუსტიკური ემისია ატარებს ინფორმაციას სხეულში მიმდინარე დეფორმაციის მექანიზმის, ადგილმდებარეობის და ინტენსივობის შესახებ. ჩვენი კვლევის მიზანია მეწყერის ნელი მოძრაობის მოდელირება, რეგისტრაცია და მონიტორინგი აკუსტიკური ემისიის ჩაწერის საშუალებით. მეწყრული სხეულის ცოცვის დროს აღძრული აკუსტიკური იმპულსების რეგისტრაცია ხდებოდა აკუსტიკური სენსორის საშუალებით. ჩვენი ექსპერიმენტების

ერთ-ერთი მიზანია აპარატურის ოპტიმიზაცია რათა მოვახერხოთ მისი გადატანა სველე პირობებში და ვიმუშაოთ მეწყრის დასრიალების წინასწარი შეტყობინების აკუსტიკური სისტემის შექმნაზე.

Акустическая эмиссия при активации оползня: лабораторное моделирование

Нодар Варамашвили, Тамаз Челидзе, Зураб Челидзе

Резюме

Предотвращение потери жизни и имущества в результате стихийных бедствий в настоящее время рассматривается очень серьезно во многих странах мира. Есть много неопределенности в оценке момента, когда произойдет движение оползня. Акустическая эмиссия является естественным явлением, которое происходит, когда твердое тело подвергается деформации. Акустическая эмиссия несет информацию о локализации, интенсивности и механизме деформации, происходящей в материале. Цель нашего исследования моделирование, регистрация и мониторинг медленного движения оползней с помощью записи акустической эмиссии. Регистрация акустических импульсов, возникающих при движении материала происходила с помощью акустического сенсора. Одна из целей нашего эксперимента, оптимизация оборудования для использования его в полевых условиях и создание акустической системы раннего оповещения активизации оползня.

Journal of Georgian Geophysical Society,
Issue (A), Physics of Solid Earth, v. 16a, 2013, pp. 11-18

Assessment of periodical forcing intensity in the spring-slider model

Nodar Varamashvili, Tamaz Chelidze, Zurab Chelidze, Victor Chikhladze, Dimitri Tefnadze

M. Nodia Institute of Geophysics of Ivane Javakhishvili Tbilisi State University,
1, Alexidze Str., 380093 Tbilisi, Georgia

Abstract

In the present study, the character of slip regimes under weak external periodical mechanical forcing has been investigated in a laboratory spring-slider system. In our experiments, the slip events are distinguished by acoustic emission bursts, which are generated by slider displacement. In addition to drag, the weak variable mechanical forcing was superimposed to the upper plate. With increasing additional forcing, which stay still much smaller than the main driving force (spring action) one can see increasing phase synchronization of the first arrivals (onsets) of stick-slip generated acoustic pulses with forcing phase. In this article we want to show that the force caused by the impact of vibrator is much less than plate dragging force. For this we used direct method of calculating the magnitude of the effect of the seismic vibrator forcing. Also, the impact of forcing was calculated from the acoustic pressure produced by seismic vibrator on piezo sensor. Besides, the method of assessment of the forcing by comparative analysis of the impacts of the pendulum and vibrator on the sliding plate was used.

Introduction

The additional mechanical or electromagnetic forcing, which can be much smaller than the main driving force may provoke triggering and synchronization during stick-slip process, which means that these phenomena are connected with nonlinear interaction of objects, namely with initiation of instability in a systems which are close to the critical state (Chelidze et al., 2002; Chelidze and Lursmanashvili, 2003; Avila, 2004; Pikovsky et al., 2001). The earlier similar works considered mainly the effect of forcing on the friction coefficient (Rice and Ruina, 1983).

Understanding of triggering and synchronization effects can be obtained in controllable experiments. We carried out laboratory experiments on the spring-slider system with periodic mechanical forcing, which is weak in comparison with the main dragging force of the spring. In the previous paper the effect on stick-slip dynamics under the weak mechanical forcing applied tangentially and normal to the slip plane was studied (Varamashvili et al., 2008). The external forcing compared with the basic forces is of several orders of magnitude smaller causes triggering different nonlinearities (Bogomolov, 2011) and the effects are not only related to the process of stick-slip.

Experimental setup

We investigated (mechanical) triggering and synchronization of instabilities in experimental spring-slider system by recording acoustic emission, accompanying the slip events [Chelidze et al., 2002; Chelidze and Lursmanashvili, 2003; [Chelidze et al., 2006].

Experimental set up represents a system of two horizontally oriented plates of roughly finished basalt (Fig. 3). A constant dragging force of order of 4N was applied to the upper (sliding) plate; in addition, the system was subjected to weak periodic mechanical perturbations of various amplitudes. Mechanical forcing was realized by the vibrator "CB-5" for normal directed forcing and by "CB-20" for tangential directed forcing. The intensity of mechanical vibration was regulated by the voltage applied to the vibrator.

The dynamics of the sliding process in the spring-slider model depends on the dragging spring stiffness K and dragging velocity V (Boettcher and Marone, 2004). At low velocity, this process is of relaxation type, at intermediate velocity it is periodic, and at high velocity the sliding became relatively stable, with random deviations.

We investigated (mechanical) triggering and synchronization of instabilities in experimental spring-slider system by recording acoustic emission, accompanying the slip events; the setup is described in detail in Chelidze *et al.* (2006) and Varamashvili et al. (2008). The supporting and the slipping basalt blocks were saw-cut and roughly finished. The height of surface protuberances was in the range of 0.1-0.2 mm.

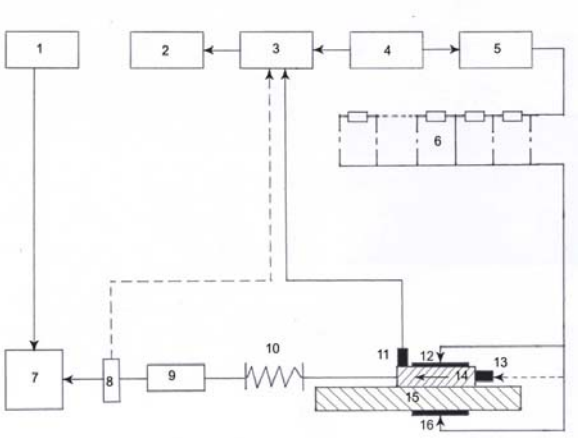

Fig. 1. Schematic representation of the experimental spring-slider model: 1 – Stabilized power source, 2 – personal computer, 3 – amplifier, 4 – forcing signal generator, 5 – external voltage generator, 6 – voltage divider, 7 – dragging device, 8 – tensometer, 9 – dynamometer, 10 – spring, 11 – piezoelectric sensor, 12 – electrode, 13 – vibrator, 14 – sliding block, 15 – fixed block, 16 – electrode.

The experiments were conducted when the forcing load is applied parallel to the slip surface (tangential forcing).

In the case of tangentially directed forcing we calculated the maximum value of mechanical forcing, which corresponds to the maximum measured voltage applied to mechanical vibrator (i.e. when the voltage applied to the vibrator equals 6 V). The mass of the oscillating element of the vibrator m is ≈ 10g, so we obtain for the natural frequency f of the oscillating element of the vibrator, $f = \sqrt{\frac{k}{m}} = 20$ Hz, where k is the stiffness of the vibrator spring. From this expression we obtain, $k = 400\ m = 4$ N/m,

The maximum deflection x_{max} of the oscillating element at the applied voltage 6 V equals $\approx 10^{-3} m$, so the corresponding (maximal) intensity of forcing F_{max} is:

$$F_{max} = kx_{max} \approx 4.10^{-3} N \quad (1)$$

As the forcing is periodic, its current value F is: $F = F_{max}\cos(2\pi\varpi t)$. The maximum rate of vibrator force change is:

$$(\frac{dF}{dt})_{max} = 2\pi\varpi f_{max} \approx 0{,}75N/s \quad (2)$$

The friction (dragging) force is $F_{fr} = Kl$, where K is the dragging spring stiffness and l is the spring elongation. The rate of dragging shear force change in our experiments was $\frac{dF_{fr}}{dt} = (Kl)' = Kv$ where v is the dragging velocity. In our experiment $v \approx 0{,}9mm/s$, $K \approx 250N/m$, i.e. $\frac{dF_{fr}}{dt} \approx 0{,}22N/s$.

.The ratio of the rate of periodic (vibrator) force to the dragging force rate is:

$$\frac{dF_{fr}/dt}{(dF/dt)_{max}} \approx 0{,}3 \quad (3)$$

The forcing rate is larger than the dragging rate, so the synchronization is possible [10].

Sound pressure test

Sound pressure or acoustic pressure is the local pressure deviation from the ambient (average, or equilibrium) atmospheric pressure, caused by a sound wave (Rienstra and Hirschberg, 2013). Sound pressure level (SPL) or sound level is a logarithmic measure of the effective sound pressure of a sound relative to a reference value. It is measured in decibels (dB) above a standard reference level

$$L_p = 10log_{10}\left(\frac{P_{rms}^2}{P_{ref}^2}\right) = 20log_{10}\left(\frac{P_{rms}}{P_{ref}}\right) \quad (4)$$

where P_{ref} is the reference sound pressure and P_{rms} is the rms sound pressure being measured.

The commonly used reference sound pressure is P_{ref} = 20 µPa.

Considering this:

$$L_p = 20log_{10}\left(\frac{P_{rms}}{20\ \mu Pa}\right) \quad (5)$$

From this we obtain, that:

$$P_{rms} = 10^{\frac{L_p}{20}}.20\ \mu Pa \quad (6)$$

The force can be calculated as:

$$F = P_{rms}S \quad (7)$$

In Fig.2 the record of noise obtained using piezo sensor and vibrator forcing record are presented. Piezo sensor was placed on the sliding plate (Fig. 4) and 2.5 V voltage was imposed on vibrator. As can be seen from Fig.3 noise value registered on the piezo sensor is approximately L_p = -30 dB. Based on these data vibrator forcing value on the plate can be calculated. P_{rms} pressure is:

$$P_{rms} = 10^{\frac{L_p}{20}}.20\ \mu Pa = 10^{\frac{-30}{20}}.20\ \mu Pa \approx \frac{1}{15}.10^{-3}\ Pa$$

Accordingly calculated forcing:

$$F = P_{rms} S \approx \frac{1}{15} \cdot 10^{-5}\, Pa \cdot 10^{-3} m^2 \approx 10^{-8} N$$

Based on these calculations, vibrator forcing effect on the upper plate is very weak ($10^{-8} N$) and it is much smaller compared to the pulling force, which is approximately 4 N. Even less forcing is applied in the direction of movement, since the area of the upper plate in this direction is several times smaller than the area in the vertical direction (Fig.1).

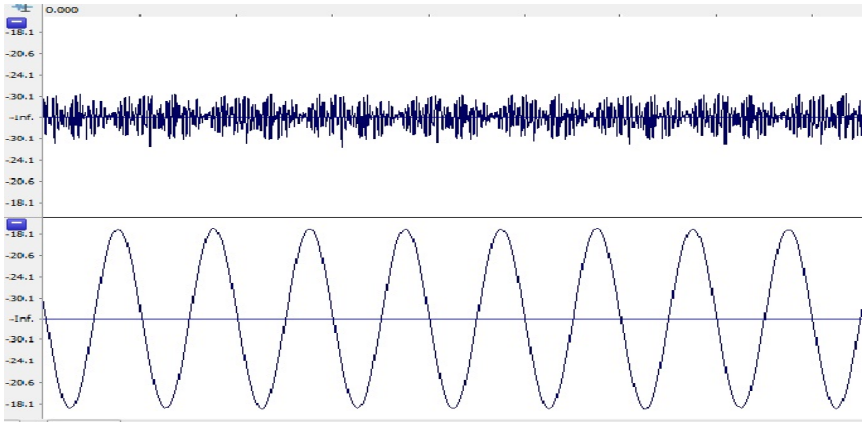

Fig. 2. Records of voltage applied to the seismic vibrator (lower channel) and noise registered by piezoelectric transducer (upper channel).y-axis shows intensity in db, x-axis time (period of forcing is 50 ms), y-axis acoustic signal intensity in dB

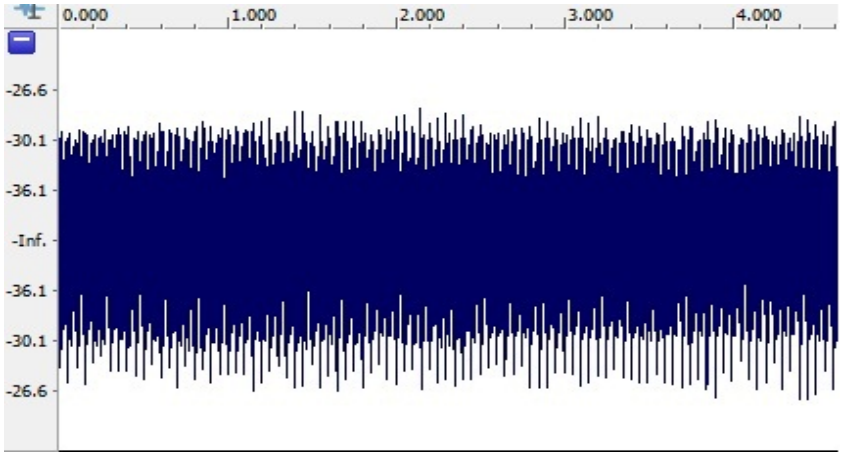

Fig. 3. Expanded record of noise on piezo sensor under action of seismic vibrator to which 2.5 V voltage is applied. y-axis shows intensity in db, x-axis time in sec., y-axis acoustic signal intensity in dB

Calibration with pendulum

To determine the order of forcing magnitude of the seismic vibrator attached to the upper plate the following experiment was carried out. The impact produced by the collision of the pendulum with sliding (upper) plate was assessed. Mass of the pendulum $m \approx 15\, g$, length of pendulum $l \approx 50\, cm$. On Figs. 3 and 4 are presented experiments, when registration was carried out using a piezo sensor (Fig.3) or seismic sensor (Fig.4). Pendulum collision with the upper plate was realized from different distances: 1, 2, 3, 4, 5, 6, 7 and 8 cm.

Our goal is to calculate force the pendulum is acting on the plate. The magnitude of this force will be different for different collision distances. It is necessary to carry out the following calculations:
We need to calculate
1. What height the pendulum reaches at various deviations from the initial position
2. Corresponding potential energy
3. Speed at collision of the pendulum weight with a plate
4. The value of impact momentum (pulse) which the pendulum passes to the plate (about a half of the full pulse)
5. Finally, knowing the duration of the collision it is possible to calculate the force

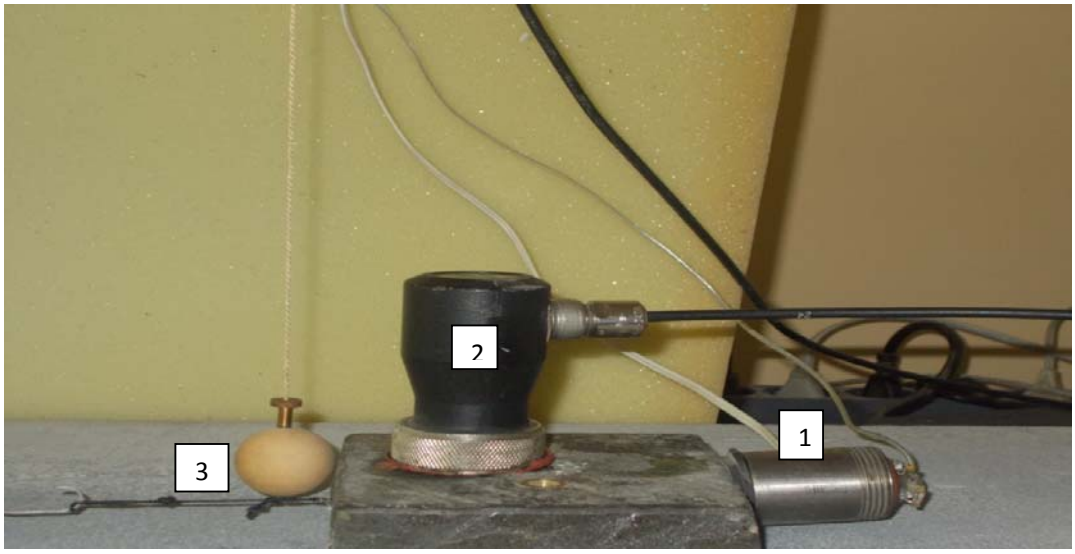

Fig. 4. Seismic vibrator (1) is attached to the sliding plate to which 2.5 v voltage is applied. Registration of the acoustic signal is produced using piezo sensor (2). Calibration of the acoustic signal is produced using pendulum (3).

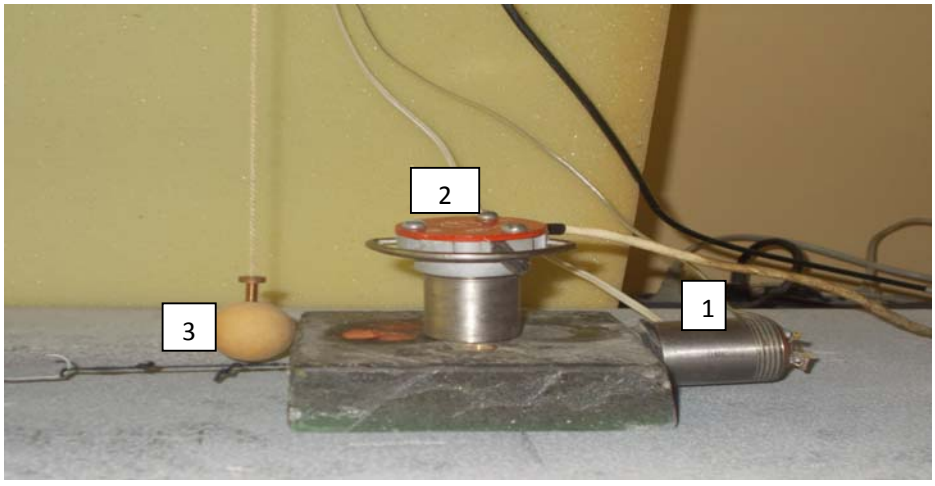

Fig. 5. Seismic vibrator (1) is placed on the sliding plate to which is applied 2.5 v voltage. Registration of the acoustic signal is produced using seismic sensor (2). Calibration of the acoustic signal is produced using pendulum (3).

Figure 6 shows recording made by an USB oscilloscope when the pendulum was deviated by 1 cm. On seismic vibrator 2.5 V voltage is applied. At 1 cm deviation the pendulum rises to a height of $h \approx 2.10^{-4} m$, corresponding potential energy equals $E_p = mgh.$ pendulum speed at collision with a plate $v = \sqrt{2gh} \approx 0.06 \frac{m}{s}$, the value of pulse which the pendulum delivers to the plate $p \approx 4,5.10^{-4} kg.\frac{m}{s}$.

From analysis of Fig.6 we conclude that the pendulum-plate interaction duration time is $t \approx 0.025s$. Accordingly, the impact force is: $F = \frac{p}{t} \approx 2.10^{-2} N$

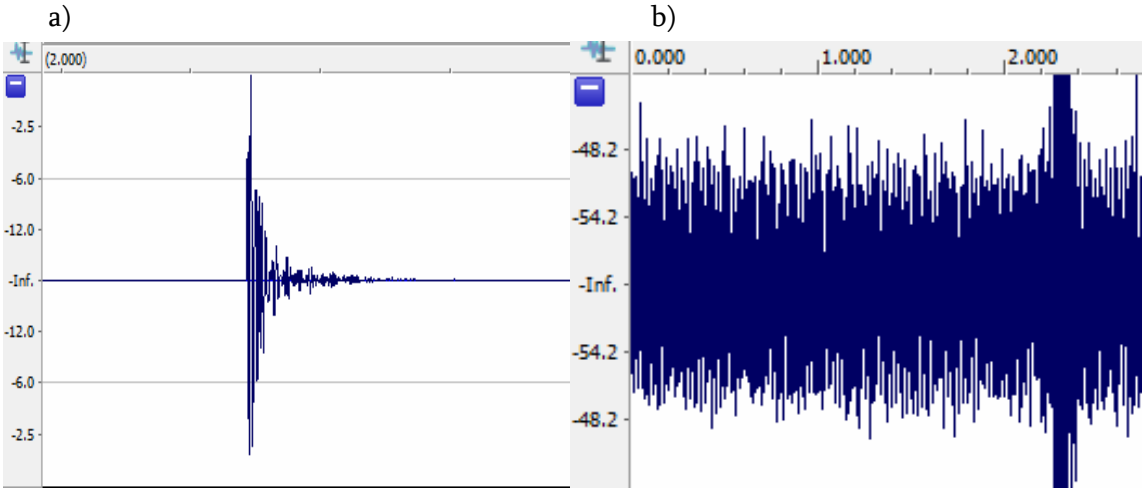

Fig. 6. a) expanded record of acoustic signal generated during clash of 1 cm deviated pendulum using seismic sensor, b) expanded record acoustic signal on piezo sensor under action of seismic vibrator to which 2.5 V voltage is applied with accompanying noise: y-axis shows acoustic signal intensity in dB, x-axis time (1 cm approximately 10 ms)

Table 1. Gradations of the pendulum deviations and corresponding forcing values on the plate

Deviation cm	1	2	3	4	5	6	7	8
Heigh, m	2.10^{-4}	8.10^{-4}	18.10^{-4}	32.10^{-4}	5.10^{-3}	$7,2.10^{-3}$	$9,8.10^{-3}$	$12,8.10^{-3}$
Pendulum forcing, N	2.10^{-2}	$2,7.10^{-2}$	6.10^{-2}	$7,3.10^{-2}$	8.10^{-2}	11.10^{-2}	13.10^{-2}	15.10^{-2}

As can be seen from Figure 6 a the signal resulting from the collision of a pendulum with a plate is clearly recorded in the corresponding channel. Acoustic pulse generated during clash of 1 cm deviated pendulum is shown. Effect of mechanical vibrator is shown on Fig. 6 b.Seismic vibrator is a bit more far from recording piezo sensor than a location of pendulum collision. The effect on the piezoelectric transducer from the collision of a pendulum with a plate is much stronger than an effect of the seismic vibrator.

Based on Figure 6 we can calculate the ratio of the intensity values of acoustic signals arising at the collision of the pendulum on the plate and the resulting from acoustic vibrator forcing. We

calculated the magnitude of the forces encountered during pendulum clashes with the plate (Table 1) and now we have to calculate the order of magnitude of the vibrator forcing.

As can be seen from Figure 6 the amplitude of the acoustic pulse from pendulum clash is approximately -2 dB and the amplitude of (noisy) vibrator forcing is approximately -50 dB. The difference between them is 48 dB, which means that amplitude of a vibrator signal 300 is times smaller than that of pendulum clash. Hence we obtain for 1 cm pendulum deviation:

$$F_v \approx 3.10^{-8} F_q \approx 6.10^{-5} N$$

where F_v is the magnitude of the vibrator forcing on the plate and F_q is the magnitude of the collision force of deflected by 1 cm pendulum.

We can conclude that the intensity of forcing on the sliding plate is several orders of magnitude less than the applied pulling force and the ratio of the forcing to the main driving force is in the range $10^{-4} – 10^{-8}$ N.

References

[1] Avila G., (2004), Synchronization phenomena in light controlled oscillators, Free University of Brussels, Belgium

[2] Boettcher, M. S., and C. Marone, Effects of normal stress variation on the strength and stability of creeping faults,. J. Geophys. Res., 109, B03406, doi:10.1029/2003JB002824, 2004

[3] Bogomolov L., Zakupin A. and Sichev V. Electric impact on the Earth's crust and variations of weak seismicity, Lambert Academic Publishing, Saarbrucken: reha gmbh. 2011. 408 c (in Russian)

[4] Chelidze T., O. Lursmanashvili, T. Matcharashvili and M. Devidze (2006), Triggering and synchronization of stick slip: waiting times and frequency-energy distribution. Tectonophysics, **424,** 139-155

[5] Chelidze T., N. Varamashvili, M. Devidze, Z. Chelidze, V. Chikhladze and T. Matcharashvili (2002), Laboratory study of electromagnetic initiation of slip. Annals of Geophysics, **45,** 587-599

[6] Chelidze T., and O. Lursmanashvili (2003), Electromagnetic and mechanical control of slip: laboratory experiments with slider system. Nonlinear processes in Geophysics, **20,** 1-8

[7] Pikovsky A., M.G. Rosenblum and J. Kurths, (2001), Synchronization: Universal Concept in Nonlinear Sciences,Cambridge University Press

[8] Rienstra S.W. and A. Hirschberg, An Introduction to Acoustics, Eindhoven University of Technology, 2013

[9] Rice J. R., and A.L.Ruina, (1983), Journal of Applied Mechanics, **50,** 343-349

[10] Varamashvili N., T. Chelidze, and O. Lursmanashvili (2008), Phase synchronization of slips by periodical (tangential and normal) mechanical forcing in the spring-slider model, Acta Geophysica, **56,** 357-371, DOI: 10.2478/s11600-008-0006-1

ზამბარა-მცოცის მოდელში პერიოდული ზემოქმედების მნიშვნელობის შეფასება

ნ. ვარამაშვილი, თ. ჭელიძე, ზ. ჭელიძე, ვ. ჩიხლაძე, დ. ტეფნაძე

რეზიუმე

სტატიაში შეისწავლებოდა სუსტი პერიოდული გარეშე ზემოქმედების პირობებში ზამბარა-ბლოკის ლაბორატორიული სისტემის სრიალის რეჟიმების ხასიათი. ჩვენს ექსპერიმენტებში სრიალის მოვლენის რეგისტრირება ხდება აკუსტიკური იმპულსებით, რომლებიც გენერირდება მოსრიალე ფილის გადაადგილებისას. გარდა გამწევი ძალისა ზედა ფილაზე მოდებულია სუსტი ცვლადი მექანიკური დატვირთვა.

დამატებითმა ზემოქმედებამ, რომელიც შეიძლება გაცილებით ნაკლები იყოს მთავარ მამოძრავებელ ძალაზე, შეიძლება გამოიწვიოს სტიკ-სლიპის პროცესისტრიგერირება და სინქრონიზაცია. გარეშე ზემოქმედების ზრდასთან ერთად დაიკვირვება სტიკ-სლიპის პროცესის დროს გენერირებული აკუსტიკური იმპულსების პირველი შემოსვლების ფაზური სინქრონიზაციის ზრდა. წარმოდგენილ ნაშრომში ჩვენი მიზანია ვაჩვენოთ, რომ სეისმური ვიბრატორის ზემოქმედებით გამოწვეული ძალის სიდიდე ბევრად მცირეა ფილის გამწევი ძალის სიდიდესთან შედარებით. გამოყენებული იქნა სეისმური ვიბრატორის ზემოქმედების ძალის პირდაპირი გამოთვლის მეთოდი. ასევე, ვიბრატორის ზემოქმედებით პიეზოგადამწოდზე წარმოებული აკუსტიკური წნევის საშუალებით ძალის გამოთვლის მეთოდი და ქანქარას საშუალებით ფილაზე ვიბრატორის ზემოქმედების შედარებითი ანალიზის მეთოდი.

Оценка величины периодической нагрузки в модели пружина-блок

Н. Варамашвили, Т. Челидзе, З. Челидзе, В. Чихладзе, Д. Тефнадзе

Резюме

В настоящей работе исследовался характер режимов неравномерного скольжения (стик-слип) при слабых внешних периодических механических воздействиях в лабораторной системе пружина-блок. В наших экспериментах, события проскальзывания идентифицируются акустическими всплесками, которые генерируются при перемещении скользящей плиты. Кроме тянущей силы, к верхней плите приложена слабая переменная механическая нагрузка.

Дополнительное воздействие, которое намного слабее основной движущей силы, может спровоцировать триггерирование и синхронизацию в процессе стик-слип. С усилением внешнего воздействия можно увидеть улучшение фазовой синхронизации первых вступлений генерируемых при стик-слипе акустических импульсов. В представленной статье мы хотим показать, что сила, вызванная воздействием вибратора намного меньше силы протяжки плиты. Для этого был использован прямой метод вычисления силы воздействия сейсмического вибратора. Кроме того был использован метод вычисления силы воздействия через акустическое давление, производимое сейсмическим вибратором на пъезодатчик. Наконец, использовался метод сравнительного анализа воздействия импульса маятника и вибратора на плиту.

Journal of Georgian Geophysical Society,
Issue (A), Physics of Solid Earth, v. 16a, 2013, pp. 19-24

Assessment the role of snow in hydrological cycle of the Borjomula-Gudjareti-Tskali rivers basin

George Melikadze, Nino Kapanadze, Mariam Todadze

Mikheil Nodia Institute of Geophysics of Ivane Javakhishvili Tbilisi State University

Abstract

During study summarizing exiting meteorological, hydrological and snow data in the studied area, installation of the monitoring network, collection of water samples, snow expeditions and a more detailed sampling during snowmelt. Regular monitoring consists of precipitation, air temperature and humidity measurements at 3 sites, and water level measurements at 2 rivers. Monthly samples for isotopic analyses (stable water isotopes) are collected from 3 raingauges, 2 rivers, 1 borehole and 2 springs since. The network build in the project provided a lot of new data on snow hydrology in the studied area that was not available before. Measurements at different altitudes were useful. Although snowfall represents just about 30% of annual precipitation, snowmelt water is an important source of water for the rivers (maximum contribution about 50%). Snowmelt affects river runoff at least 2-3 months. Yet, stable water isotopes in the snowmelt water significantly differ among the sites and they are different from those in the snow cover.

Study area

Investigation was caring out in the frame of IAEA project. Studied area (Fig. 1) is situated in the southwestern part of Georgia, in the Little Caucasus Mountains, the Adjara-Trialeti range. It is drained by two main rivers, namely the Gudjareti-Tskali river (catchment area 316 km^2, its mean altitude is 1700 m) and the Borjomula river (catchment area 168 km^2, mean altitude 1600 m). The rivers are the right-hand tributaries of the Mtkvari (Kura) river which is the most important transboundary river in the region of Georgia and Azerbaijan. Apart from the mountains surrounding the study area, the dominant geological unit is the lava body forming the plateau between the two rivers. The Borjomula and Gudjareti rivers flow in their middle and lower sections in narrow valleys (1, 2).

The altitude ranges from about 800 m a.s.l. at the Borjomi city to about 2900 m a.s.l. at the highest mountain peaks. Mean annual mean air temperature is 8.3°C in Borjomi (altitude 794 m a.s.l.), 4.4 °C in Bakuriani (altitude 1703 m). Mean air temperatures of the warmest months (July, August) in Borjomi, Bakuriani and the slopes of the study area are 19°C, 14°C and 9-10°C, respectively. Mean air temperatures in January are 2.8, -5.5 and -9°C, respectively. Mean annual precipitation in the area varies from 650 to 950 mm in Bakuriani (3).

The objectives of the project are:

- Quantification of the amount and residence time of snowmelt water discharging into streams and recharging the captured springs
- Contributions of snowmelt water to stream flow in the Borjomula and Gudaretis-Tskali rivers
- Groundwater recharge from the snow (springs/ boreholes at Daba, Sadgeri and Tba)

Sampling methodology

There was no network providing climatic and hydrological data for the studied area. Therefore, it had to be established within this project from December 2010. Since the study area is mountainous, the network

attempts to describe altitudinal evolution of main climatic characteristics. That way, monitoring station was installing on the several place:

- Monthly composite samples of precipitation are collected in Hellman raingauge and air temperature and air humidity data (hourly time interval) measured by the HOBO sensor, at 3 elevations- Tsagveri, Tba (new station) and Bakuriani (existing station).
- Two gage was installed at the Borjomula and at the Gudjareti river equipped with the pressure transducer (HOBO diver, hourly measurements).
- Isotopic sampling on monthly step carried out on the this two rivers and 2 springs Daba and Sadgeri. Also, on the Tba boreholes.
- Snow course measurements (SD, SWE) at 5 locations (elevations), along with samples for isotopes
- Snowmelt water sampling at 3 locations-Tba, Bakuriani and Tsagveri (extended funnel gauge, plastic and tin snow lysimeters, passive (Frisbee) samplers at 1 location-Tba)

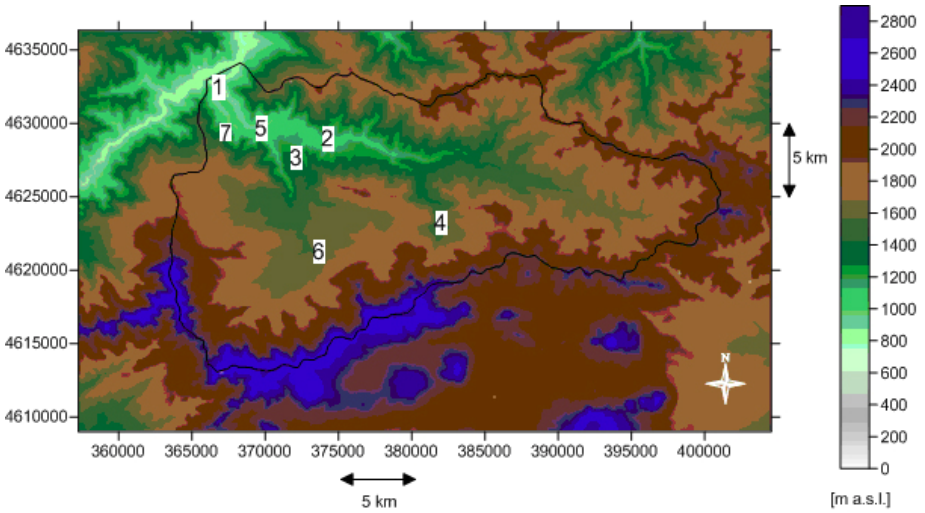

Fig. 1. Monitoring and sampling points in the studied area.

This figure 1 shows digital elevation model and the network. WS stands for water stage measured on the rivers, P and T are precipitation and air temperature measurements, respectively. SWE denotes the sites where we measure snow depth and water equivalents at snow courses. SLYS is the abbreviation for snowmelt lysimeters where we sample water from melting snow that is consequently analyzed for stable water isotopes (4).

Stable water isotopes are analyzed by the LGR isotope analyzed in Prague

Monitoring results

During monitoring period (33 months) found out very good correlations between air temperature variations among sites. Air temperature at different altitudes was very well correlated. The data confirm that winter 2013 was warmer and negative temperatures lasted shorter than in winter 2012. At Tsagveri and Tba stations we have observers the solid precipitation represents about one third of annual precipitation. Annual precipitation is relatively small considering mountain character of the area. Number of days with precipitation at the highest altitude is significantly higher than at lower altitudes.

Water pressure data revealed that runoff regime of both rivers is the same.

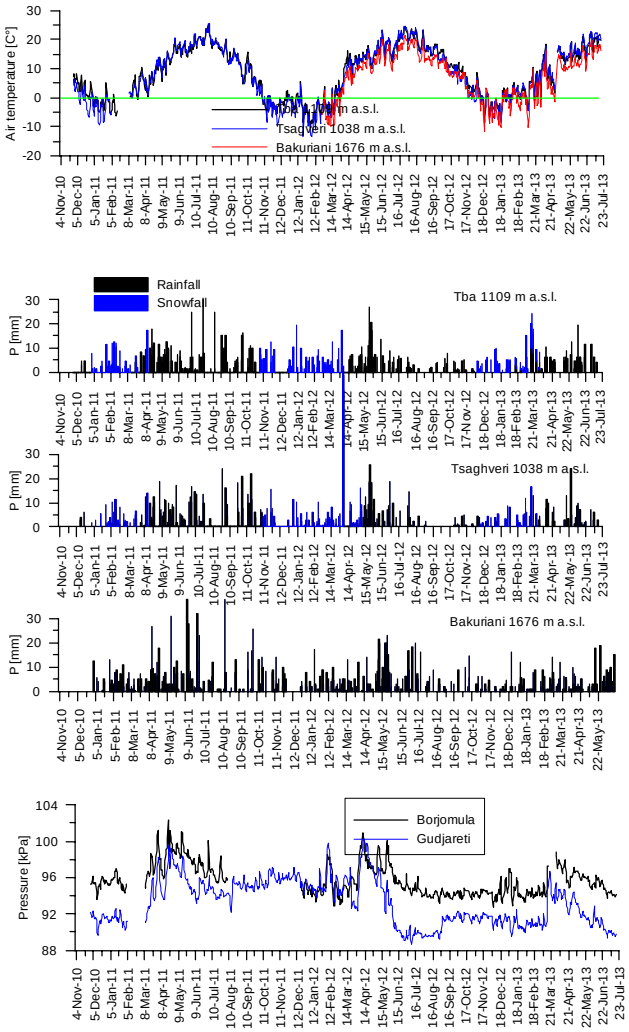

Fig 2 Snowmelt periods

Combined figure of climatic conditions and runoff regime indicates that snowmelt period in 2011 lasted approximately from 11 March to the beginning of June. Snowmelt in 2012 started later (at the end of March) to the end of May. Snowmelt period in 2013 was same, started approximately in the mead part of March to the end of May.

We measured snow courses on the 5 sites at altitudes 952-1676 m a.s.l., measured 4 times in 2011, 5 times in 2012 and 2 time in 2013, SWE gradients about 4-9 mm/100 m, significantly less snow in forest. SWE exhibited altitude gradients of about 5 mm of SWE per 100 meters of altitude. However, the gradients are applicable only until the beginning of snowmelt.

Measurements of snow water equivalents in 2011 covered mostly the snow accumulation period, measurements in 2012 and 2013 covered also the snowmelt period. Measured maximum of snow water equivalent varied from about 120 to reached about 180 mm.

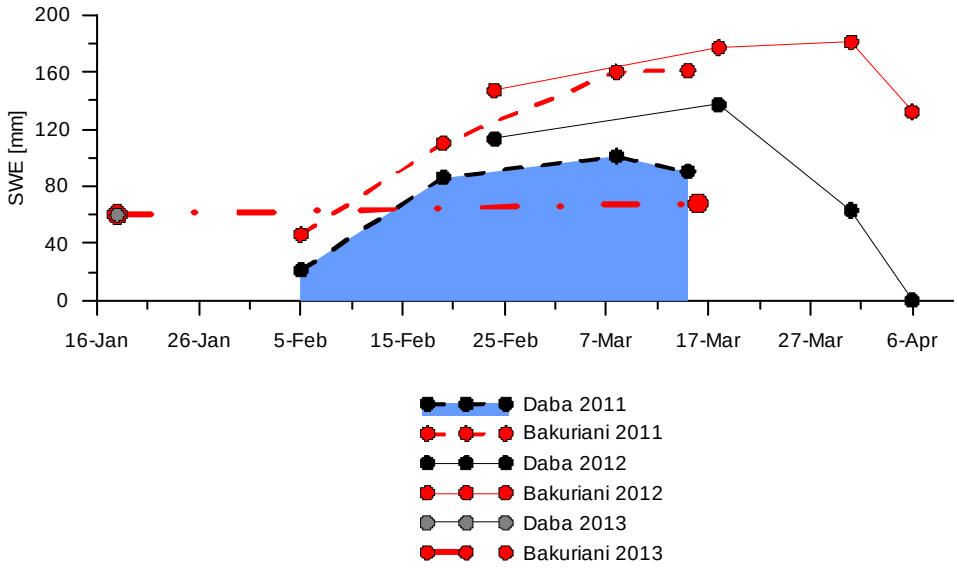

Fig 3 Snow Water equivalent

Fig 3 show, that, maximum SWE in the lower part of the study area represented about 60-80% of solid precipitation. The duration of the melting period varies between 2-3 weeks.

This figure #4 shows spatial variability of deuterium in precipitation at different altitudes, rivers and groundwater. We present also longer data series from GNIP station in Bakuriani and GNIR station on Mtkvari very close to the study area. The data at this step indicate appearance of lighter water in the streams and groundwater in spring.

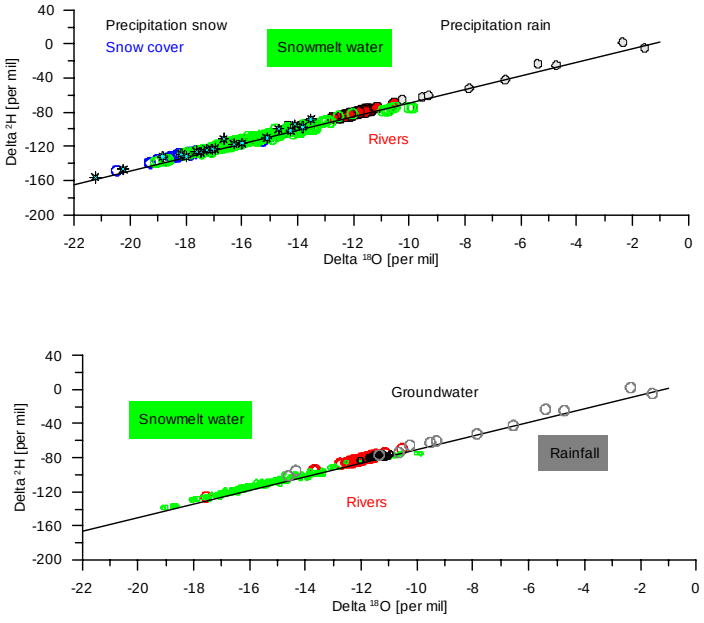

Fig 4 Isotopic composition of water

Groundwater does not differ from the rivers. It indicates that both the rivers and shallow groundwater come from the same source. As expected, the groundwater is generally isotopically heavier than river water.

Snow cover during the snowmelt becomes isotopically enriched.

Data in spring 2011 show that air temperatures increased approximately around the middle of March, but a more intensive snowmelt started a few days' later Water levels in the rivers increased as a response to the snowmelt and later the typical snowmelt runoff regime (diurnal variability of runoff) evolved

Isotopic composition of snowmelt water sampled at Bakuriani by means of the smaller tin and the larger plastic lysimeters were mostly similar, except the beginning of the snowmelt period

Snowmelt water at Tsagveri (lower altitude) during more intensive snowmelt was isotopically lighter than at Tba (higher altitude, but more exposed to sunshine radiation)

River water reacted to increased snowmelt input in the middle of March, following rainfall on March 19 and continuation of snowmelt since March 26

Because the isotopic composition of infiltrating snowmelt water at different sites and times significantly varied, a range of values was used in hydrograph separation

Hydrograph separation in spring 2011 for the Borjomula river. Maximum calculated contribution to total runoff was 21%. Snow contributions to runoff in the Gudjareti river were a higher

In 2012. intensive snowmelt started at the beginning of April (about 2 weeks later than in warmer winter of 2011)

Sampling at Bakuriani confirmed the finding from 2011 that at the beginning of snowmelt the isotopi composition of snowmelt water samples by plastic and tin lysimeters significantly differed

Isotopic composition of snowpack was relatively similar to that of snowmelt water

In 2013 snowmelt started at the end of March and finished at the end of May.

Conclusions

- The network build in the project provided a lot of new data on snow hydrology in the studied area that was not available before (solid-liquid precipitation, hourly variability of water levels in the rivers, snow cover characteristics, SWE modelling, stable water isotopes, snow-covered area from MODIS)
- Measurements at different altitudes were useful
- Although snowfall represents just about 30% of annual precipitation, snowmelt water is an important source of water for the rivers (maximum contribution about 50%)
- The importance of snow is indicated also by the overall distribution of isotopic composition of waters
- Snowmelt affects river runoff at least 2-3 months
- Snowmelt is thus important also for water availability in dry summer period
- Isotopic composition of snow cover does not show an altitude gradient
- Yet, stable water isotopes in the snowmelt water significantly differ among the sites and they are different from those in the snow cover
- Method of snowmelt water sampling influences the obtained data on stable water isotopes (perhaps also a consequence of the small-scale differences in isotopic composition of the snowpack)

References

1. George I. Melikadze, Tamaz Chelidze, Natalia Jukova, Peter Malik,and Tomas Vitvar, 2011, Using Numerical Modeling for Assessment of Pollution Probability of Drinking Water Resources in Borjomi Region (Southern Georgia),Climate Change and its Effects on Water Resources, Issues of National and Global Security (Edit Baba, A., Tayfur, G., Gunduz, O., Howard, K.W.F., Fridel, M.J., Chambel, A.), 2011, NATO Science Series. Springer. ISBN:978-94-007-1145-7. Chapter 29, pp.267-275.
2. GEORGE I. MELIKADZE, NADEZHDA DOVGAL , NATALIA ZHUKOVA, USING NUMERICAL MODELING FOR BORJOMI-BAKURIANI DRINKING WATER RESERVOIR, Workshop materials "Exploration and exploitation of groundwater and thermal water systems in Georgia,, 124 -132, 2010, Tbilisi, GEORGIA, http://dspace.nplg.gov.ge/handle/1234/9081
3. W. Dansgaard. Stable isotopes in precipitation. Tellus 1964, 5, 436.
4. I. D. Clark, P. Fritz. Environmental Isotopes in Hydrogeology, Lewis Publishers, New York, 1997.

Исследование роли снега в гидрологическом цикле в басейнах рек Воржомула Гуджаретис-Цкали

Г.Меликадзе, Н. Капанадзе, М. Тодадзе

Резюме

Исследование посвящено изучению оценки роли снега в гидрологическом цикле. Во время изучения обобщены и уточнены метеорологические, гидрологические данные, данные о снеге в изучаемой области, создана сеть наблюдений, осуществлен сбор образцов воды, снега и других образцов в период таяния снегов в период март-май 2013. Регулярный мониторинг включает измерение осадков, температуру воздуха и влажности в 3-х точках наблюдения (высота 1038, 1109, 1676 метров над уровнем моря), а также измерение уровня воды в 2-х реках. Ежемесячные образцы для изотопного анализа были отобраны с 3-х дождемеров, 2-х рек, 1-й скважины и 2-х источников. Сеть наблюдений, созданная в рамках проекта, обеспечила многими новыми и ранее недоступными данными о гидрологии снега в изучаемой области (атмосферние осадки осадки, почасовые изменения уровня воды в реках, характеристики снежного покрова, SWE-моделирование, стабильные изотопы воды,). Измерения на различных высотах было полезными. Несмотря на то, что снегопады обеспечивают только примерно 30% годовых осадков, талая вода является важным источником воды для рек (максимальный вклад около 50%). Таяние снегов влияет на речной сток 2-3 месяца. Отметим, стабильные изотопы в талых водах значительно отличаются на местах и отличаются от снежного покрова.

თოვლის როლის განსაზღვრა წყალბრუნვის ციკლში ბორჯომულა გუჯარეთის წყლის მდინარეთა აუზებში

გ. მელიქაძე, ნ. კაპანაძე, მ. თოდაძე

აბსტრაქტი

კვლევების მიზანს წარმოადგენდა თოვლის როლის განსაზღვრა წყლის ციკლში. კვლევების პერიოდში გაანალიზდა არსებული მეტეოლოგიური, ჰიდროგეოლოგიური და თოვლის საფარის მონაცემები. ხორციელდებოდა ექსპედიციები წყლის და თოვლის საფარის სინჯების აღების მიზნით. ორგანიზება გაუკეთდა სამონიტორინგო ქსელს ნალექების რაოდენობის, ჰაერის ტემპერატურის და ტენიანობის გადაზომად სამ სადგურში. ასევე, მდინარის დონის გაზომვებს ორივე მდინარეში. ყოველთვიურად ხდებოდა იზოტოპური სინჯების აღება 3 ნალექმზომიდან, 2 მდინარიდან, 1 ჭაბურღილიდან და 2 წყაროდან. მოპოვებული იქნა უახლესი მასალა თოვლის ჰიდროლოგიაში, რომელიც არ არსებობდა მანამდე. სხვადასხვა სიმაღლეზე განხორციელებული გაზომვები გამოდგა წარმატებული. თოვლის ნალექმა შეადგინა მთლიანი ნალექების მოცულობის 30%. ის წარმოადგენს მდინარეების მკვებავი წყლის მნიშვნელოვან წილს (მაქსიმალური წილი 50%). თოვლის დნობის შედეგად მდინარეების წყალუხვობა გძელდება 2–3 თვე. დადგინდა, რომ თოვლის ნადნობი წყლის იზოტოპური შემადგენლობა განსხვავდება სხვადასხვა სიმაღლეზე და ასევე, განსხვავდება თოვლის საფარის იზოტოპური შემადგენლობისაგან.

Journal of Georgian Geophysical Society,
Issue (A), Physics of Solid Earth, v. 16a, 2013, pp. 25-31

USING ENVIRONMENT TRACERS FOR INVESTIGATION OF SUBMARIN GROUNDWATER DISCHARGE

[1]George Melikadze, [2]Michael Schubert, [3]Christos Tsabaris, [1]Nino Kapanadze, [1]Mariam Todadze, [1]Zurab Machaidze, [1]Alexander Chankvetadze

[1]Mikheil Nodia Institute of Geophysics of Ivane Javakhishvili Tbilisi State University
[2]Helmholtz-Zentrum für Umweltforschung GmbH – UFZ
[3] Institute of Oceanography,Hellenic Center for Marine Research (HCMR)

Abstract

The investigation of material transport via submarine groundwater discharge (SGD) is more challenging. In order to determine the groundwater discharge areas into the sea during studies had been implemented and selected the new methodology of using ecological tracers. During marine and land investigations studies had been successfully used the complex of ecological tracers – stable isotopes 18O and 2H, radionuclide Rn and Ra and other parameters. On the territory of Kobulety had been defined the groundwater flow direction and the areas of their submarine discharge. Within the identified areas was defined the intensity of eutrofication – the value of nitrate and phosphate content in groundwaters and in the sea. Also, had been studied their distribution on the surface and intensity of outwash into the sea.

1. INTRODUCTION

The sustainable management of the coastal ocean generally requires a comprehensive understanding of the processes related to solute and particulate material transport from the terrestrial to the marine environment. Whereas river and sewage discharge into the sea are bound to distinct locations, thus allowing straightforward quantification of discharge rates and material budgets, the investigation of material transport via submarine groundwater discharge (SGD) is more challenging. Adding to the general difficulties in locating and investigating groundwater sources on the coastal seabed is the spatial and temporal variability that is typical for SGD.

SGD provides a major potential pathway for solute and particulate transport across the aquifer/ocean interface. Nutrients and contaminants carried by the groundwater have a significant potential to cause deterioration of the overall quality of the coastal environment. Related detrimental environmental impacts include contamination and eutrophication of the coastal sea, contamination of seafood, coral reef damage, and harmful algal blooms.

Aqueous tracers provide an appropriate tool for investigating SGD. “Environmental tracers” are defined as natural or anthropogenic substances that are ubiquitously present in the environment originating from defined sources. In contrast to artificially injected tracers they have the general advantage of not contaminating the studied environment by introducing chemicals that may prove persistent into the water body of concern. In addition, due to their ubiquitous occurrence environmental tracers are most suitable for large-scale and/or long-term studies, which are essential for comprehensive SGD investigation.

The scientific aim of the “SGD Black Sea” research project was the application of a multi-tracer approach for SGD research at two exemplary sites on the Black Sea coast. It was the intention to combine several appropriate aqueous tracer methods for SGD localization and quantification and to confirm the achieved findings by a novel approach based on satellite data. The applied satellite-based information allow (i) a water flow accumulation modelling approach based on a terrestrial

digital elevation model (DEM) and (ii) an assessment of large scale and long term temperature patterns of the coastal sea. The two suggested study sites have been chosen in order to show strong exposure to anthropogenic pressure on the mountainous eastern coast of the Black Sea (Georgia).

2. DESCRIPTION OF STUDY AREA

Georgian team has collected all geological, geophysical, hydro-geological, hydrological and other data about study area. All data was digitized and created data-base (1,2,3).

The coastal zone of study area is located between confluence of river Kintrishi and Kelenderi cape (Sarphi). The coastal zone has a concave form. The coastal zone is built by the sediments transported by rivers. Sediments are distributed by the coastal sea flows –for the south part of study area sea flow changes its directions - from the south to the north. Along The mentioned coastal zone sea water mineralization is 12-17 % and at the confluences of big rivers it decreases till 0-10 %. This fact should be given much attention as we see that continental water flow takes an important part in hydrochemical regime of the coastal zone. It means that toxic and contaminative substances keep a high concentration for a long time. This fact was proved during the observations in Batumi and Poti in 1988-1990. From 1923-1925 due to global climate changing processes Black sea level is increasing. in 1875-1925 it was 40 cm. it should be noted, that the in 1925-2000 the water level increase was 18 cm.

3. DATA COLECTION

3.1. FIELD WORK ON THE GROUNG SURFACE

During the 2012-2013 on the territory of Adjara the field work along the coastline and the surrounding areas had been started. The main research goal was to explore and outline the contaminated areas along the coastline, which represent the potential sources of sea contamination. Along the coastline were sampled every kind of underground water outflow (river, spring, well and borehole). During field work the mobile group was moving by car, which was equipped with special devices (for Ph, conductivity, temperature, free oxygen as well as for Radon and Helium measurements). Besides, the selected points were sampled and the samples were shipped to the laboratory (Tbilisi) for further analyzing.

The sampled points were mapped by GPS and on the next step the data was processed by ArcMap. By the same software was mapped geological, hydrogeological and hydrochemical data. Above mentioned gave us possibility complex studies.

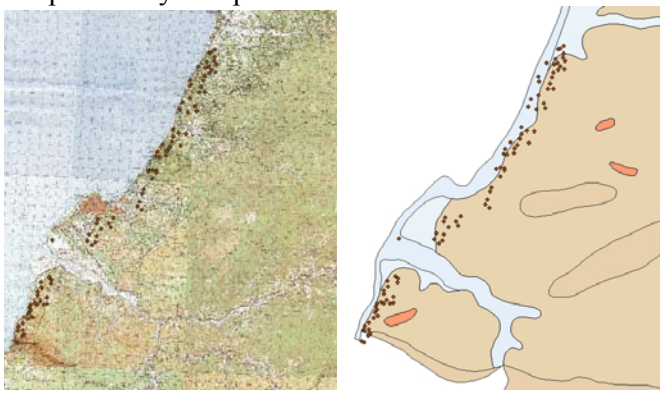

Fig. #1 Dislocation of sampled point on the Topographical and Geological map

Had been observed the radon and helium distribution (4, 5) and their background values as well as hydrochemical parameters (Na, Ca, K, Mg, HCO3, SO4 and Cl) in underground waters.

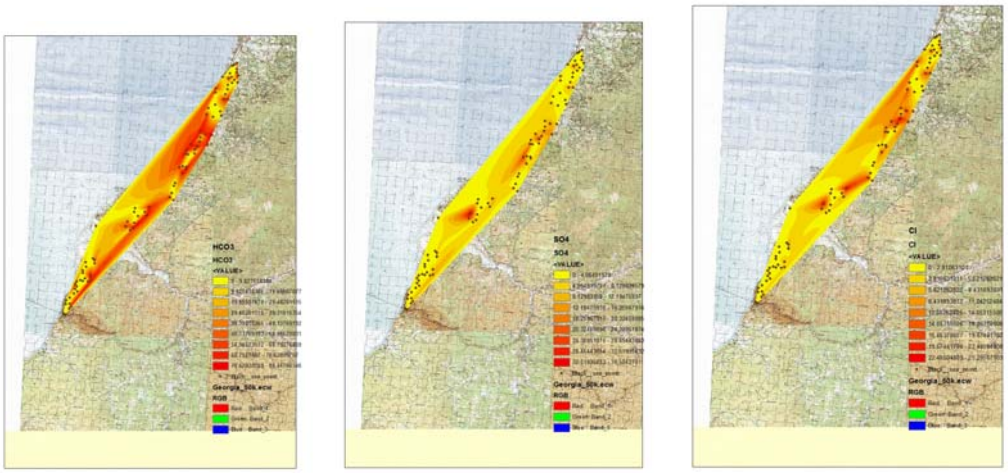

Fig. #2 Distributions of HCO_3, SO_4, Cl in the groundwater along the seaside

There are fixed some anomalies located Northern from Batumi and on the territory of Kobuleti

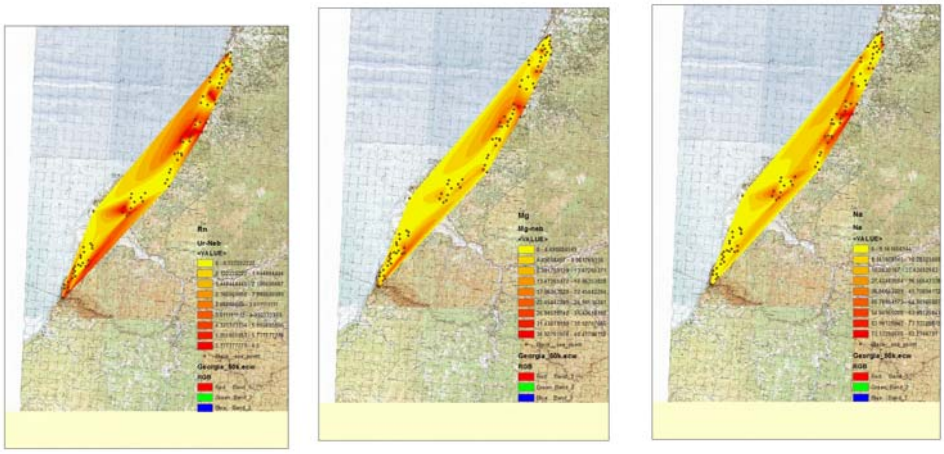

Fig. #3 Distributions of Rn, mineralization and Na in the groundwater along the seaside

During mapping arte fixed anomalies in the distribution of Rn in the groundwater. This zone consisted with anomalies zone of hydrochemical parameters. The observed anomalies may indicate on the polluted areas and represent the object of our interest for further detail studies.

3.2. MARIN SURVEYS

The preparation work for marine expedition had been done together with German colleagues. Namely, the satellite data processing was done by German colleagues. Had been processed and analyzed thermal background data of sea and ground surface.

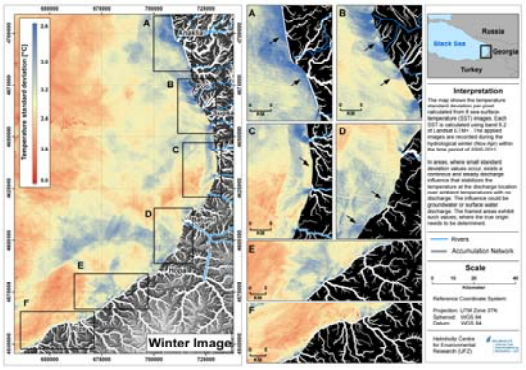

Fig. #4 Satellite data

On the picture shows the cold water discharge areas in the sea at the confluences of rivers as well as at the underground water discharge places. After analyzing two areas had been selected – the one North from Batumi and another one close to Kobuleti, where was expected to reveal the areas of underground waters discharge.

In September 2012 German colleagues arrived in Georgia. During their scientific visit the marine expedition in the Black sea coast was organized. There was done a profile From Batumi till Choloqi by boat and the water physical properties (conductivity, temperature and etc) and Radon concentration were measured continuously.

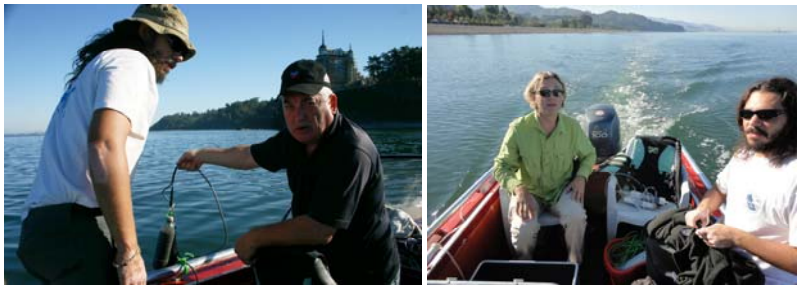

Fig. #5 Marin field study

Fig. 6 Illustrates the radon concentrations and the related salinities that were detected along the coastline and on the perpendicular profile. Fig. 7 shows the same information as diagrams.

Fig. 6A (left): Radon data recorded during the 1st sampling campaign in September 2012. The size of the circles corresponds to the detected radon concentration.

Fig. 6B (right): Salinities recorded during the 1st sampling campaign in September 2012. The size of the circles corresponds to the detected salinity values.

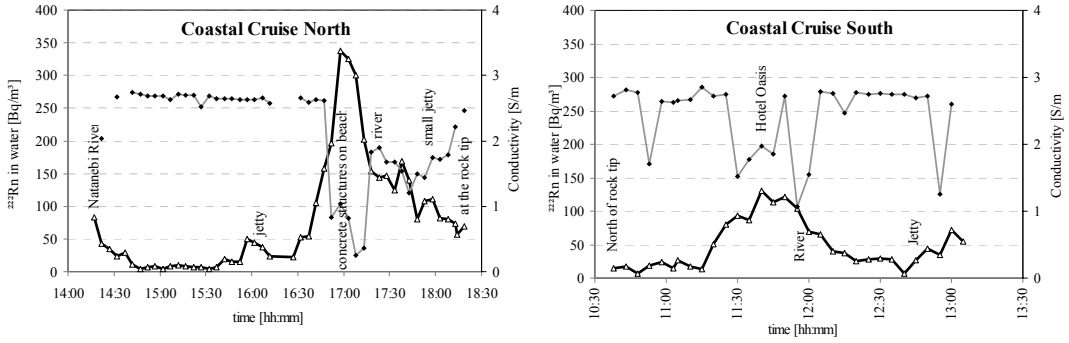

Fig. 7A (left): Radon and salinity recorded during along the northern part of the coastal survey in September 2012.

Fig. 7B (right): Radon and salinity recorded during along the southern part of the coastal survey in September 2012.

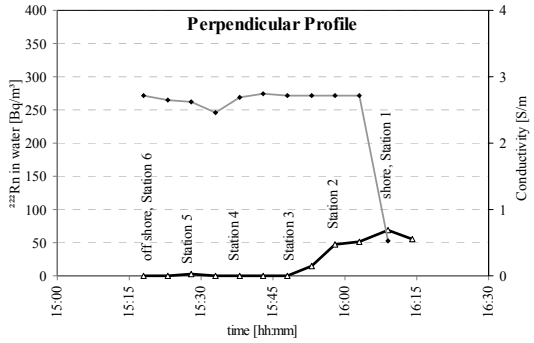

Fig. 7C: Radon and salinity recorded during along the perpendicular profile in September 2012.

As an additional parameter the pH of the seawater was recorded. As it becomes obvious in Fig. 8A the pH showed a distinct peak at the same location where elevated radon concentrations occur, indicating strong SGD. The data displayed in Fig. 8B, illustrating the findings along the southern part of the coastal survey, do also show a negative correlation between radon and pH, which is however not as distinct as the observation displayed in Fig. 8A.

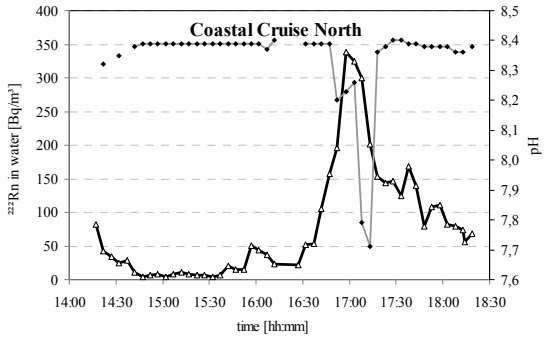

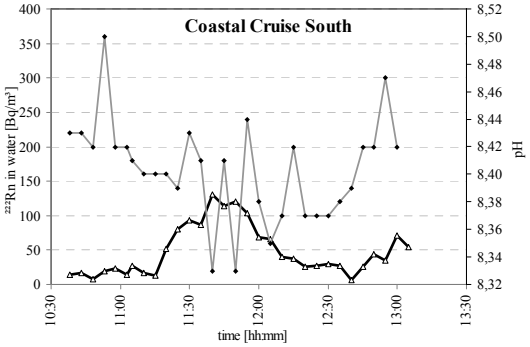

Fig. 8A (left): Radon and pH recorded during along the northern part of the coastal survey in September 2012.

Fig. 8B (right): Radon and pH recorded during along the southern part of the coastal survey in September 2012.

Along the perpendicular profiles also had been done sampling of stable isotopes – 18O and 2H in order to use them as additional tracers. The results showed that mixing of underground water with sea water occurs about 300 meters from the shore and the contribution of underground water is about 5 %. By The joint marine and land investigations showed that found anomalous areas can be identified as continuation of each other.

In order to determine the intensity of eutrophication (nitrate and phosphate pollution) had been measured the nitrate and phosphate content in groundwaters and sea water in areas of revealed groundwater submarine discharge. Their values are less than the allowable standard for nitrates and range from 0.2 - 3 mg / l and for phosphates 0.18 -1 mg / l.

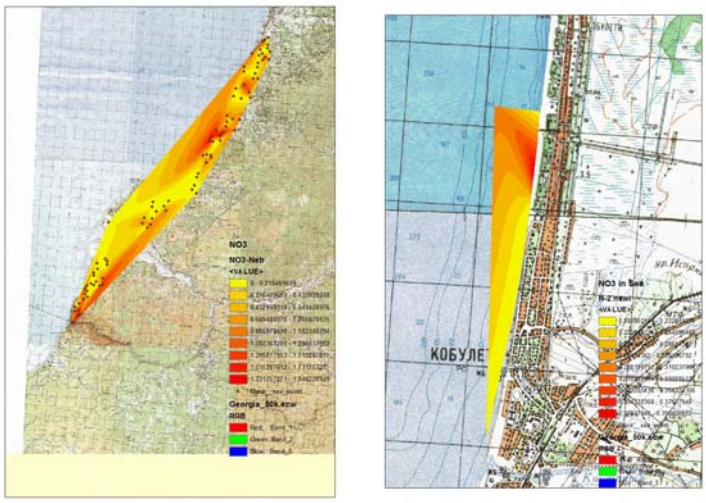

Fig. #9 Distributions of NO3 in the groundwater (left) and sea water (right) along the seaside

Despite the fact that their values are lower than the permissible limit in the sea water – fro nitrates 0.2 - 0.4 mg / l and phosphates of 0.02 - 0.04 mg / l, the amount of run-off of pollutants into the sea is significant. For example, the average annual discharge of Kintrishi river is 0.003 million. m^3, and the Chakvis-Tskali - 0.002 million m^3, which is for nitrates and phosphates 9000 tons per year to 3000 tons per year, accordingly for Kintrishi river and for Chakvi tskali river accordingly 6000 tons and 2000 tons per year. The mentioned tendency will decrease in time if the arable lands are not enriched by chemicals in future.

4. CONCLUSIONS

On the territory of Kobulety had been defined the groundwater flow direction and the areas of their submarine discharge; had been defined the surface character of contamination. Within the identified areas was defined the intensity of eutrofication – the value of nitrate and phosphate content in groundwater and in the sea. Also, had been studied their distribution on the surface and intensity of outwash into the sea.

5. REFERENCES

1. Buachidze I. M at all, ”Hydrogeology og USSR” Book X, Georgia, “Hedra”, Moscow, 1970.
2. Buachidze I. M at all, ”Distrubition of artesian basene on the territory of Georgia”, Geologic Institute of Academi Science of Georgia, Book XII, 1953.
3. Kharatishvili L. A. “Report of geological Department of Kolkheti 1966-68”, Geological Department of Georgiia, 1967.
4. Janja Vaupotič, Mateja Bezek, Nino Kapanadze, George Melikadze, Teona Makharadze, RADON AND THORON MEASURMENTS IN WEST GEORGIA, Journal of the Georgian Geophysical Society 2012, in print
5. George I. Melikadze, Avtandil G. Amiranashvili, Kahha G. Gvinianidze, David G. Tsereteli, Mariam Sh. Todadze “Correlation Between Radon Distribution and prevalence of lung Cancer in West Georgia”, “Environment and Recourses”, Association of Academics of Science in Asia Workshop, 25-27 September 2009, Izmir, Turkey, pp 176-180

Использование экологических трассеров для изучения субмаринной разгрузки подземных вод

Г. Меликадзе, М. Шуберт, Х. Цабарис, Н. Капанадзе, М. Тодадзе, З. Мачаидзе, А. Чанкветадзе

Резюме

Изучение движение материалов по подводному стоку подземных вод (SGD) является сложной проблемой. Чтобы определить области разгрузки подземных вод в море во время исследования была выбрана и осуществлена новая методология- использование экологических индикаторов. Во время морских и наземных исследований был успешно применен комплекс экологических индикаторов: стабильных изотопов 18O и 2H, радионуклидов Rn и Ra и других параметров. На территории Кобулети было определено направление движения подземных вод и места их выхода (излива) на дне моря. В локализованных областях была определена интенсивность эвтрофикации – величина нитратов и фосфатов в подземных водах и в море. Кроме того, было изучено их распределение и интенсивность смыва в море.

ეკოლოგიური ტრასერების გამოყენება მიწისქვეშა წყლების სუბმარინული განტვირთვის შესწავლაში

გ. მელიქაძე, მ. შუბერტი, ქ. ცაბარისი, ნ. კაპანაძე, მ. თოდაძე, ზ. მაჩაიძე, ა. ჭანკვეტაძე

რეზიუმე

მიწისქვეშა წყლების სუბმარინული განტვირთვისას მასალის ტრანსპორტირების საკითხის შესწავლა მეტად საინტერესოა სამეცნიერო თვალსაზრისით. ზღვაში განტვირთვის უბნების დასაფიქსირებლად შერჩეული და დანერგილი იქნა ახალი ეკოლოგიური „ტრასერების“ ტექნოლოგია. მიწისზედა და საზღვაო კვლევების პროცესში წარმატებით იქნა გამოყენებული ეკოლოგიური „ტრასერების“ კომპლექსი– სტაბილური იზოტოპების 18O და 2H, რადიონუკლიდების Rn და Ra ნაკრები. ქობულეთის ტერიტორიაზე გამოვლენილი იქნა მიწისქვეშა წყლის ნაკადის მიმართულება და მისი განტვირთვის არეალები. გამოვლენის უბნებში განისაზღვრა აითროფიკაციის სიდიდეები– ნიტრატების და ფოსფატების კონცენტრაციები ნიადაგში და ზღვაში. ასევე, შესწავლილი იქნა მათი განაწილება ზედაპირზე და ზღვაში მათი ჩარეცხვის ინტენსივობა.

Journal of Georgian Geophysical Society,
Issue (A), Physics of Solid Earth, v. 16a, 2013, pp. 32-36

Investigation of carbon dioxide fluxes and possibility its storage in Georgia

George Melikadze[1], Olga Körting[2] Nino Kapanadze[1], Birgit Müller[3] Mariam Todadze[1], Tamar Jimsheladze, Alexander Chankvetadze,

Mikheil Nodia Institute of Geophysics of Ivane Javakhishvili, 1 Aleqsidze, Tbilisi State University
[2]Institute of Applied Geosciences, Karlsruhe Institute of Technology, Adenauerring 20b, 76131 Karlsruhe, Germany
[3]Landesforschungszentrum Geothermie, Adenauerring 20b, 76131 Karlsruhe, Germany.

Abstract

The major objective of investigation was study the natural CO_2 sources, to investigate the properties of rocks, which contain and absorb CO_2 during its emission. Later mentioned rocks will be considered as an underground Carbon dioxide reservoirs. For this case it is important to determine the potential of save sequestration in Carbon dioxide reservoirs and aquifers and to understand the geochemical and mechanical processes associated with long-term storage of CO_2 including methods to assess zones of weakness.

Field study

In this period, to conduct the joint researches, German partners arrived in Georgia and was organized the complex expedition to the South Georgia and Kazbegi region.

In order to study the CO_2 distribution and define its quantitative characteristics the field work was organized on the territory of South Georgia, Tbilisi and Kazbegi region were studied all main CO_2 sources which in the gas composition contain mostly carbon dioxide – Vardzia, Naqalaqevi, Tmogvi, Akhaltsikhe, Truso and Kazbegi springs.

Fig.# 1 Spring with CO_2 and sampling process in Kazbegi (left) and Vardzia (right) region

For field studies the mobile group was equipped with special devices and moved by car along the pre-defined routes and carried out the sampling of natural and artificial springs. For field measurements they used WTW340i (for pH, conductivity, temperature, free oxygen) as well as "SISIE" and "INGEM-1" for Radon and Helium measurements (1,2). Also, special equipment for gas content measuring had been purchased, namely PGD3-IR (Methan, Oxigen, CO2 and HS). Selected points were sampled for typical

chemical analysis ((Na, Ca, K, Mg, HCO_3, SO_4 და Cl) and the samples were shipped to the laboratory (Tbilisi) for further analyze.

Fig #2 Sampling and gas composition measurement process

Fig #3 Radon measurement process on the Tmogvi and Vardzia borehole

The sampled points were mapped by GPS and on the next step the data was processed by ArcMap. By the same software the results of water and gas hydrochemical analysis, as well as geological, hydrogeological and hydrochemical data of the region have been processed. This gave us the possibility of complex studies

During field work had been observed hydrochemical parameters (Na, Ca, K, Mg, HCO_3, SO_4 and Cl) in underground waters as well as gas content and general peculiarities of Radon distribution. For all observed parameters were determined the background values.

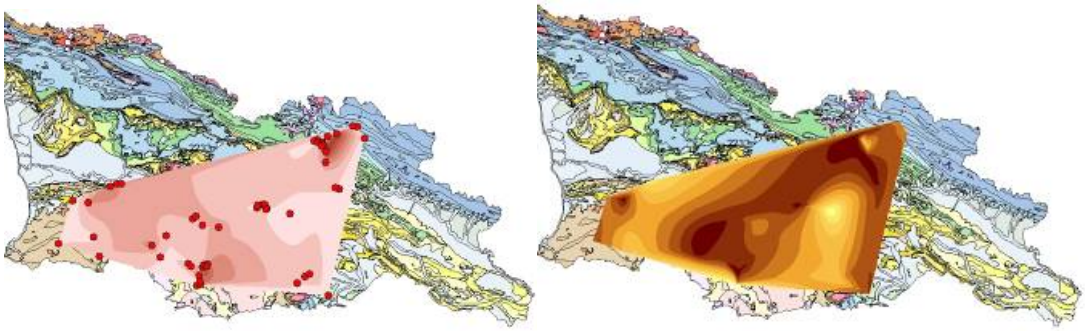

Fig.# 4 Distribution of mineralization (left) and HCO_3 (right) of groundwater between difference Geological region

Natural gases are a very sensitive indicative for geological, especially for geotectonic state. As it was expected in distributing of gas associations the properties of the geological structure of Georgia has been obviously revealed. Researches were done in two zones:

1. the northern zone – containing much carbonic acid gases;
2. The southern zone– with the content of nitrogen and carbonic acid gases.

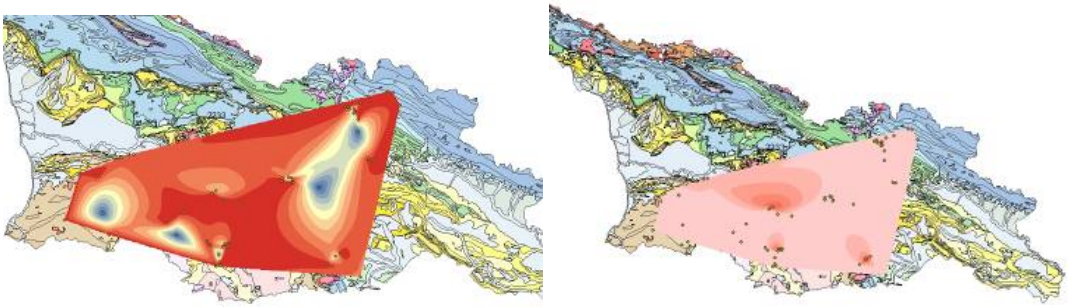

Fig.# 5 Distribution of CO_2 (left) and CH_4 (right) value of groundwater between difference Geological region

The northern zone contains two geotectonic elements – the main Caucasian anticline block and the great Caucasian folded ridge without the extreme segments in the east and west.

In gas associations of these zones that are connected especially with mineral waters, Carbon dioxide obviously dominates. Investigations do not reveal a clear chemical link between underground waters and carbon dioxide, but the bulk of its exposure is connected with Narzan, the main type of mineral waters on the given territory.

The total content of free CO_2 in the waters of North zone, as it was mentioned above, is 1-2 g/l. So high concentration is related with special groups of underground waters and shows the genetic connections of CO_2 concentration with magmatic-metamorphic processes. So, the It is evident the volcanic origin of CO_2

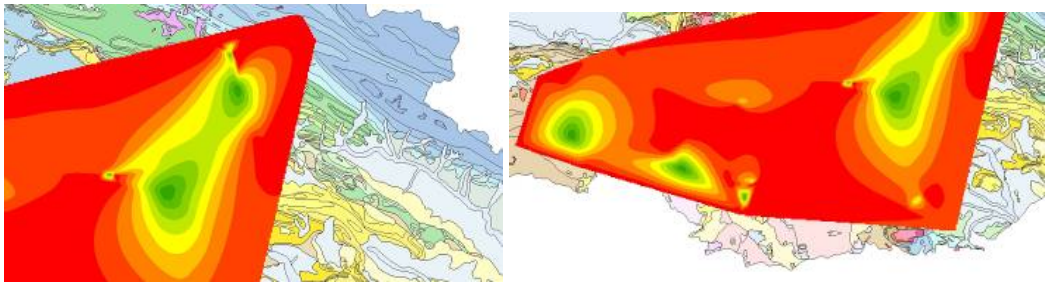

Fig.# 6 Distribution of CO_2 value in the North (left) and South (right) region

Carbon dioxide gas exposures in the southern zone are very numerous. Gas factor of Borjomi group as well as Vardzia, Nakalakevi and others often reach 7-10 g/l. Besides, the horizon pressure is quite high (25 atmospheres in a bore hole). Seldom, but dry outlets of carbon dioxide gas are observed anyway. Exposed carbon dioxide amounts to 2 g/l.

All the above mentioned refers to the existence of strong carbon dioxide escalations. Genetic links of carbon dioxide and the young post-magmatic processes cannot be doubtful; besides, the Quaternary lava discovered here refers to the recent volcanic activity (3).

The gas content rock samples were taken from above mentioned places and were sent to Germany for laboratory investigations (Tab. #1).

Tab. #1 Chemical composition of water and rock from study area

Rocks sample									
Components	Borjomi altered	Borjomi fresh	13_1 fresh	13_2 altered	14_1 fresh	14_2 altered	14_3 altered	16A altered	16B fresh
Na2O (%)	0.94	2.09	3.76	3.71	3.77	3.58	4.41	1.59	0.86
MgO (%)	1.89	1.27	3.05	3.00	2.79	2.74	1.64	1.43	1.10
Al2O3 (%)	8.00	6.42	16.92	17.42	17.02	16.38	16.36	14.66	15.92
SiO2 (%)	44.07	40.43	61.33	61.45	60.53	58.40	67.57	70.22	68.26
P2O5 (%)	0.12	0.04	0.20	0.23	0.24	0.24	0.12	0.05	0.06
K2O (%)	1.34	0.59	2.27	2.28	2.36	2.24	2.10	1.97	0.85
CaO (%)	39.57	44.39	5.35	5.16	5.52	5.23	3.47	5.01	7.23
TiO2 (%)	0.38	0.23	0.70	0.74	0.72	0.71	0.52	0.34	0.37
MnO (%)	0.20	0.51	0.11	0.10	0.11	0.11	0.07	0.05	0.04
Fe2O3 (%)	3.07	2.80	4.60	5.13	5.04	4.84	3.11	3.26	3.05
Loss on ignition	11.36	26.60	0.89	1.40	0.09	1.39	0.00	7.89	7.94
Water samples									
[mg/L]	Borjomi		Caucas-1		Caucas-			Tbilisi	
B	8.40		14.35		12.58			2.81	
Na	1380.20		238.90		220.70			83.64	
Mg	41.12		35.85		38.35			0.07	
Al	0.06		0.10		0.02			0.04	
P	0.00		0.16		0.26			0.04	
K	31.98		4.88		4.70			0.65	
Ca	94.04		114.40		112.50			2.32	
Mn	0.05		1.18		0.85			0.00	
Fe	2.31		21.30		17.03			0.01	
Sr	8.92		1.18		1.21			0.07	
Ba	3.58		0.19		0.20			0.00	
HCO3	3837.65		829.76		768.75			158.63	
Cl-	245.91		167.52		140.46			49.37	
SO4(2-)	0.35		12.98		31.58			16.86	
F-	5.73		0.28		0.01			1.79	
Br-	0.67		0.37		n.a.			n.a.	
NO3-	0.37		0.40		n.a.			n.a.	

After the analyzing of existing data on geologically safe places for CO2 storage, have been selected few zones: Low craterous age carbonate layer in West Georgia, Middle Eocen age volcanic layer in East Georgia, etc. Tbilisi middle Eocene age thermal and oil bearing horizons have been considered as the best Zone. The suitability of the zone depends on the solidity of cap rocks as well as on possible activation of crack systems in them.

In order to estimate the solidity and suitability of the Middle Eocene water bearing horizon as a gas reservoir, the digital modeling will be carried out by the computer programm FEFLOW (4,5).

Conclusions

Was study the natural CO_2 distribution on the territory of South and North Georgia and investigated the properties of water samples and of rocks which contain and absorb CO_2 during its emission. Later mentioned rocks will be considered as an underground CO_2 reservoirs. Next, will be study fluid/rock interactions, will allow us to model these effects and make predictions for CO_2 storage sites.

Acknowledgments: Authors acknowledge financial support of FP7 foundation in the frame of BLACK SEA ERA.NET - Pilot Joint grant “Natural analogue investigation for CCS in the Southern Caucasus

References

1. Avtandil G. Amiranashvili, Tamaz L. Chelidze , George I. Melikadze , Igor Y. Trekov , Mariam Sh. Todadze, “Quantification of the radon distribution in various geographical areas of West Georgia”, Journal of Georgian Geophysical Association, №12, 2008.
2. [1] Janja Vaupotič, [1] Mateja Bezek, [2] Nino Kapanadze, [2] George Melikadze, [2] Teona Makharadze, RADON AND THORON MEASURMENTS IN WEST GEORGIA, Journal of the Georgian Geophysical Society, Issue A. Physics of Solid Earth, vol. 15A, 128-137, 2012.
3. Buachidze I. M at all, ”Hydrogeology of USSR” Book X, Georgia, “Hedra”, Moscow, 1970.
4. GENADY KOBZEV, NINO KAPANADZE, GEORGE I. MELIKADZE, NATALIA ZHUKOVA, CREATION OF NUMERICAL MODEL OF TBILISI GEOTHERMAL DEPOSIT, Workshop materials “Exploration and exploitation of groundwater and thermal water systems in Georgia, 110-124, 2010, Tbilisi, GEORGIA
5. Nino Kapanadze, George I. Melikadze, and Genadi Kobzev, 2011, Modeling of the Tbilisi (Georgia) Geothermal Deposit Under Climate Change Conditions, Climate Change and its Effects on Water Resources, Issues of National and Global Security (Edit Baba, A., Tayfur, G., Gunduz, O., Howard, K.W.F., Fridel, M.J., Chambel, A.), 2011, NATO Science Series. Springer. ISBN:978-94-007-1145-7. Chapter 30, pp.277-284.

Изучение потоков углекислого газа и возможности его захоронение в Грузии

Георгий Меликадзе, Олга Кортинг, Нино Капанадзе, Виргит Мюлер, Мариам Тодадзе

Резюме

Главной целью исследований было изучение источников природного газа CO_2, изучение свойств пород, которые содержат и адсорбируют CO_2 при их эмиссии. Упоминаемые позже породы будут рассматриваться как подземные резервуары углекислого газа. В этом случае является важным определение потенциала сохранения в резервуарах и водоносных слоях углекислого газа, а также понимание геохимических и механических процессов, связанных с долговременным хранением CO_2, включая методы оценки нарушенных зон.

ნახშირორჟანგის ბუნებრივი ნაკადების და მათი შენახვის შესაძლებლობის შესწავლა

გიორგი მელიქაძე, ოლგა კორტინგ, ნინო კაპანაძე, ბირგიტ მიულერ, მარიამ თოდაძე

აბსტრაქტი

კვლევის მთავარი მიზანი იყო ნახშირორჟანგის ბუნებრივი წყაროების შესწავლა, ნახშირორჟანგის შემცველი ქანების თვისებების შესწავლა. ეს ქანები შემდგომში განიხილება, როგორც რეზერვუარი ნახშირორჟანგის მიწისქვეშა შენახვისთვის. ამ შემთხვევაში მნიშვნელოვანია განისაზღვროს ნახშირორჟანგის რეზერვუარებში და მიწისქვეშა ჰორიზონტებში შენახვის შესაძლებლობის განსაზღვრა, ასევე გეოქიმიური და მექანიკური პროცესების გაგება, რომლებიც დაკავშირებულია ნახშირორჟანგის ხანგძლივი დროით შენახვასთან, მათ შორის რღვევის ზონებში.

Journal of Georgian Geophysical Society,
Issue (A), Physics of Solid Earth, v. 16a, 2013, pp. 37-43

THE GEOMAGNETIC VARIATIONS IN DUSHETI OBSERVATORY JANUARY- JUNE 2013

Tamar Jimsheladze, George Melikadze, Alexander Chankvetadze, Robert Gagua, Tamaz Matiashvili

Mikheil Nodia Institute of Geophysics of Ivane Javakhishvili Tbilisi State University

Abstract

Georgia is a part of the far-extending seismically active region, which includes the whole Caucasus, Northern parts of Turkey, Bulgaria, etc. These territories witnessed several intense destructive earthquakes. Thus carrying out possible short-term prognosis of earthquakes is very important for the country. The statistic evidence for reliability of the geomagnetic precursor is based on the distributions of the time difference between occurred and predicted earthquakes for the period January-June of 2013 for Dusheti region. Before strong earthquake magnetic precursors denoted by many authors, but must to say, that more of them don't satisfy stern criterions.

For estimation of the geomagnetic variations as reliable precursor it was discovered the specific time analysis for digital definition of Geomagnetic Quake and proposed way for interval defined from the extremum of local tide variations. The method of earthquake's predictions are based on the correlation between geomagnetic quakes and the incoming minimum (or maximum) of tidal gravitational potential. The geomagnetic quake is defined as a jump of day mean value of geomagnetic field one minute standard deviation measured at least 2.5 times per second. The probability time window for the incoming earthquake or earthquakes is approximately ± 1 day for the tidal minimum and for the maximum- ± 2 days.

4. INTRODUCTION

The precursors list includes usual geophysical and seismological monitoring of the region, including hydrochemical monitoring of water sources and their Radon and Helium concentrations, crust temperature, and hydrogeodeformation field, monitoring of biological precursors and etc. During the monitoring of earthquake precursors including extra information as the variations of electromagnetic fields analysis, it is possible to define earthquakes precursors and estimate earthquake occurrence's intended time what is very actual and important problem

The problem of "when, where and how" earthquake prediction cannot be solved only on the basis of seismic and geodetic data (1; 10; 6).

The possible tidal triggering of earthquakes has been investigated for a long period of time.

Including of additional information in the precursors monitoring, such as the analysis of the electromagnetic field variations under, on and above the Earth surface, can contribute towards defining a reliable earthquake precursor and estimating the most probable time of a forthcoming earthquake.

Simultaneous analysis of more accurate space and time measuring sets for the earth crust condition parameters, including the monitoring data of the electromagnetic field under and over the Earth surface, as well as the temperature distribution and other possible precursors, would be the basis of nonlinear inverse problem methods. It could be promising for studying and solving the ,,when, where and how" earthquake prediction problem.

Some progress for establishing the geomagnetic filed variations as regional earthquakes' precursors was presented in several papers (7; 9).

The approach is based on the understanding that earthquake processes have a complex origin. Without creating of adequate physical model of the Earth existence, the gravitational and electromagnetic interactions, which ensure the stability of the Sun system and its planets for a long

time, the earthquake prediction problem cannot be solved in reliable way. The earthquake part of the model have to be repeated in the infinity way "theory- experiment- theory" using nonlinear inverse problem methods looking for the correlations between fields in dynamically changed space and time scales. Of course, every approximate model (16; 12; 13; 14; 3; 4; 5) which has some experimental evidence has to be included in the analysis. The adequate physical understanding of the correlations between electromagnetic precursors, tidal extremums and incoming earthquake is connected with the progress of the adequate Earth's magnetism theory as well as the quantum mechanical understanding of the processes in the earthquake source volume before and in the time of earthquake.

The achievement of the Earth's surface tidal potential modeling, which includes the ocean and atmosphere tidal influences, is an essential part of the research. In this sense the comparison of the Earth tides analysis programs (Dierks and Neumeyer, ws) for the ANALYZE from the ETERNA-package, version 3.30 (Wenzel, 1996 a, b), program BAYTAP-G in the version from 15.11.1999 (Tamura, 1991), Program VAV (17) is very useful.

The role of geomagnetic variations as precursor can be explained by the hypothesis that during the time before the earthquakes, with the strain, deformation or displacement changes in the crust there arise in some interval of density changing the chemical phase shift which leads to an electrical charge shift. The preliminary Fourier analysis of geomagnetic field gives the time period of alteration in minute scale. Such specific geomagnetic variation we call geomagnetic quake. The last years results from laboratory modelling of earthquake processes in increasing stress condition at least qualitatively support the quantum mechanic phase shift explanation for mechanism generating the electromagnetic effects before earthquake and others electromagnetic phenomena in the time of earthquake (2; 11; 15). The future epicentre coordinates have to be estimated from at least 3 points of measuring the geomagnetic vector, using the inverse problem methods, applied for the estimation the coordinates of the volume, where the phase shift arrived in the framework of its time window. For example the first work hypothesis can be that the main part of geomagnetic quake is generated from the vertical Earth Surface- Ionosphere electrical current. Sea also the results of papers (Vallianatos, Tzanis, 2003 ; Duma, Ruzhin, 2003, Duma, 2006) and citations there.

In the case of incoming big earthquake (magnitude > 5 - 6 the changes of vertical electropotential distribution, the Earth's temperature, the infrared Earth's radiation, the behaviour of debit, chemistry and radioactivity of water sources, the dynamics and temperature of under waters, the atmosphere conditions (earthquakes clouds, ionosphere radioemitions, and etc.), the charge density of the Earth radiation belt, have to be dramatically changed near the epicentre area- see for example papers .

The achievements of tidal potential modeling of the Earth's surface, including ocean and atmosphere tidal influences, multi- component correlation analysis and nonlinear inverse problem methods in fluids dynamics and electrodynamics are crucial for every single step of the constructing of the mathematical and physical models.

2. Data

Dusheti Geomagnetic Observatory is located in Dusheti town (Georgia, Lat 42.052N, Lon44.42E), Alt900m). It is equipped with modern precise Fluxgate Magnetometer Model LGI and it accomplishes non-stop registration of X, Y, Z elements. The data includes minute and second records of the field elements. It is measured with 0,1nT accuracy daily.

There was analyzed earthquakes data in region with Lat42.052N and Long44.42E for January-June of 2013, reported in EMSC: Earthquake research results, magnitude range from 3.5 to 9.0, data selection 115 earthquakes; Minute data of Geomagnetic fields elements received from Dusheti Geomagnetic observatory or 60 samples per hour, with 0,1nT accuracy; Coordinate of Dusheti Geomagnetic observatory: 42.052N, Lon44.42E Alt900m. About the method of Earthquake's

prediction see (18).The distributions of earthquakes' magnitudes and depths, (Mgnitude >3.5) are presented in Fig.1 and Fig.2. (Epicentral distances up to 300km and magnitudes M>3.5).

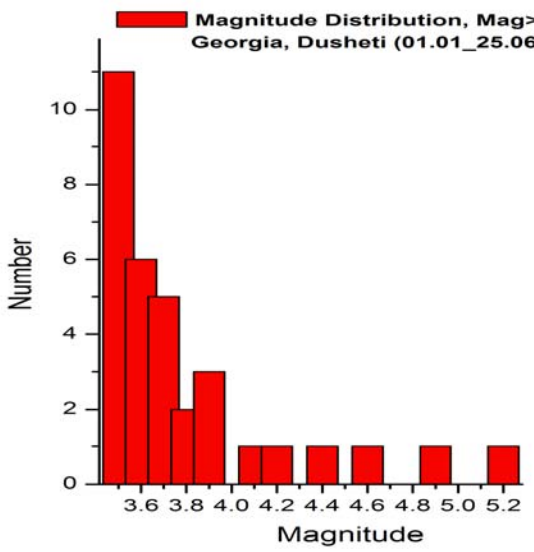

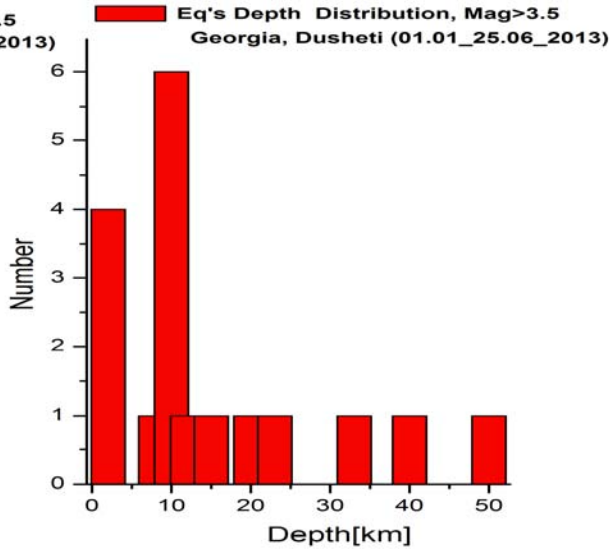

Fig.1 Magnitude distribution

Fig.2 The earthquake's depth distribution

Fig3. Presents the SChtM and magnitude distribution for all occurred in the region earthquakes as function of distance from the monitoring point with magnitude>3.5.

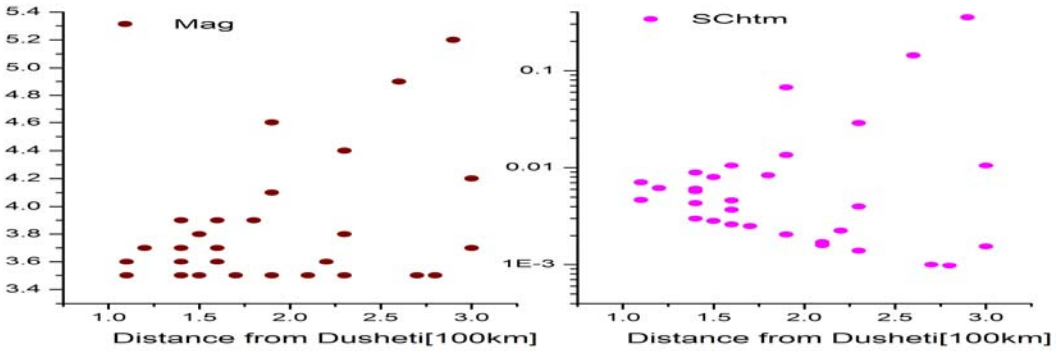

Fig.3. the distribution of SChtM and Magnitude (>3.5) on distances for all occurred earthquakes in the region

The comparison of the distribution in the Fig3 and Fig.4 can give some presentation for distance and magnitude sensibility of the geomagnetic approach.

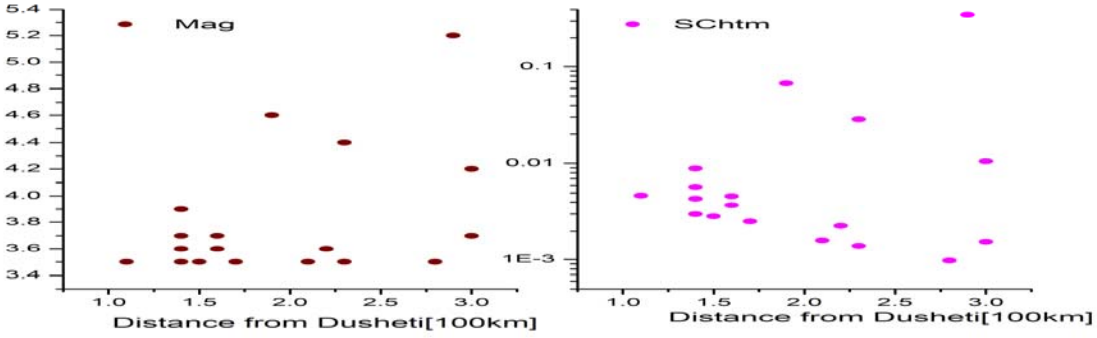

Fig.4. the distribution of SChtM and Magnitude (>3.5) on distances for predicted earthquakes

3. Analysis

The next Table contains the monitoring data for Dusheti and its analysis, described above, which illustrate that the geomagnetic quake is regional reliable earthquake precursor. The columns present: the number of signals preceding the incoming tidal extreme data, information for the tidal minimum (1) or maximum (2), the time of tidal extreme, the time of occurred earthquake, latitude [degree], longitude [degree], depth [km], magnitude, the difference between the time of tidal exstreme and the time of occurred earthquake [in days], distance from monitoring point [in 100 km], the value of function SChtM [J/km2],. The table consists a data for the earthquake with magnitude grater then 3.5

Number of Signals	Tidal min,max	Signal Time	Tidal Min,Max time	Eq Time	Lat	Long	Depth [100km]	Mag	DayDiff	Dist [100km]	SChtM [J/km^2]
1	min	02/02/2013	02/02/2013 10:44	2/3/2013 23:48	40.8	47.9	42	3.7	1.57	3	0.002
1	max	04/26/2013	04/27/2013 11:15	4/30/2013 9:29	40.9	48	5	4.2	2.95	3	0.011
2	max	05/22/2013	05/25/2013 11:07	5/28/2013 0:09	43.2	41.5	2	5.2	2.56	2.9	0.354
		05/24/2013									
2	max	03/20/2013	03/29/2013 11:13	3/27/2013 21:25	40.4	47.2	24	3.5	-0.55	2.8	9.76E-04
		03/23/2013									
1	max	02/20/2013	02/25/2013 12:37	2/22/2013 1:16	43.8	43.2	10	3.5	-3.45	2.3	0.001
2	min	04/09/2013	04/19/2013 12:41	4/18/2013 20:38	41.1	47.2	26	4.4	-0.66	2.3	0.028
		04/14/2013									
1	max	06/01/2013	06/08/2013 11:02	6/7/2013 10:42	43.7	43.4	10	3.6	-1	2.2	0.002
1	max	02/25/2013	02/25/2013 12:37	2/27/2013 4:24	40.9	46.7	18	3.5	1.68	2.1	0.002
2	max	03/27/2013	03/29/2013 11:13	3/31/2013 7:02	42.8	46.8	40	4.6	1.85	1.9	0.067
		03/29/2013									
1	min	06/08/2013	06/16/2013 14:24	6/15/2013 0:46	43.2	46	2	3.5	-1.55	1.7	0.003
3	min	05/15/2013	05/18/2013 13:57	5/18/2013 4:14	43.2	45.8	20	3.7	-0.39	1.6	0.005
		05/16/2013									
		05/18/2013									
1	min	02/02/2013	02/02/2013 10:44	2/2/2013 14:06	43.4	44.4	10	3.6	1.17	1.6	0.004
1	max	04/26/2013	04/27/2013 11:15	4/29/2013 14:26	42.6	46.3	12	3.5	2.15	1.5	0.003
1	min	02/02/2013	02/02/2013 10:44	2/2/2013 8:36	43.2	44.1	10	3.6	0.94	1.4	0.004
2	min	03/15/2013	03/19/2013 11:26	3/17/2013 14:04	43	45.8	15	3.7	-1.86	1.4	0.006
		03/17/2013									
2	max	1/25/2013	1/26/2013 13:25	1/24/2013 11:00	42.8	46.1	40	3.9	-2.08	1.4	0.009
		1/26/2013									
1	max	04/06/2013	04/10/2013 11:01	4/7/2013 17:16	43.3	44.8	10	3.5	3.24	1.4	0.003
2	max	04/23/2013	04/27/2013 11:15	4/28/2013 0:01	42.5	43.5	2	3.5	0.55	1.1	0.005
		04/24/2013									

At the next figures are presented the samples of material work-up for 01.02-23.03_ 2013 Dusheti data. From up to down are presented the curve of tidal gravitational potential, density of earthquake energy (Schtm), earthquake's distribution at the same period, values of SigD and its standard deviation.

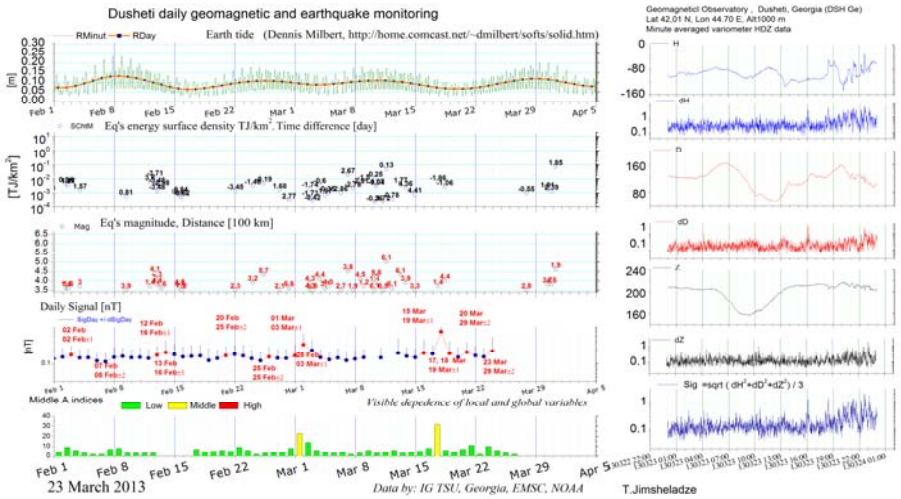

Fig.5 The reliability of the time window prediction for the incoming earthquake.

At Dusheti station, during the period of January-June 2013, there was revealed important disturbances before 26.03.2013 and 28.05.2013 earthquakes, Mag 5.1 and Mag.4.9, epicenter Gagra, which is located from Dusheti in 290km. The disturbance was detected 3 days earlier before earthquake. The disturbance was recorded as before earthquake as its aftershocks period.

Fig.6. Presents the comparison of the number of all occurred and predicted earthquakes For Dusheti. Fig6 Presents the map graphic for earthquakes with magnitude grater then 4 predicted simultaneously from Dusheti measurement.

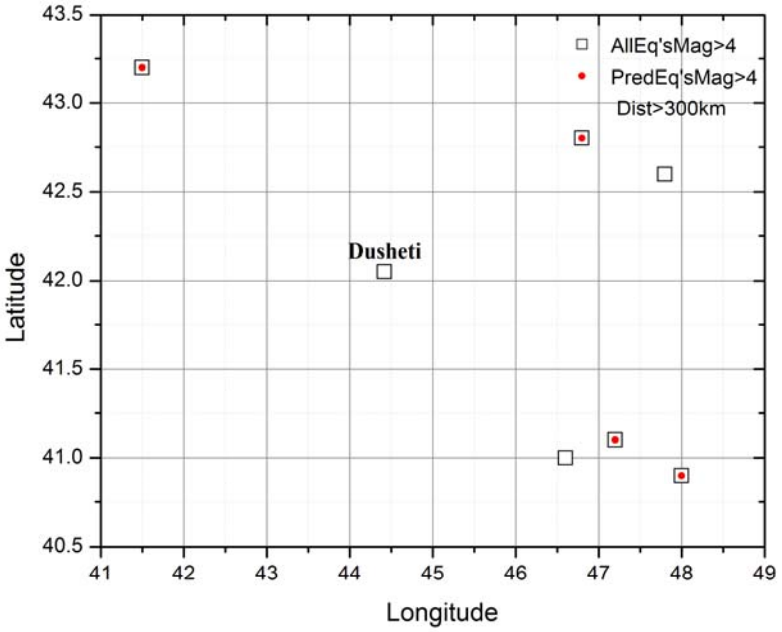

Fig.6 Map graphic for earthquakes with magnitude grater then 4 predicted simultaneously from Dusheti measurement.

It is clear from the picture that among 6 earthquakes for Mag>4; 4 of them were fixed by us.

It is obvious that the occurred in the predicted time period earthquake with maximum value of function SChtM (proportional to the Richter energy density in the monitoring point) is the predicted earthquake. But sometimes there are more than one geomagnetic signals in one day or some in different days. It is not possible to perform unique interpretation and to choose the predicted earthquakes between some of them with less values of energy density. The solution of this problem can be given by the analysis of the vector geomagnetic monitoring data in at least 3 points, which will permit to start solving the inverse problem for estimation the coordinates of geomagnetic quake source as function of geomagnetic quake. The numbering of powers of freedom for estimation the epicenter, depth, magnitude and intensity (maximum values of accelerator vector and its dangerous frequencies) and the number of possible earthquake precursors show that the nonlinear system of inverse problem will be over determinate.

4. CONCLUSIONS

The correlations between the local geomagnetic quake and incoming earthquakes, which occur in the time window defined from tidal minimum (± 1 day) or maximum (± 2 days) of the Earth tidal gravitational potential are tested statistically. The distribution of the time difference between predicted and occurred events is going to be Gaussian with the increasing of the statistics.

The presented results can be interpreted as a first reliable approach for solving the "when" earthquakes prediction problem by using geomagnetic data. Georgian Geomagnetic station inputs important information for space dependences of precursor intensity as part of complex regional NETWORK

of **PrEqTiPlaMagInt** collaboration (**Pr**ediction **E**arth**q**uake **Ti**me **Pla**ce **Mag**nitude **Int**ensity) which includes Bulgaria, Makedonia and Ukraine.

5. REFERENCES

1) Aki K., Earthquake prediction, societal implications, U.S. National Report to IUGG, 1991-1994, Rev. Geo-phys. Vol. 33 Suppl., © 1995 American Geophysical Union, *http://www.agu.org/revgeophys/aki00/aki00.html* , 1995.

2) Freund F.T., A.Takeuchi, B. W.S. Lau, Electric Currents Streaming out of Stressed Igneous Rocks – A Step Towards Understanding Pre-Earthquake Low Frequency EM Emissions, Special Issue "Recent Progress in Seismo Electromagnetics", Guest Editors M. Hayakawa, S. Pulinets, M. Parrot, and O. A. Molchanov, Phys. Chem. Earth, 2006

3) Duma G., Modeling the impact of telluric currents on earthquake activity, EGU06-A-01730; NH4.01-1TH5P-0571, Vienna, 2006

4) Eftaxias K., P.Kapiris, J.Polygiannakis, N.Bogris, J.Kopanas, G.Antonopoulos, A.Peratzakis and V.Had-jicontis, Signature of pending earthquake from electro-magnetic anomalies, Geophysical Research Letters, Vol.28, No.17, pp.3321-3324, September 2001.

5) Eftaxias K., P.Kapiris, E.Dologlou, J.Kopanas, N.Bogris, G.Antonopoulos, A.Peratzakis and V.Hadjicontis, EM anomalies before the Kozani earthquake: A study of their behaviour through laboratory experiments, Geophysical Research Letters, Vol. 29, No.8 10.1029/ 2001 GL013786, 2002.

6) Ludwin, R.S., 2001, Earthquake Prediction, Washing-ton Geology, Vol. 28, No. 3, May 2001, p. 27, 2001.

7)Mavrodiev S.Cht., Thanassoulas C., Possible correlation between electromagnetic earth fields and future earthquakes, INRNE-BAS, Seminar proceedings, 23- 27 July 2001, Sofia, Bulgaria, ISBN 954-9820-05-X, 2001, http://arXiv.org/abs/physics/0110012, 2001.

8) Mavrodiev S.Cht., On the Reliability of the Geomagnetic Quake Approach as Short Time Earthquake's Precursor for Sofia Region, Natural Hazards and Earth System Science, Vol. 4, pp 433-447, 21-6-2004

9) Mavrodiev S.Cht., Pekevski, L., and Jimsheladze T., 2008, Geomagnetic-Quake as Iminent Reliable Earthquake's Preqursor: Starting point Future Complex Regional Network, Electromagnetic Phenomena related to earthquake s and volcanoes. Editor: Birbal Singh.
Publ., Narosa Pub.House, new Delhi, pp. 116-134.

10) Pakiser L, Shedlock K.M., Predicting earthquakes, USGS, http://earthquake.usgs.gov/hazards/prediction.html, 1995.

11) St-Laurent F., J. S. Derr, Freund F. T. , Earthquake Lights and the Stress-Activation of Positive Hole Charge Carriers in Rocks, Special Issue "Recent Progress in Seismo Electromagnetics", Guest Editors M. Hayakawa, S. Pulinets, M. Parrot, and O. A. Molchanov, Phys. Chem. Earth, 2006

12) Thanassoulas, C., Determination of the epicentral area of three earthquakes (Ms>6R) in Greece, based on electrotelluric currents recorded by the VAN network., Acta Geophysica Polonica, Vol. XXXIX, no. 4, 373-387, 1991.

13) Thanassoulas, C., Tsatsaragos, J., Klentos, V., Deter-mination of the most probable time of occurrence of a large earthquake., Open File Report A. 4338, IGME, Athens, Greece, 2001a.

14) Thanassoulas, C., Klentos, V., Very short-term (+/- 1 day, +/- 1 hour) time-prediction of a large imminent earthquake, The second paper, Institute of Geology and Mineral Exploration (IGME), Athens, Greece, Open File Report A. 4382, pp 1-24, 2001b.

15) Vallianatos F., Tzanis A., On the nature, scaling and spectral properties of pre-seismic ULF signals, Natural hazards and Earth System Science, Vol. 3, pp 237-242, 2003.

16) Varotsos P. A., N. V. Sarlis, E. S. Skordas, H. K. Tanaka, and M. S. Lazaridou1, Additional information for the paper `Entropy of seismic electric signals: Analysis in natural time under time-reversal' after its initial submission, ftp://ftp.aip.org/epaps/phys_rev_e/E-PLEEE8-73-134603, 2006.

17) Venedikov A.P., Arnoso R., Vieira R., A program for tidal data processing, Computers & Geosciences, vol. 29, no.4, pp. 487-502, 2003.

18) Jimsheladze T., Melikadze G., Chankvetadze A., Gagua R., Matiashvili T., ,,The geomagnetic variation in Dusheti observatory related with earthquake activity in East Georgia"., Journal of the Georgian Geophysical Society, Issue A. Physics of Solid Earth, vol 15A

ВАРИАЦИИ ГЕОМАГНИТНОГО ПОЛЯ НА ДУШЕТСКОЙ ОБСЕРВАТОРИИ
(Январь – Июнь 2013)

Тамар Джимшеладзе, Георгий Меликадзе, Александр Чанкветадзе,
Роберт Гагуа, Тамаз Матиашвили

Резюме

Геомагнитные аномалии перед землетрясениями были зафиксированы многими авторами, однако надо отметить, что большинство из них не удовлетворяет строгим критериям. Этот метод прогноза землетрясений базируется на корреляции между землетрясениями, геомагнитными аномалиями и наступающими максимумами (или минимумами) приливных вариаций гравитационного поля. Геомагнитное отклонение определяется как отклонения в поле средних значений стандартного отклонения, измеряемых минимум 2.5 раз в секунду. Окно вероятности совпадения во времени событий равняется±1 день для приливно–отливного минимума и ±2 дня для приливно–отливного максимума. Статистическая достоверность геомагнитных предшественников, зафиксированных Душетской обсерваторией, еще раз подтверждается данными распределения разницы между прошедшими и спрогнозированными землетрясениями для периода Январь-Июнь 2013 года.

დუშეთის ობსერვატორიაზე დაფიქსირებული გეომაგნიტური ველის ვარიაციები
(იანვარი - ივნისი 2013)

თ. ჯიმშელაძე, გ. მელიქაძე, ა. ჩანკვეტაძე, რ. გაგუა, თ. მათიაშვილი

რეზიუმე

მიწისძვრის წინ გეომაგნიტური ანომალიები დაფიქსირებულია მრავალი ავტორის მიერ, თუმცა აღსანიშნიე რომ მათი უმეტესობა ვერ აკმაყოფილებს მკაცრ კრიტერიუმებს. პროგნოზის ეს მეთოდი ეყრდნობა კორელაციას მიწისძვრებსა, გეომაგნიტურ ანომალიებს და მიზიდულობის ველის მიმოქცევითი ვარიაციების მოსალოდნელ მაქსიმუმს (ან მინიმუმს) შორის. გეომაგნიტური გადახრა განისაზღვრება როგორც სტანდარტული გადახრების საშუალო მნიშვნელობებიდან, რომლების განისაზღვრება მინიმუმ 2.5 ჯერ წამში. მოვლენების თანხვედრის ალბათობის ფანჯარა უდრის +-1 დღეს, მიმოქცევითი ვარიაციების მინიმუმებისთვის და +-2 დღეს -მაქსიმუმებისთვის. დუშეთის ობსერვატორიის მიერ დაფიქსირებული გეომაგნიტური წინამორბედების სტატისტიკური დამაჯერებლობა, კიდევ ერთხელ დასტურდება 2013 წლის იანვარ-ივნისის მონაცემებით .

Journal of Georgian Geophysical Society,
Issue (A), Physics of Solid Earth, v. 16a, 2013, pp. 44-51

CREATION OF NUMERICAL MODEL OF THE TSAISHI GEOTHERMAL REZERVIOR FOR ORGANIZATION OF GEOTHERMAL CIRCULATION SYSTEM

George Melikadze, Genadi Kobzev, Nino Kapanadze, Mariam Todadze

Mikheil Nodia Institute of Geophysics of Ivane Javakhishvili Tbilisi State University

Abstract

The main aim of the project was to arrange the first geothermal circulation/re_injection system on Tsaishi geothermal filed in Georgia and rehabilitation of heating system of Tsaishi public school, by using environmentally clean, renewable energy source. In order to implement the main aim of the project had been organized the hydrogelogical testing the existing boreholes in order to determine the boreholes' properties and to create a model of aquifer. The digital modelling represents the main steps of calibration and simulation process, which gives the possibility to estimate and study the different scenarios of exploatation and development of precesses.

.

1. Introduction

There are five deep wells arranged on a short distance from each other in settlement Tsaishi #4k, #8k and #10t, from where thermal water outpours uselessly or is used by handmade pipes and only a small part of it.

Fig. 1 Project design scheme

Out of existed thermal wells as a result of hydro geological study only two #10t as exploitation and #4k - as injection wells were selected. The geothermal circulation system had been arranged and the heat system of Tsaishi public school building was connected to this system. For more details see the scheme below (Fig. 1). The school had been supplied with thermal water from well 10 (red line on the scheme). After heating of school the used water is transported (blue line) by pipe to Tsaishi 4k well for the reinjection.

2. Hydrodynamic Research Methods

In order to determine the hydrodynamical parameters (coefficient of filtration, permeability, conductivity, debit, temperature, static and dynamic pressure and etc) of main water bearing horizon, which are necessary for digital modeling, should be done field tests of the boreholes according to the standard method (1, 2, 3) using licensed softwares.

As it is already known, two boreholes - #10 and #4k were considered to be used for geothermal circulation system implementation – first one as productive and second – reinjection. Nearby boreholes that are in 20-50 m distance from #10 borehole were used for monitoring. Measurement and registration works were conducted on these boreholes during the entire exploitation season.

Simultaneously, for measurement equipment installation boreholes unit were prepared and afterwards equipment was installed (water pressure, temperature and discharge measurement sensors, atmosphere and neutral gas measurement sensor). Whole debit and the quantity of water utilized by school heating system were measured on #10 borehole. After heat was deprived, water flow was pumped in #4k borehole by using special pump. All parameters of reinjection process were recorded.

Continuous monitoring was organized. Monitoring was continued till the end of the project and separate boreholes hydrodynamic parameters determination was conducted through testing;

3. Determination of hydrodynamic parameters

In order to define hydro dynamic parameters of exploitation and injection boreholes on #4 and #1K injection boreholes experimental testing was conducted.

Special water pressure and temperature measurement device was installed on boreholes that in a frequent mode (once in a minute) was recording data. In order to define boreholes interaction as well as horizon filtration characteristics #4 borehole along with #1 borehole was closed and reopened few times. Example of observed variations sees on pics (Fig. 2, 3).

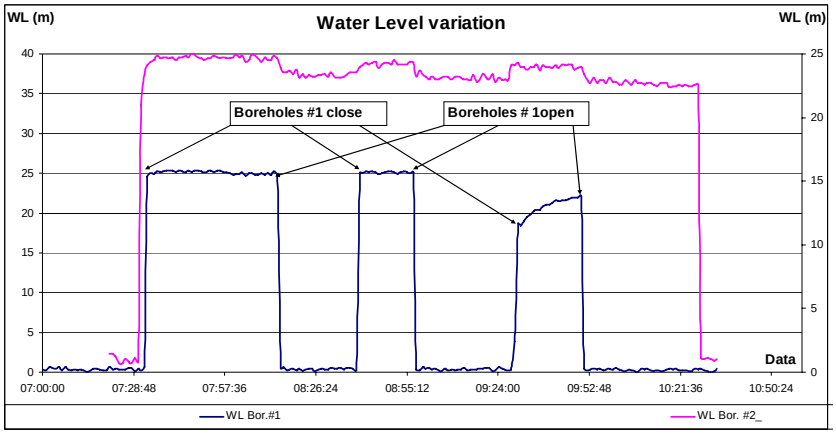

Fig. 2 Water pressure and temperature variation graphics on #4 K regime borehole during experimental testing

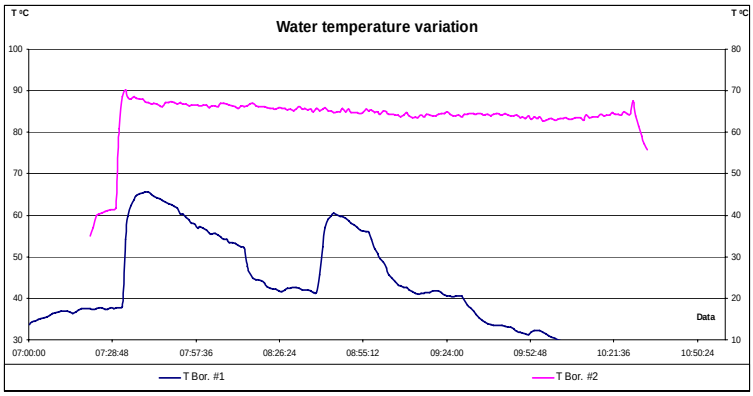

Fig. 3 Water pressure and temperature variation graphics on #1 K regime borehole during experimental testing

Hydrodynamic parameters had been calculated based only on data from #4 borehole (Fig. 4)

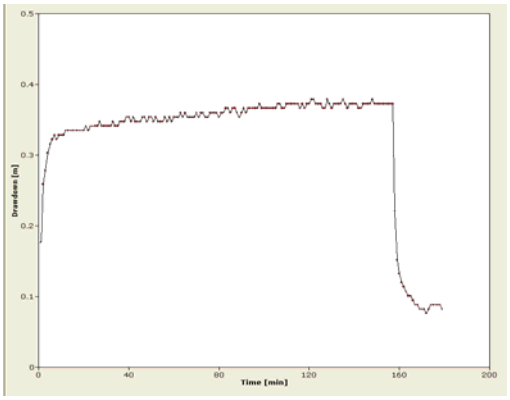

Fig. 4 Water level restoration graphics on a N4 K borehole

Recorded row data during pump test had been processed by the specific programme Aquifertest pro 4.2. (Fig. 5)

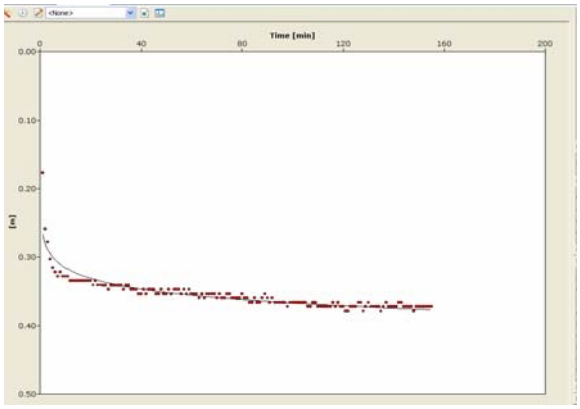

Fig. 5 Water level change logarithmic curve

In order to calculate search options Jacobs method was used. For this aim straight section was selected on a water level fall curve (indications from 15 up to 155) (Fig.6).

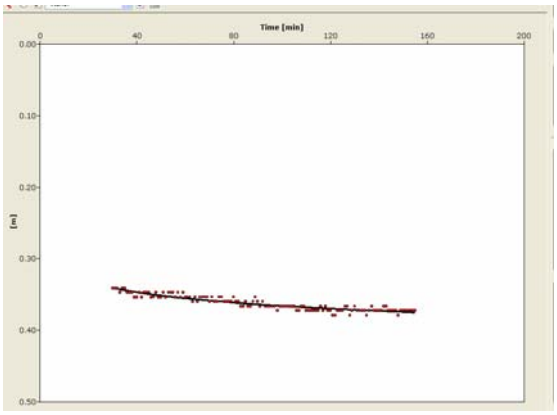

Fig. 6 Water level change logarithmic curve for selected section

As given graphic demonstrate, there is complete convergence between calculated and theoretical curves. Water consist horizon hydrodynamic parameters were calculated - distribution of water T=4620 m^2/ during day/night period and water output S=4.18*10-8.

In order to define interdependence of boreholes testing was repeated, during this process # 10 productive borehole was included as well. During testing boreholes were closed an open in sequence and #4 K borehole was observed. As a result a good hydrodynamic connection between boreholes was again demonstrated.

Based on field researche's received data, section's digital modelling and determination of geothermal circulation system efficiency was started.

Eleboration of digital modeling was conducted according to famous methods like (Domenico and Schwartz, 1998; Middlemis, 2000) by using computer program Feflow and was consist of several stages:

4. Research area's boundary conditions definitiona and elaboration of conceptual model

As it was mantioned above, modeling was conducted by using program package Feflow 5.3, that give a possibility to calculate thermal area's three-dimensional model. In addition, environmental three-dimensional geometrical model was intialy prepared by using programs ArcMap 9.2 and ArcView 3.2 a.

Based on existed geological and hydrogeological materials analysis, following conceptual model for Tsaishi hydrothermal basin was eleborated, according to it, water consist layer is formed by cretaceous age limestones. They are about ten different capacity water conductor layer and less water conductor layers. Model's area constitute $23.6*10^6$ m^2 .

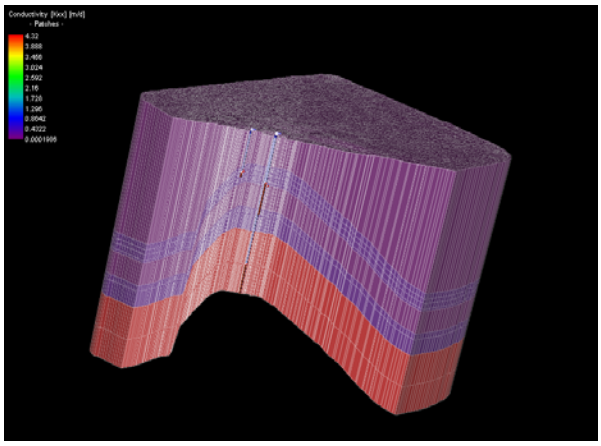

Fig. 7. Conceptual models block-scheme elaborated for Tsaishi hydrothermal area.

Water consist horizons filtration coefficient values are presented in the table 2

Table 2

Layer number	Kx,Ky, m/sec	Kz, m/sec
#1,#6	$2.3*10^{-9}$	Kx/10
#2#3#4#5#7#8	$0.024*10^{-4}$	Kx/2
#9#10	$0.5*10^{-4}$	Kx/2

From the table it is evident, that # 1 and #6 are non water conductor layers, #2, #3, #4, #5, #7, #8 are good water conductor layers, thermal water from # 9 and # 10 layres is taken by # 10 borehole. Basin's piezometric maps, mineralization and thermal profiles indicate on underground water movement regional direction from north-east to south-west. Accordingly, water inflow into aquifer is secured from north-east, that is shown in pink points in model and process of outflow from model by blu points. For # 2 and #5 layers flux capacity-water output constitute 0.005m/ in a day and for # 7 and #10 layers 0.12m/in a day.

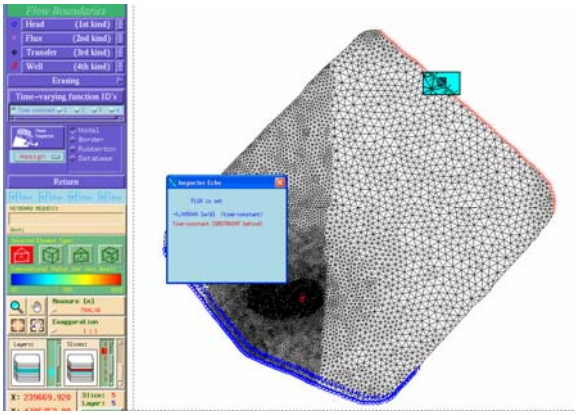

Fig. 8. Flux movement block system for Tsaishi hydrothermal sector

West and east borders of hydrothermal basin show on the model are conditionally non water conductor (Fig. 8).

5. **Implementation of digital modeling**

With the given model we can conduct any type of simulation of thermal area – define balance, field exploitation forcast and etc.

First of all, Tsaishi field's forcast was prepared including current conditions fo exploitation purpose and thermal water balance was calculated from the period of its opening (1983year) up to present, during 30 years period and for next 30 years period operation in the same regime. 60 years in total. As it is shown from drawing, borehole pressure gradually decreases and due to this process discharge is reduced by 4000m^3/24h(from the period of its opening) and by 3000m^3/24has for to date (borehole # 10 shown in red color, # 4 in a blue color). Afterwords, in the case of this kind regime operation, pressure will continue to fall down and we will face so called *Horizon landing*.

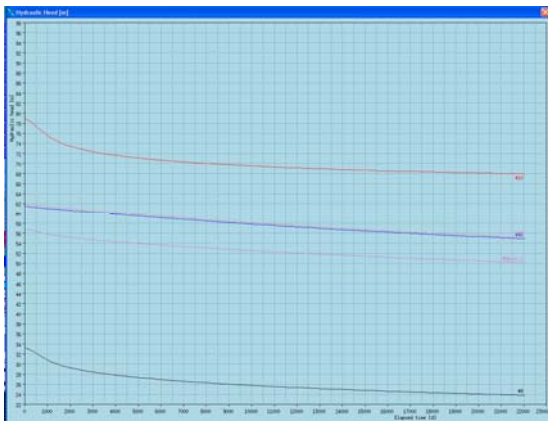

Fig. 9. Pressure changes graphic in the boreholes for 70 years period .

In the process of balance calculation, thermal water's energy lose effect from thermal line borders as well as negative balance fot whole field was detected (Fig. 9-10).

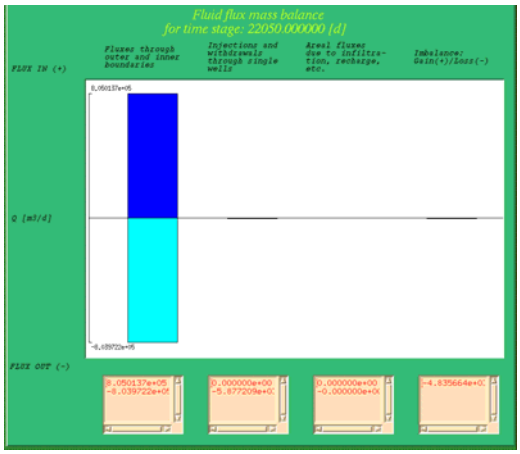

Fig. 10. Balance graphic

On the second stage, possible effectiveness of field's explotation by returning of thermal water was calculated in case if so called geothermal circulation condition will be implemente on Tsaishi area. Namely, the following case was simulated, the hot water taken from the borehole # 10 was pumped into borehole # 4 and at the the same time its effectiveness was calculated for 70 years (Fig. 11).

Fig 11. Pressure changes graphic by reinjection for 70 years period

As it is shownt from Fig. 11, pressure restoration process is evident in # 4 and # 1 boreholes after starting reinjection process and reduction of falling tendency.

Accordingly, in minor, but improvement in whole balance for Tsaishi area can be seen where reinjection was conducted (Fig. 12).

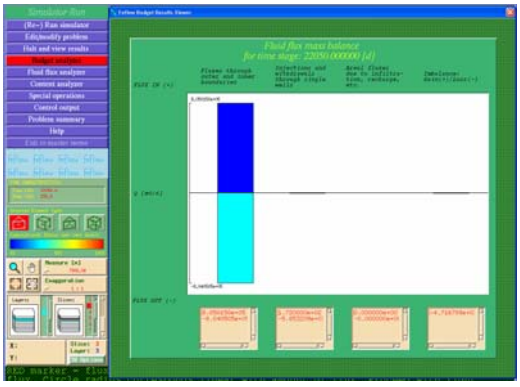

Fig.12. Thermal balance graphics of Tsaishi are for nex 30 yaers

As a result, geothermal circulation system implementation will give an opportunity to avoid outpouring of discharged water that causes thermal pollution of environment and creation of marshes; although by returning discharged thermal water in water exchanger horizon water massive waste will practically be equal to zero. So, pressure fall in water exchanger layer will not occur and this will increase reservoir exploitation period for a long time.

6. Conclusion

The following achieved after project implementation:
Improved Tsaishi public school heating system's efficiency that will ensure normal micro climate in the building;
Hot water supply system operated
Tsaishi geothermal field's section digital model created and possibilities for Geothermal circulation system arrangement determined.

7. Reference

1. A Correia, J. Carneiro, G. Buntebarth, T Chelidze, G. Melikadze, Numerical simulation of groundwater flow and heat transport in the Tbilisi hydrothermal reservoir. printed by M. NODIA INSTITUTE OF GEOPHYSICS, GEORGIAN. ACADEMY OF SCIENCES, EUROPIAN CENTER "GEODYNAMICAL HAZARDS OF HIGHDAMS" OF OPEN PARTIAL AGRREEMENT ON MAJOR DISASTERS, COUNCIL OF EUROPE. Editors: G. Buntebarth, T. Chelidze Tbilisi 2005.
2. Bunterbart G. Kapanadze N, Kobzev G and Melikadze G "Re-assessment of the Geothermal Potential of Tbilisi region: The Hydrodynamic Digital Model Project", "Environment and Recourses", Association of Academics of Science in Asia Workshop, 25-27 September 2009, Izmir, Turkey, pp 154-161
3. Melikadze G., Jimsheladze T., Kapanadze N. „Microtemperature observation in Tbilisi seismoactive region" "New Directions of Investigations in Earth Sciences", the 3rd International Scientific Conference of Young Scientists and Students, Azerbaijan National Committee of Geologists, October 5-6 2009,

Создание цифравой модели Цаишского геотермального резервуара для организации геотермальной циркулационной системы

Георгий Меликадзе, Генадий Кобзев, Нино Капанадзе, Мариам Тодадзе

Резюме

Главной целью данного проекта является создание первой циркуляционной, с повторным закачиванием воды, системы на геотермальном поле Цаиши (Грузия) для тепло и горячоводоснабжения Цаишской государственной школы с использованием чистого возобновляемого источника энергии.

Для достижения главной цели проекта было организовано гидрогеологическое тестирование существующих скважин для определения свойств скважин и создания модели водоносного горизонта. Цифровое моделирование отражает главные шаги калибровки процесса симуляции, дает возможность оценить и изучить различные сценарии эксплуатации и развития процессов.

ცაიშის გეოთერმულ საბადოზე გეოთერმული ცირკულაციური სისტემის ორგანიზების მიზნით ციფრილი მოდელის შექმნა

გიორგი მელიქაძე, გენადი კობზევ, ნინო კაპანაძე, მარიამ თოდაძე

აბსტრაქტი

პროექტის მთავარ მიზანს წარმოადგენდა საქართველოში პირველი გეოთერმული ცირკულაციის სისტემის შექმნა ცაიშის გეოთერმულ საბადოზე და ცაიშის საჯარო სკოლის გათბობის სისტემის რეაბილიტაცია ეკოლოგიურად სუფთა, განახლებადი ენერგიის წყაროთი. არსებულ ჭაბურღილებზე მოხდა ჰიდროგეოლოგიური ტესტირების ორგანიზება რათა განსაზღვრულიყო ჭაბურღილთა თვისებები და შექმნილიყო წყალშემცველი ჰორიზონტის ციფრული მოდელი. ამის შემდგომ განხორციელდა მოდელის კალიბრაციისა და სიმულაციის პროცესები, რაც საშუალებას იძლევა შეფასდეს ექსპლოატაციისა და პროცესების განვითარების სხვადასხვა სცენარები.

Journal of Georgian Geophysical Society,
Issue (A), Physics of Solid Earth, v.16a, 2013, pp. 52-54

Results of the Investigation on the Building Territory

N. Ghlonti, G. Jashi, A. Tarkhnishvili, D. Odilavadze, Z. Arziani, Z. Amilakhvari.

In order to verify engineering-geological conditions ordinary investigations were carried out by electrical prospecting and georadiolocation methods on one of the building objects. We studied the engineering-geological state of the object by electrical prospecting method according to the variation of the resistivity (ρ) in the vertical and lateral direction [1], and by means of georediolocation method we determined the relative dielectric conductivity and equiphase condition of the diffracted electromagnetic waves in the formations within the territory [2].

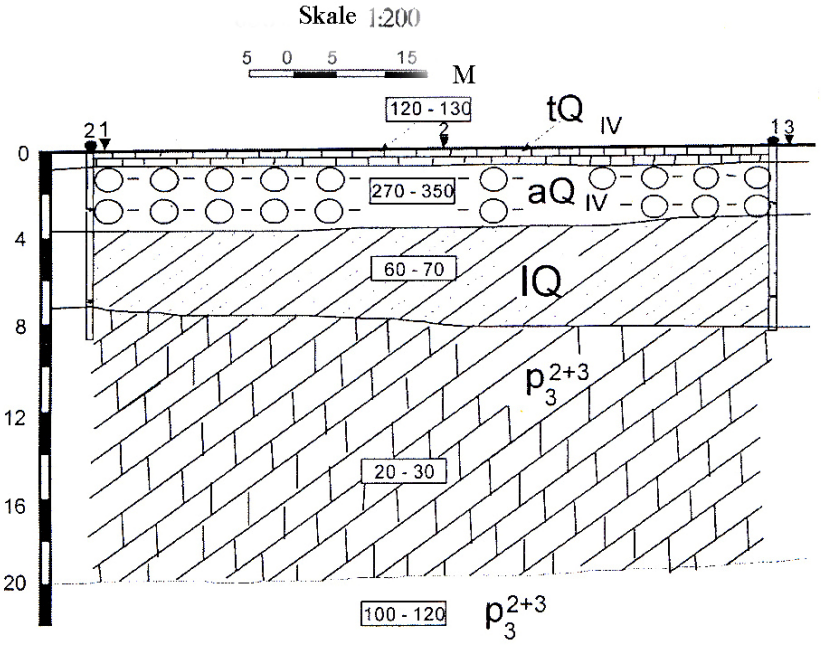

The *figure 1* shows the positions of geophysical profiles and observation points in the 1:500 scale. On the basis of the investigations we constructed geoelectric and radiolocation sections.

For interpretation of the obtained material we used the results of the earlier geological investigations. For illustration our article includes images of typical sections constructed according to electrical prospecting and georadiolocation methods. The *figure 2* shows the geoelectrical sections along the 1-1´ profile.

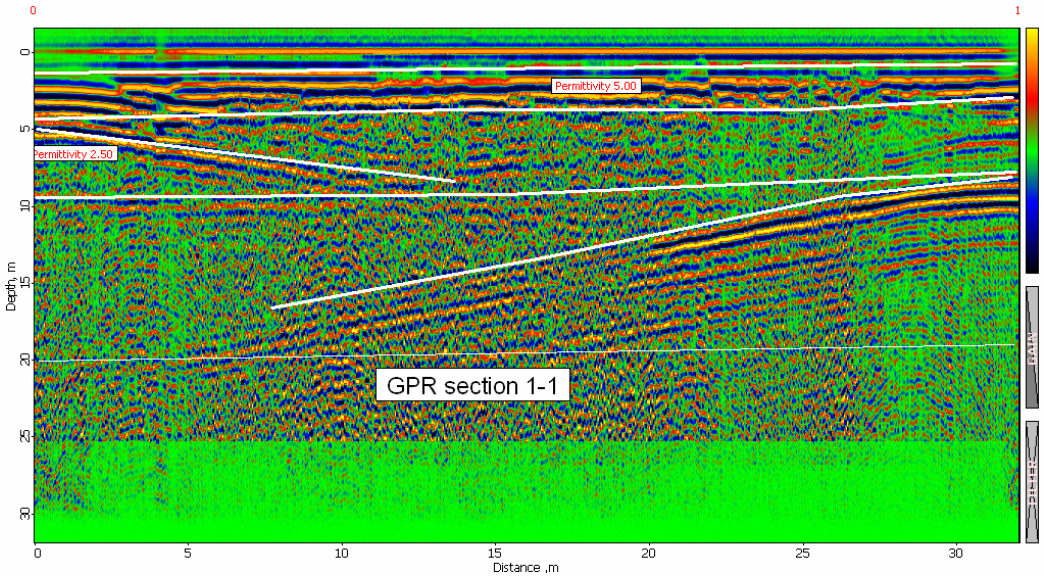

Fig. 2.

The received curves mainly belong to KQH type. The parameters of the first three layers were verified on the basis of the bore well data: the first layer ρ_1=120-130 ohmmeter, h_1=0.5-0.8m of the section corresponds to debris presented by detritus, pebbles and builder's rubble (tQ_4). The second layer ρ_2=270-350 ohmmeter, h_1=3-3.5m is presented by pebbles and stone fragments (aQ_4). The third layer ρ_3=60-70 ohmmeter, h_1=3.5-4.5m corresponds to clay and gravel fragments JQ. According to the vertical electrical sounding (VES) interpretation we divided the fourth layer (sandstones and argillites P_3^{2+3}) in two parts: the upper part must correspond to slightly intruded by water and fissured argillites and sandstones, and the lower part must be presented by relatively solid sandstones. The geo-electric sections are analogous to the above mentioned profile sections shown in the *figure 1*.

As mentioned above the radiolocation profiles are situated alongside the geo-electric profiles. For the radiolocation investigations we used certified GEORADAR "ZOND-12" with supporting 75MHz antenna and software PRIZM-2,5. The thicknesses of the layers distinguished by this method coincide with the thicknesses of the geo-electric section layers, though in the sections constructed by radiolocation method some breaking horizons were distinguished. This might be caused due to the local fragments in these layers (*figure 3*).

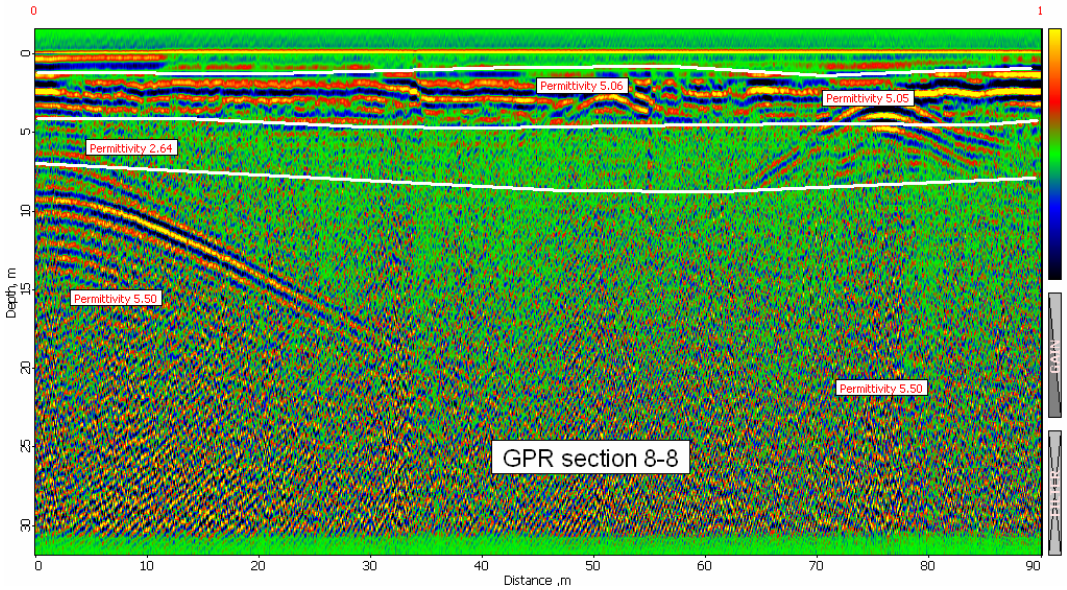

Fig. 3

Thus, by means of geophysical exploration (electrical prospecting, georadiolocation method) on the territory we verified the engineering-geological condition of the object, determined the spatial orientation and physical parameters of the layers.

References:

1. Guide to interpretation of Vertical Eleqtrical Sounding. L.M. Pilayev
2. Enviromental and Engineering Geophysics. Prem V. Shanma, Cambridge University Press.

Результаты геофизических исследований на строительных объектах

Н. Глонти, Г. Джаши, А. Тархнишвили, Д. Одилавадзе, З. Арзиани, З. Амилахвари

Резюме

На одном из строительных участков города Тбилиси методами лектроразведки и георадиолокации было установлено пространственная ориентация и физические параметры составляющих осадочных формаций.

სამშენებლო ობიექტებზე გეოფიზიკური კვლევების შედეგები

ნ. ღლონტი, გ. ჯაში, ა. თარხნიშვილი, დ. ოდილავაძე, ზ. არზიანი, ზ. ამილახვარი

რეზიუმე

ელექტროძიებისა და გეორადიოლოკაციური მეთოდებით თბილისის ერთ-ერთ სამშენებლო ობიექტზე დადგენილ იქნა იქ გავრცელებული დანალექი ფორმაციების სივრცობრივი ორიენტაცია და მათი ფიზიკური პარამეტრები.

Journal of Georgian Geophysical Society,
Issue (A), Physics of Solid Earth, v. 16a, 2013, pp. 55-60

FEATURES OF SEISMICITY OF AZERBAIJAN PART OF THE GREATER CAUCASUS

Yetirmishli G.J., Mammadli T.Y., Kazimova S.E.

Republican Seismological Survey Center
of National Academy of Sciences of Azerbaijan
Az 1001 Baku, N.Rafibeily str. 9,
sabina.k@mail.ru

The article is devoted to the strong Zagatala, Balakan and Ismayilli earthquakes in Azerbaijan in 2012. The analysis of seismicity of focal zones of the indicated districts - macroseismic field, mechanisms of earthquakes' foci, aftershock activity at the foci of strong shocks, as well as geological and tectonic conditions of epicentral zones are presented. Using a pair of right strike-slips of geodynamic model, the interpretation of mechanisms of the Zagatala earthquakes' source is given and the mechanism of the General-Caucasian release with left strike-slip component has been established. The amplitude spectra have been built and dynamic parameters of focus have been calculated from digital seismograms of shear waves of the Zagatala earthquakes of May 7, 2012.

Introduction

The territory of Azerbaijani part of the Greater Caucasus is prone to high seismic activity, where strong and catastrophic earthquakes with a magnitude of M ≥ 6 occurred for the historical period (Fig. 1).

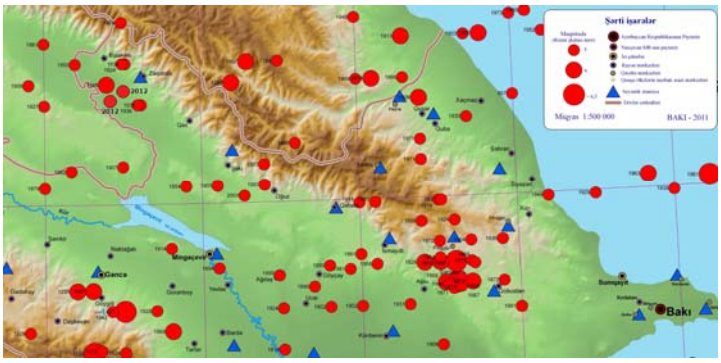

Fig. 1 Map of the epicenters of strong earthquakes of Azerbaijan occurred for the period of 427-2012

Continuous tectonic movements in the Caucasus lead to activation of seismicity of its territory in 2012. The earthquakes occurred in Zagatala district of magnitude M=5.6-5.7 on May 07, 2012 at 04:40:21 and 14:15:13 on Greenwich time (on local time 19:15), in Ismayilli district with a magnitude of M=5.3 on October 7, 2012 at 11:42:50 on Greenwich time; strong earthquake occurred also in Balakan district on October 14, 2012 at 10:13:13 on Greenwich time with a magnitude of M=5.6.

Zagatala earthquakes, 2012

As it was noted above 2 strong earthquakes of magnitude M=5.6-5.7 occurred in Zagatala district in May 7, 2012. According to the data of instrumental observations, earthquakes' coordinates are: φ = 41,57°N, λ= 46,64°E, M = 5.6-5.7, depth h = 8-12 km. It was felt in Zagatala, Balakan, Gakh and in other settlements (Fig. 2).

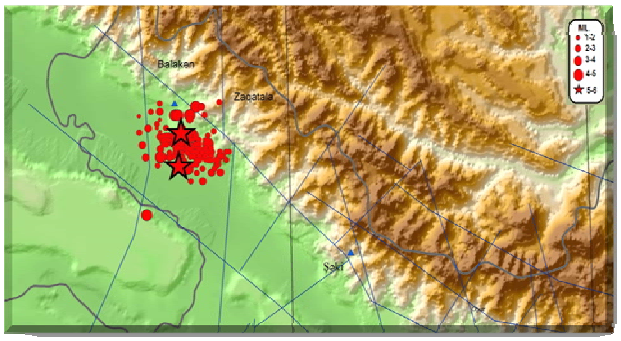

Fig. 2 Map of epicenters of earthquakes in Zagatala district in 07.05.2012

A complete destruction and severe damage of many (hundreds) of residential houses happened in the epicentral zone.

Earthquakes were felt at the epicenter and in nearby settlements with intensity of up to 7-8 points on MSK-64 scale. As a whole, intensity of earthquakes reached 5-6 magnitude in the larger part of the territory of Zagatala, Balakan and Gakh districts.

Isoseismal map was constructed on the basis of immediately collected macroseismic information after earthquakes.

It isn't difficult to note from the form of isoseists that movements, which have resulted in these earthquakes occurred along the Vandam's fault extending in the General-Caucasusian orientation.

Earthquakes were accompanied by numerous aftershocks. 170 aftershocks were noted after the earthquake only in a day, many of which were felt. Eight mobile digital seismic stations (Fig.2) were established at the epicentral zone after 3 days of main shocks that allowed registering all weak aftershocks including large number of microearthquakes in the focal zone ($M_l \leq 2$) (Fig. 3). All aftershocks are located very close and both on lateral and depth (H = 9-20 km). Many of them were quite strong (up to magnitude 4-5) and were felt in the epicentral zone.

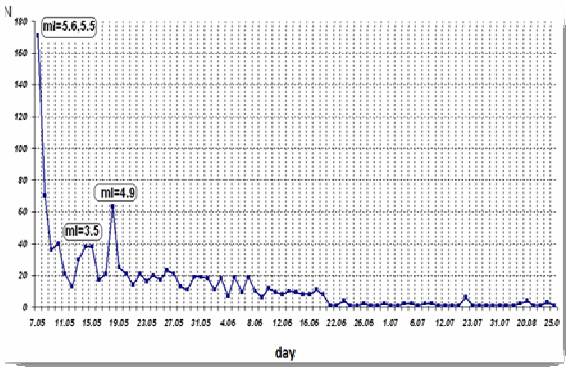

Fig. 3 Distribution of earthquakes' numbers by day in Zagatala district for the period of 07.05-27.08, 2012.

The mechanisms of Zagatala earthquakes' foci were solved according to the data of 31 digital seismic stations of Azerbaijan on "FPFIT" program of "Kinemetrics" system [Reasenberg, 2008]. It was established that left-side movements with strike-slip component occurred in the foci of strong earthquakes. Slip and strike-slip movements were observed at a depth of 10 km in the foci of aftershocks (Fig. 4) [Yetirmishli G.J, 2010, 2013]. Strike-slip movements dominated at a depth of 10-20 km. These results are completely consistent with Agalarova E.B. [Agalarova E.B., 1975] and Aghayeva S.T. [Agayev S.T., 1999] results obtained by analyzes of mechanisms of earthquakes' foci of the Azerbaijani part of the southern slope of the Greater Caucasus.

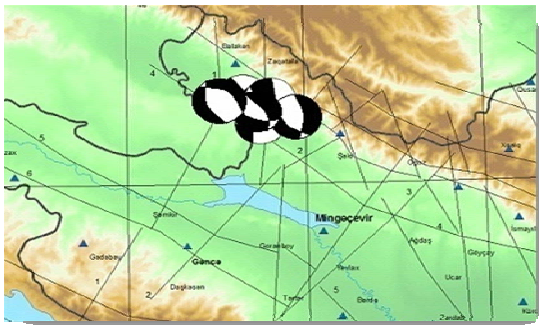

Fig. 4 Mechanisms of earthquakes (ml>4) in Zagatala district

Sheki earthquake

The earthquake occurred in the south-east of Zagatala in Sheki district with an average magnitude (M=4.1) exactly one week later on May 14, 2012 at 09:58:17 on Greenwich time which was felt at the epicenter and nearby settlements and in Sheki with an intensity of 5 on MSK-64 scale.

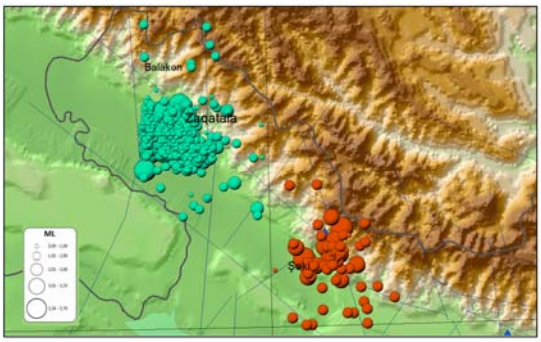

Fig.5 Map of epicenters of earthquakes in Zagatala and Sheki district

In contrast to the strong Zagatala earthquake, after which hundreds of aftershocks occurred, Sheki earthquake was accompanied by a small number of aftershocks.

Ismayilli earthquake

The earthquake of magnitude M=5.3 occurred on October 7, 2012 at 11:42:50 on Greenwich time in Ismayilli district, which was felt at the epicenter and in adjacent districts with an intensity of I=5 on the MSK-64 (Fig. 6).

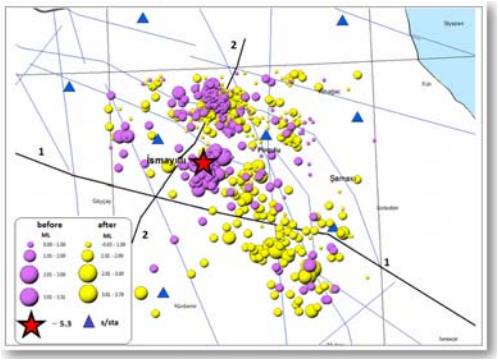

Fig. 6 Map of epicenters of earthquakes in Isamyilli district

We should note that deep location of the earthquake hypocenter caused relatively low intensity of shaking at the epicenter and covered some large territory.

Aftershocks of the earthquake are distributed at the depth interval N = 35 ÷ 45 km; due to great depth few of them were felt on the surface of the Earth.

Balakan earthquakes

Seismic situation in the focus of strong Zagatala earthquake was barely stabilized, when the earthquake of magnitude M=5.6 (that's almost equal to the magnitude of Zagatala earthquake) occurred near to it in Balakan district on October 14, 2012 at 10:13:13 on Greenwich time. Focus parameters on data of seismic stations of Azerbaijan are as follows: φ = 41,66 º N, λ = 46,27 º E, H = 8 km (Fig. 7).

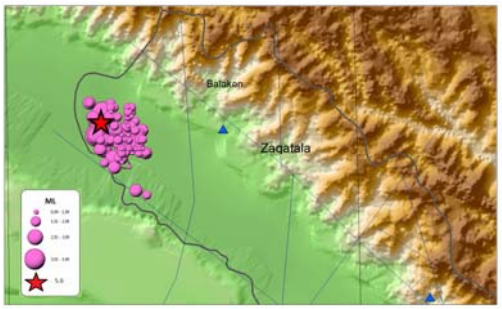

Fig. 7 Map of epicenters of earthquakes in Isamyilli district

The earthquake was felt at the epicenter and also in nearby settlements, as well as in Zagatala and Balakan with an intensity of up to 7 on the MSK-64 scale. Injuries and the destruction of houses happened in the district of the epicenter (Fig. 8).

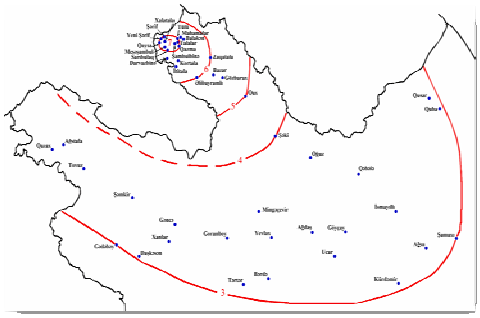

Fig. 8 Macroseismic map of earthquake effects in Balakan district in 2012.

It should be noted that hypocenters of both Zagatala and Balakan earthquakes were shallow, which was reflected in the size of small pleistoseist zones.

Balakan earthquake was preceded by two foreshocks of average strength (M = 4.5 and M = 4.0) for a few hours that were felt with an intensity of 4 on the MSK-64. A large number of aftershocks followed after the earthquake.

Mechanism of the first earthquake was – strike-slip, of the second – left-horizontal strike-slip which is determined by geodynamics of a pair of right-slip faults – Kazakh-Signakh and Ganjachay-Alazani (Fig.9).

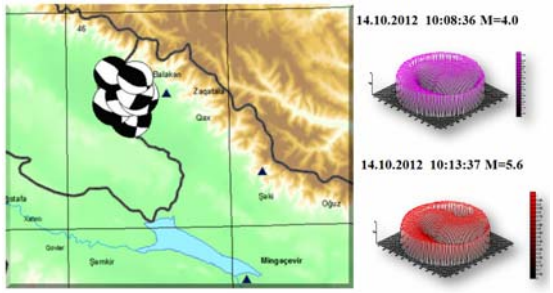

Fig. 9 Mechanisms of earthquakes (M_l>4) in Balakan district

Discussion

Fourier amplitude spectra were built using digital seismograms for shear waves of earthquakes, which gave the possibility of determining the maximum level of the spectrum and upper boundary frequency of maximum level f_0 from values of the amplitude and period of the maximum displacement on the seismogram D. Brunn's classical model was used in calculations. Only records of S-waves at "Zagatala" station were used (Fig. 10). Interval of epicentral distances for the considered earthquakes was equal to Δ = 10-34 km.

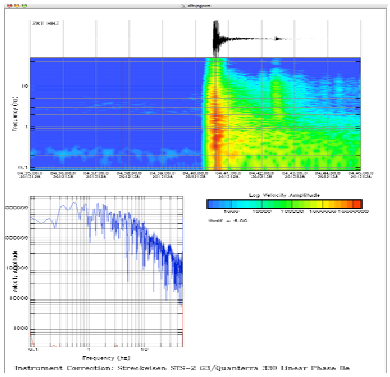

Fig. 10 Frequency response curve of strong Zagatala earthquake.

The following spectral characteristics have been determined: angular frequency f_0, seismic moment M_0, radius of the circular dislocation R, stress drop $\Delta\sigma$, average movement on dislocation D and focus volume V (Tab. 1).

Table. 1. Dynamic parameters of strong earthquake in 2012.

Data	Stantions	Δ, km	f_0, Hz	M_0, 10^{17}, din·sm	M_w	r_0, km	$\Delta\sigma$, 10^{10}din/m^2	D, km	V, km^3
07.05.2012 $t_0=04^h40^m25^s$, φ=41.49, λ=46.60, h=8 km, ml=5.6									
07.05.2012	ZKT	10	5,4	3,0	5,6	0,017	2,54	0,019	0,02
07.05.2012 $t_0=14^h15^m13^s$, φ=41.56, λ=46.62, h=12 km, ml=5.5									
07.05.2012	ZKT	10	5,0	2,0	5,5	0,018	1,33	0,011	0,02
14.10.2012 $t_0=14^h15^m13^s$, φ=41.56, λ=46.62, h=12 km, ml=5.5									
14.10.2012	QZX	10	4.5	3.2	5.6	0.005	0.08	0.02	0.05
	ZKT	15	5.6	3.2	5.6	0.002	3.1	0.02	0.03
	SEK	25	4.3	3.2	5.6	0.002	1.4	0.01	0.03
07.10.2012 $t_0=14^h15^m13^s$, φ=41.56, λ=46.62, h=12 km, ml=5.5									
07.10.2012	IML	11	6	1.1	5.3	0.004	0.64	0.012	0.03
	PQL	15	3	1.1	5.3	0.003	1.6	0.015	0.01
	QBL	34	3.4	1.1	5.3	0.002	2.4	0.012	0.03

Conclusions

The similarity of separate seismoactive zones of the Azerbaijani part of the Greater Caucasus is observed not only in their tectonic conditions but also in the character of seismicity.

The Shamakhy-Ismayilli zone is characterized by high seismic activity. Catastrophic earthquakes with M=6.0-6.9 occurred repeatedly here as a result of which Shamakhy and many surrounding villages were destroyed. Weak earthquakes arise quite often in the Western-Ismayilli part of this zone, however strong earthquakes (M=5.0) also aren't rare here. The last strong earthquake (M=5.0) occurred in 1981, which entailed the destruction of many houses.

Zagatala and Balakan earthquake also confirmed this conclusion. The exception is Ismayilli earthquake which hypocenter depth H = 41 km, whereas PCF is located at a depth of 10-12 km here. We should note that this is not the only earthquake in Ismayilli district with such focus depth. And before that

there were a number of weak and moderately strong earthquakes with hypocenter depth of 40 km. We consider that such anomalous seismotectonic phenomenon for this district is related with a complex fault tectonics of the given area and requires additional researches.

References

Agalarova E.B. A detailed study of the stress state of the seismic regions of Azerbaijan: Abstract PhD diss. M., 1975, 18.

Agaeva S.T. The elastic stress field of seismogenic structures of the southern slope of the Greater Caucasus: Abstract diss. Candidate. geol-min. sciences, Baku, 1999, 25 p.

Yetirmishli G.J., Kazimova S.E., Ismaylova S.S. Comparative analysis of earthquake focal mechanisms of the South Caspian Basin and the continental part of the territory of Azerbaijan. Seismic prognostic monitoring in Azerbaijan. Baku, 2010 p.75-81.

Reasenberg P., Oppenheimer D., FPFIT, FPPLOT, and FPPAGE FORTRAN computer programs for calculating and displaying earthquake fault-plane solutions, Distributed to depository libraries on microfiche, 2008.

Hanks T.S., Kanamori H. A. A moment magnitude scale. J. Geophys. Res. – 1979, 84, № 135, p.2348-2350.

ОСОБЕННОСТИ СЕЙСМИЧНОСТИ АЗЕРБАЙДЖАНСКОЙ ЧАСТИ БОЛЬШОГО КАВКАЗА

Етирмишли Г.Д., Маммадли Т.Я., Казымова С.Э.

Национальная Академия Наук Азербайджана
Республиканский Центр Сейсмологической Службы
Az 1001 Баку,ул.Нигяр Рафибейли, 9,

Аннотация

Статья посвящена сильным Загатальским, Балакенским и Исмаиллинским землетрясениям Азербайджана в 2012 году. Представлен анализ сейсмичности очаговых зон указанных районов - макросейсмические поля, механизмы очагов землетрясений, афтершоковая деятельность очагов сильных толчков, а также геолого-тектонические условия эпицентральных зон. С использованием геодинамической модели пары правосторонних сдвигов дана интерпретация механизмов очага Закатальских землетрясений и установлен механизм общекавказского сброса с левосторонней сдвиговой компонентой. По цифровым сейсмограммам поперечных волн Закатальских землетрясений 07 мая 2012 г. построены амплитудные спектры и вычислены динамические параметры очага.

დიდი კავკასიონის აზერბაიჯანის ნაწილის სეისმურობის თავისებურებანი

გ. ეტირმიშლი, ტ. მამადლი, ს. კაზიმოვა
აზერბაიჯანის მეცნიერებათა ეროვნული აცადემია
სეისმოლოგიური სამსახურის რესპუბლიკური ცენტრი

Journal of Georgian Geophysical Society,
Issue (A), Physics of Solid Earth, v.16a, 2013, pp. 61-68

The geophysical approaches to ground condition assessment in densely populated areas

Durgaryan R., Babayan S., Avanesyan M., Gevorgyan M.

INSTITUTE OF GEOLOGICAL SCIENCES NAS RA

Introduction

It is a common knowledge that the Republic of Armenia, and the Gyumri city, in particular, is located within a seismically active zone. Within such zones, periodically recurring strong earthquakes of varying size (magnitudes) can produce strong ground motions, which may cause increased seismic impacts in the upper strata of the Earth crust. The problem becomes more urgent if there is a case of multiple layers, bedded in versatile layering, and severely inhomogeneous environments. In the meantime, seismic impacts in soft soils can be times stronger than in rocky soils.

In general, information on the seismic effects within the upper section of the Earth crust (30 meters) determined by these and other natural and man-made conditions is presented in detail in the Building Code (Khachian et al., 2006) according to soil classification and seismic zones (baseline value of seismic hazard).

As part of the entire set of investigations, works implemented in this direction were aimed at evaluation of seismic hazard for the master plan of the Gyumri City, accounting for local soil conditions, which would provide sound basis for the activities on seismic risk assessment. To ensure comprehensive and impartial assessment of local soil conditions, we took into account and considered the following databases and work stages (Fig. 1):

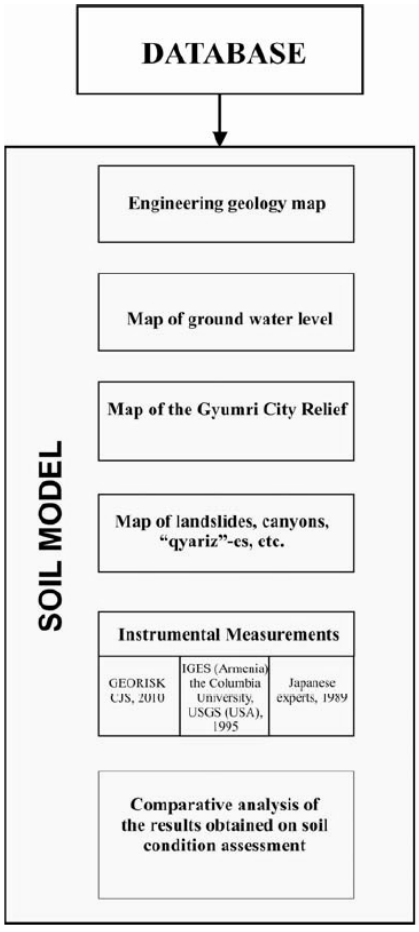

Fig. 1: The strategy of analysis of soil conditions in the Gyumri City

Geology of the Gyumri city area

The Shirak depression is a typical intermountain trough with flat bottom, filled with Quaternary lacustrine, lake-and-alluvial and alluvial sediments that overlie the Akchaghil dolerites, basaltic andesites, various horizons of strongly dislocated deposits of the Miocene, Oligocene,Eocene, Cretaceous and Jurassic. The Shirak Plain and the Akhourian River valley stand out clearly there. The Shirak Plain represents the surface of the same-name depression built with the Early-Middle Pleistocene sediments of Lake Shirak. (Sayadyan Yu. V.2007).The geological structure of the Shirak Depression was studied by many researchers in detail. In particular, Paffenholtz K. N. (Geology of the Armenian SSR, 1964) described the lithological stratigraphic section of the depression in the following way (top to bottom):

1. Alluvial and proluvial formations up to 7.5 m thick;
2. Volcanic tuff of dark color up to 12 m thick;
3. Old alluvial-proluvial sediments (pebblestone, clay, sands) up to 35 m thick;
4. Typical lake sediments represented by clays (sandy in places) with inclusions of pebble, inter-layers of volcanic sand in the form of lenses, diatomite clays and tuff limestones. The overall thickness of the stratum is 250 m.

Engineering geology

From the standpoint of engineering geology, presence of this kind of clayey and sandy-clay unconsolidated and highly plastic sediments, "sandwich"-type inter-layering of strata that have different physical and mechanical properties (Fig. 2), as well as the high level of ground water are among the main factors of the disastrous effect seismic impacts can have within the Gyumri City area, which was demonstrated during both the Spitak earthquake of 1988, and the earthquake of 1926.

Many studies have mentioned the contribution of unfavorable soil conditions and amplification of the seismic effect during the Spitak earthquake (Borcherdt 1989, Yegian 1992, Babayan 2001, Khachyan et al. 2006).

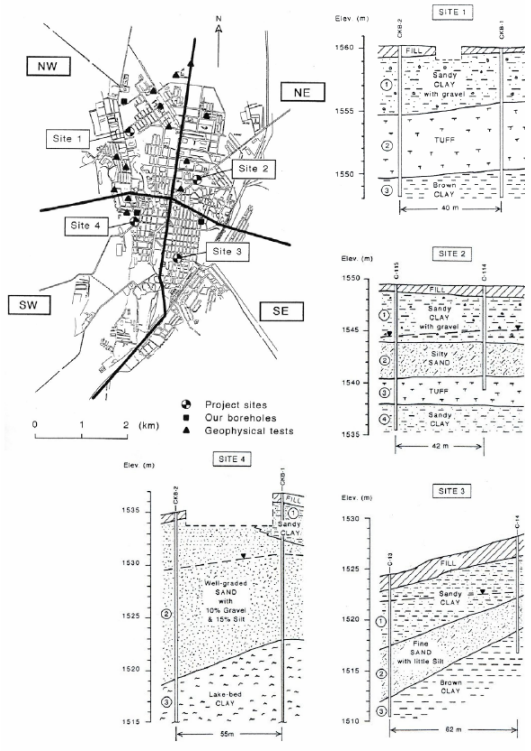

Fig. 2: Geotechnical cross-sections for the four project sites in Gyumri (Yegian 1992)

Hydro-geological conditions

There are two main horizons of ground waters within the Gyumri City area – the supra-tuff and sub-tuff horizons. These waters pour out within central parts of the city at the sites, where tuffs, serving as the confining bed for the supra-tuff water, are common. Large portion of surface and atmospheric water

penetrates into the sub-tuff strata of sandy-clayey and pebble-gravely soils, forming a sub-tuff water horizon, for which lake clays serve as the confining bed. This horizon is up to 15 m thick and is intensively drained within the valleys of the Akhourian River, Gyumri River and Cherkezi-Dzor River. This water horizon feeds also springs and marshes in the city stadium district and the Cherkezi-Dzor, as well as the swamps located in the southern area of the city (IGES, "ArmProyekt", 2001).

Landslide processes and dangerous man-made effects in the area of the Gyumri city

The main landslide effects - soil subsidence and rock falls - are common also over the valley of the Cherkezi-Dzor River, displaying thicknesses of up to 25 m, and vertical displacements up to 20 meters. Some of the landslides are in relatively stable condition, but if water is present, the hazard of landslide activation builds up. Moreover, the over-loading of slopes, construction activities, agricultural use of land on the slopes and their undercutting activate landslide processes sharply (Fig. 3).

Along with landslides, such effects as rock collapses, falls, soil subsidence and other are observed as well. Landslide effects developed mostly in the areas of the so-called Arapi Suite, represented by lacustrine-river deposits, pebble, sands, plastic clays, loams and diatomite clays of Middle-Quaternary age. At some sites, landslide phenomena involve also ignimbrite tuffs of the Yerevan-Leninakan type, overlying the lake and fluvial sediments. In the majority of cases, these processes are represented by regressive block-type or flow-type landslides when displacement develops regressively (landslide head part spreads gradually upwards on the slope).

Landslide effects have activated drastically after the Spitak earthquakes as it had triggered activation of more or less stabilized sites. The uncontrolled land use within these areas, construction and slope loading with various structures, slope undercutting, and the malfunctioning or complete unavailability of drainage systems to provide for surface and ground water run-off has led to a significant increase of the rate of activity of landslide processes and of the potential of development of new areas, where slope effects are manifested.

It is important to note that no engineering protection measures have been actually realized for these areas during the last years. In addition to the listed effects, underground processes related to natural and man-made voids have been observed in Gyumri, in particular, in the central district of the city (Gasparyan, R., Babayan, T.). Periodically, these underground discontinuities manifest themselves in deformation, settlement and destruction of buildings in some parts of the city. The results of geophysical surveys indicate that the area of Gyumri is characterized by very complex and tangled network of the underground infrastructure, the greater part of which corresponds to qyarizes (qavriz, kanat, qanqan and other) (Gasparyan R., 2009).

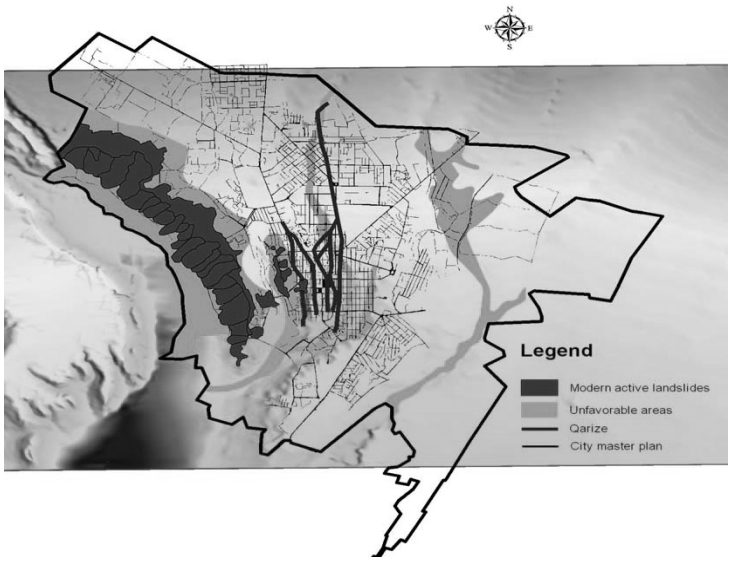

Fig. 3: Map of distribution of landslides and hazardous man-made /anthropogenic/ effects within the area of the Gyumri City

Analysis of the preceding geophysical studies of soils completed for the areas of Gyumri City and the Shirak Depression

The first map of seismic micro-zoning (SMZ) of the Gyumri City area prepared by the Institute of Geophysics and Engineering Seismology (IGES) of the NAS of RA in 1971 was tested by the earthquake of 1988. Detailed study of the Spitak earthquake of 1988 has demonstrated that complex structure of the Shirak Depression determined sharp increase of earthquake size, velocities and duration of seismic shakings, which led to large casualties and high-rate destruction in Gyumri. Apart from this, it is necessary to consider not only the first tens of meters, but also the deeper strata (Khaltourin,1997).

From the standpoint of seismic hazard assessment in seismically active regions it is extremely important to study local soil conditions ("site effect"). Depressions of similar structure in San- Francisco, Mexico, and elsewhere have been studied during many years to assess this kind of effects during earthquakes. Among empirical methods, the most common is the H/V approach known also as the Nakamura method (Nakamura 1989). This method was for the first time proposed by Nogoshi and Igarashi (1971) that had based on the preliminary studies by Kanai and Tanaka (1961). Similar measurements were made also by the Japanese specialists in the Gyumri City area directly after the Spitak earthquake of 1988.

According to the findings of the conducted studies, predominant period values for the central part of Gyumri fall in the range of 0.51-0.64 s (1.5-2.0 Hz) (E. Khachian 2008; Suyehiro S. et al. 1989), and 0.6-0.8 s (1.25-1.6 Hz) (A. Godzikovskaya, Y. Aisenberg, 1989), while during aftershocks predominant soil vibration periods were 0.2-2.5 Hz (0.4-5 s) (Borcherdt et al. 1989). The joint study conducted by the Columbia University, United States Geological Survey (USGS), and the Institute of Geophysics and Engineering Seismology (IGES of the NAS of RA) in 1994 applied the Nakamura method and measured soil vibration spectra, with predominant periods of 2 s (0.5Hz) (Field E. H. et al, 1995). Out of the four measurement sites, Point AGA was the only one located on bedrock, while Points LMD, MAR and SLO were measured within the Shirak Depression.

In 2001, IGES of the NAS of RA prepared the map of seismic micro-zoning of the Gyumri city area where engineering geology, hydrogeology, seismic prospecting and other types of data were used. This map served as the basis for the master plan of Gyumri, it identified zones with different values of peak ground acceleration (0.28 g – 0.56 g) «ArmProyekt», 2001. That map (prepared at the scale of 1:10000) passed through all required stages of getting concurrence, complex expert evaluation and approval, and represents the basic urban development document.

However, according to the new Building Code adopted in 2006 (CH PA II-6.02-2006) the Gyumri city falls within Seismic Zone 3 with estimated seismic hazard level of 0.4g. In 2010, the new concept of seismic safety development adopted in the Republic of Armenia set forth the requirements with respect to application of new approaches and techniques, which necessitated revision of the seismic hazard assessment studies.

In 2010, in the framework of this Project, GEORISK Scientific Research CJS conducted new geophysical surveys aimed at revealing dynamic characteristics of soils within the Gyumri City, considering the requirements of the above legislative acts and norms, as well as the results of earlier studies, and international standards.

Analysis of the obtained results and dynamic characteristics of soils and soil model

Considering dense network of urban development in Gyumri, military and industrial facilities, and other infrastructure available in the city, the Contractor (GEORISK CJS) assessed the situation and found it appropriate to realize geophysical surveys using a multi-channel seismic station (36 observation points) and the method of micro-tremor records (50 observation points) to enable determination of the seismic properties (shear wave propagation velocities, natural periods of soil vibration) within the upper 30 meters section and establishing soil categories (Fig. 4). To record seismic waves, vertical seismic sensors with natural vibration period of 4.5Hz were used. The method of multi-channel analysis of seismic waves (MASW) was applied (Nazarian, S., Stokoe, K., 1983).

In compliance with Subclause 5.3.3, Clause 5.3 of RA Building Code II – 6.02 – 2006, the average V_S value of shear wave propagation velocity and the value of predominant T_0 period for a soil, in case of heterogeneous soil section, are determined theoretically or by testing during engineering-geology surveys and seismological investigations, and values of $V_S/1.3$ and $1.3T_0$ are applied as their estimated values (Khachiyan et al., 2006).

In terms of geology, the upper 6 m-deep layer corresponds to sands and loamy sands, including the soil and vegetation layer, and the second layer includes tuff and has the depth of 6 m. According to the observations made by GEORISK CJS in 2010, these layers are immediately underlain with sands, loamy sands and plastic clays (Fig. 5). The latter can be up to 120 m thick, as attested by the integral analysis of the relevant frequencies of micro-tremors and surface wave propagation results.

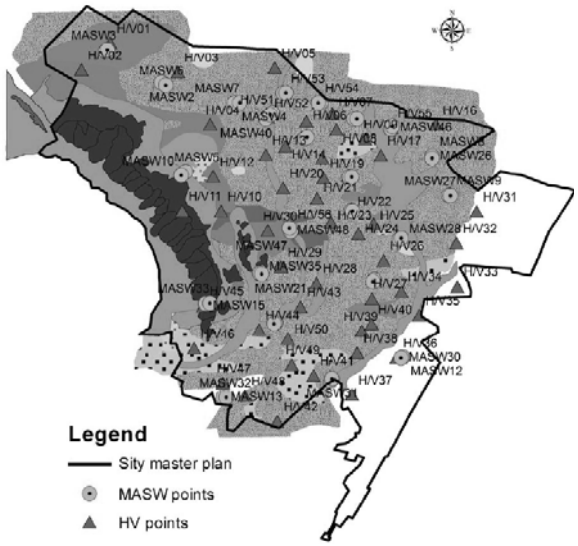

Fig. 4: Locations of geophysical record points (GEORISK-2010) on the map of engineering geology conditions within the area of the master plan of the Gyumri city

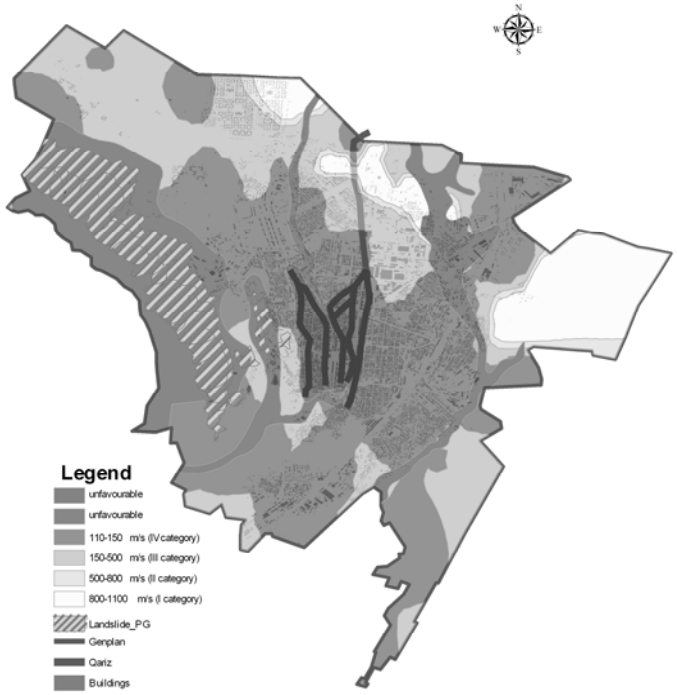

Fig. 5: Model of average velocities of surface wave distribution

As an outcome of the integral analysis of all collected data, the map of distribution of average shear wave propagation velocities over the area of the Gyumri city master plan (general plan) was prepared (Fig. 6).

Considerable share of damages caused by destructive earthquakes worldwide is related to the amplification of seismic waves in the near-surface layers of the Earth crust, which is determined by local soil conditions. Recognizing the above, we conclude that from the standpoint of seismic hazard assessment for seismically active regions, it is extremely important to study local soil conditions. For this purpose, a series of investigations shall be carried out. Among of the empirical methods, most common is the H/V method, named also as the Nakamura method. A few studies carried out based on spectral ratios micro-tremors (Nakamura, 1989; Tenorio, 1997) for hard soils and bedrocks have demonstrated the credibility of these statements SESAME, 2004).

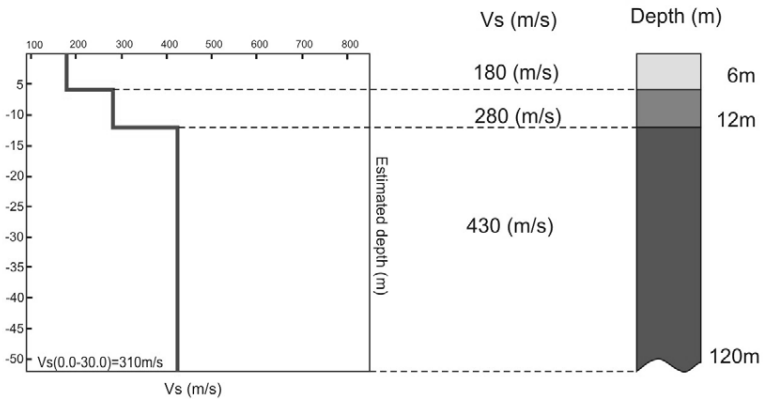

Fig. 6: The map of V_S 30 velocity distribution superimposed with the map of qyarizes, gullies and landslide effects

Site effects associated with local geological conditions are important part of any seismic hazard assessment. Many examples of disastrous earthquake consequences have demonstrated the importance of reliable analytical procedures and hazard calculation methods as well as risk mitigation strategy. In this regard, micro-tremor records with the H/V processing technique, or the Nakamura method, were proposed to help deriving characteristics of local soil conditions – the "site effect" (European research project SESAME). This method proved to be most efficient in assessment of natural vibration predominant periods of Quaternary sediments. The curves of predominant soil vibration periods shown in Fig. 7a and 7b have high rate of matching and reflect predominant periods of natural vibrations of the sedimentary basin and surface layers.

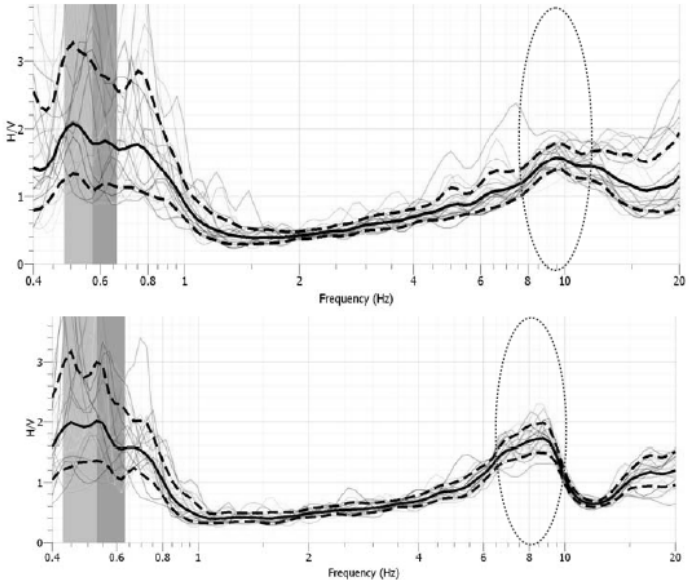

Fig. 7 ab: Characteristic curves of natural vibrations for the soils in Gyumri city (GEORISK 2010)

According to the recommendations of the SESAME Project and the presented consensus results achieved by participants of the European Research Project based on the comprehensive and detailed investigation, the spectral ratios derived by us are characteristic for thick (up to 800 m) sedimentary basins, to which lake-fluvial and lake sediments are corresponding. Based on this example, predominant period F0<1 (Hz) corresponds to natural vibrations of a basin, while F1≈10 (Hz) reflects vibrations of the surface layer. In addition to the dynamic properties of soils, the derformed works enabled us to apply overall analysis of geological and geophysical data to build the model of surface wave propagation average velocities for the Gyumri city area.

Conclusions

1. From the standpoint of seismic hazard assessment for seismically active regions, it is extremely important to study local soil conditions (site effect), and it is necessary to take into account dynamic characteristics of not only the first tens of meters, but also those of deeper layers.
2. The predominant periods of natural vibrations of soils according to the CHPA 2006 document fall in the range of 0.1-3.33 s (0.3-10 Hz), with two distinct sub-ranges of F0<1 (0.45 Hz on average) and 5<F1<10 (7Hz on average).
3. In compliance with the European research project SESAME and worldwide experience, F0 ≈ 0.45Hz corresponds to the natural vibrations of a sedimentary basin, and F1≈7.0 (Hz) is typical for surface layer vibrations.
4. The results of processing of surface wave measurements demonstrated that velocities of surface wave propagation (V_S30) fell in the range of 150-400 m/s (110-310 m/s with allowance for the CH PA 2006).
5. The average characteristic velocity value of 310 m/s was calculated based on the models of propagation of surface waves within the first 30 m section in Gyumri City.

References

1. **Бабаян Т.О.** Сейсмическое микрорайонирование территории города Гюмри. Научно-технический отчет. ИГИС НАН РА, Гюмри, 1977г. и 2001г.
2. **Гаспарян Р.К., Гаспарян В.Р.** Подземные пустоты как факторы обострения геоэкологических условий г. Гюмри, Сборник научных трудов конференции, посвященной 20-летию Спитакского землетрясения. Гюмри.2009г., с. 135-141.
3. Генеральный план г. Гюмри. «Армпроект», Ереван, 2001г. (на арм.яз.).
4. **Халтурин В.., Б.Такер, Л.Двелли.** (1997) Землетрясение неизбежно. Stanford, GeoHazard. С.17.
5. **Хачиян Э.Е., Маркарян Т. Г., Амбарцумян В.А.** "Сейсмостойкое строительство. Нормы проектирования". CHPA II-6.02-2006. Ереван 2006 [Khachiyan E. E., Markaryan, T. G., and Hambartsoumyan, V. A., 2006. Earthquake Engineering: Design Norms, CHPA II-6.02-2006].
6. **Borcherdt, R. D., Glassmoyer, G., Andrews, M., and Cranswick, E**. (1989). Effect of site conditions on ground motion and damage, in Armenia earthquake reconnaissance report, Earthquake Spectra, **5**, 23-42.
7. **Field E. H., Clement A. C., Jacob K. H., Aharonian V., Hough S. E., Friberg P. A.,Babaian T. O., Karapetian S. S.,. Hovanessian S. M, and Abramian H. A.** Earthquake Site-Response Study in Giumri (Formerly Leninakan), Armenia, Using Ambient Noise Observations Bulletin of the Seismological Society of America, Vol. 85, No. 1, pp. 349-353, February 1995.
8. **Nakamura Y.** (1989). A method for dynamic characteristics estimation of subsurface using microtremor on the ground surface, Quaterly Report of the Railway Technology Research Institute, 30, 25–30.
9. **Nazarian, S., Stokoe, K.H., and Hudson, W.R.** (1983) Use of spectral analysis of surface waves method for determination of moduli and thicknesses of pavement systems: Transportation Research Record, 930, 38-45.
10. **SESAME,** (2004), Guidelines for the implementation of the H/V spectral ratio technique on ambient vibrations. Measurements, processing and interpretation, *European Commission – Research General Directorate Project No.EVG1-CT-2000–00026 SESAME*, report D23.

Гефизические методы оценка свойств грунтов в плотно населенных районах

Дургарян, Р., Бабаян, С., Аванесян, М., Геворкян, М.

Абстракт

Целью данной работы является моделирование грунтовых условий в осадочных бассейнах. Для выполнения поставленной задачи были учтены следующие составляющие: геологические условия и структура, уровень подземных вод, антропогенное влияние на грунтовые условия, вторичные геологические эффекты и т.д. Для дополнения имеющейся базы данных, для территории города Гюмри был выполнен комплексный анализ грунтовых условий и проведены новые сейсморазведочные измерения.

Данные новые записи были использованы для изучения структуры пространственной корреляции между скоростями S-волн и доминирующими частотами микротреморов для территории города Гюмри, которая является частью Ширакского осадочного бассейна. Полученные результаты измерений дают представления о масштабах изменения скоростей S-волн внутри осадочных бассейнов, которые имеют важное влияние для дальнейшего построения точной модели и оценки влияния грунтовых условий исследуемой территории.

The geophysical approaches to ground condition assessment in densely populated areas

Durgaryan R., Babayan S., Avanesyan M., Gevorgyan M.

INSTITUTE OF GEOLOGICAL SCIENCES NAS RA

Abstract

The main goals of study are to numerically modeling the effects of local soil conditions in sedimentary basins. Taken in to the consideration other impacts: geological situation and structure, under ground water level, man made effects on ground condition, secondary geological effects and etc. we are generally focused on complex analyses of ground condition. For this case we involved and collecting a dense set of in-situ seismic measurements in Gyumri City to supplement existing knowledge's. We are used this dataset to study the spatial correlation structure of S-wave velocities and microtremors predominant frequencies in the Gyumri City part of Shirak sedimentary basin. These measurements results provide insight into the scale of variation of S-wave velocity within sedimentary basins, which has important implications for how accurately can it be modeled and how the effects of the soil conditions are estimated at different locations.

ნიადაგის თვისებების შეფასების გეოფიზიკური მეთოდები მჭიდროდ დასახლებულ რაიონებში

რ. დურგარიანი, ს. ბაბაიანი, მ. ავანესიანი, მ. გევორქიანი
რეზიუმე

სომხეთის მეცნიერებათა ეროვნული აკადემიის გეოლოგიურ მეცნიერებათა ინსტიტუტი

Journal of Georgian Geophysical Society,
Issue (A), Physics of Solid Earth, v.15a, 2013, pp. 69-76

Block structure of the earth crust of the territory of Armenia

Sergey Nazaretyan[1], Tigran Shahbekyan[2]

1. National Survey for Seismic Protection MES RA, V. Sargsyan str. 5a, Gyumri, Armenia
2. Yerevan State University, A. Manukyan str. 1, Yerevan, Armenia

Introduction

The results of investigations about the block construction of the territory of Armenia in different times by different autors are generalized and some suggestions are given for solution of the problem [1]. Particularly was mentioned that the specialists haven't given any determination for more or less acceptable term "earth crust block", the suggested block schemes were severely different and there wasn't a unit classification for separated blocks, etc. In frame of this study we trying to give the block structure of the territory of RA coming out from the suggestions is done.

To build the block structure scheme of the territory of RA it is necessary to solve at least the following important problems: a) give more or less acceptable determination for the term "block"; b)correct the location and the class of adjacent faults; c) determine the comparable homogeneous fragments of the earth crust that different from the adjacent regions and represent the territory of given block coming out from geological, geophysical, geomorphological, geodynamical data; d) give the classification of the blocks coming out from the class of the adjacent faults, location in tectonic construction, sizes of the block, deep structure, etc; e)taking into account the characteristics of modern movements of the earth crust give the directions and average velocities of movements of the blocks. Let us briefly tern to these problems coming out from the peculiarities of geological structure of RA, existing factual data and in main existing conceptions about the block construction of the earth crust.

By the term **"earth crust block"** we understand the comparable homogeneous fragment of the earth crust bound by faults that by it contracture, including depth contracture, differs from the adjacent regions. Thus in the limits of the block that part of the earth crust is more or less homogeneous by which it differents from adjacent regions. The main condition is that the block of RA necessarily must be bound by faults at least 20kms in depth. So it is important to determine the geometric parameters of the fault: length, angle of fall, width of the fragmentation zone of the fault and types of possible movements, etc. For solution of above mentioned problems the geological, geophysical, geomorphologic**,** tectonic and other data must be used, as only by complex application of the data the reliability of separation of the blocks and their boundaries will arise and it will become possible to use the data on depth constructions of blocks in maximum. The statement of the first question is comparable clear, but the difficulties and complexities connected with the second question are a lot, as the data on depth structure of the earth crust are not enough, their reliability is low, and the idea about stretching of the block into the depth is indefinite, particularly as it concerns to the blocks of low classes.

Materials for separation and investigation of blocks

It is obligatory to use the following data for the territory of RA:

- Maps of regional and local components of gravity, magnetic and geothermal fields with the results of interpretations done by different authors [2-11].
- The results accepted from the seismic stations "Zemlya" and "Cherepakha" interpreted by the method of exchange waves of earthquakes (MEWE), particularly the data of separation of blocks in the structure of the earth crust and vertical movements due to this. It is necessary to use the relief maps of depth layers as

a generalization of those data [4]. These data are important as on the territory of Armenia the seismic researches of sounding haven't been done.

- The maps of separated regional faults built by different methods, particularly by complex geological and geophysical methods [3-12].
- The maps of active regional faults built during the last 20-30years on field observations and the values of movements and velocities by faults [6, 12].
- The GPS and other data about the horizontal movements of the earth crust and the data about the source mechanisms of comparable strong earthquakes and their aftershock zones [13-15].
- The velocity maps of waves built on the records of regional stations by teleseismic methods in different depths of the earth crust and mantle [16, 17].
- The interpretation of results and factual geological, geo morphological data about the structures located nearer to the surface [5, 7, 9, 12].

The separation of the blocks of the earth crust of the territory of RA

Methods and approaches developed by different authors [3-5,7-9,11-13], above mentioned and other data for the structure of the earth crust of the territory of RA are used for solution of the problem.

The faults as the boundaries of the blocks

It is known that in separation of the faults of the territory of RA different specialists have used different initial data and approaches due to those there are serious disagreements about the location of separated faults, their depths, classes, dynamics and other questions, so an attempt was done to give an important place to more or less reliable initial data including the more productive methods of separating of depth faults.

In main the results of analysis of geological material that were approved and accepted by broad masses of specialists were used. Usually the specialists give a special place to geophysical field, which contains information about the depth structure. In that range the data on the faults separated by the method of exchange waves of earthquakes, regional geophysical fields, earthquakes, their depths and source mechanisms, etc. occupy a significant place[2-4,6-9,11-15,18,19]. For separation of the borders of blocks by geological data the structural separation of territorial faults, magmatic and other factual data of sedimentary nature and their tectonic interpretations were used. From the morphological data the distance and field observation data and their results are more important. The great part of geologists separate 3 tectonic zones and Kapan anticliniorium on the territory of RA and adjacent regions as a separate segment. The all specialists as the borders of those zones accept the regional (deep) faults [2-3, 7-12]. As this problem, the following tectonic formation complexes(megablocks): 1) simple folded plate structure of Virahayots-Kapan tectonic complex, 2) compound folded plate construction of Bazum- Zangezur zone, 3) moderate folded plate construction of Araks zone[5]. It is clear that the separated by these and other specialists tectonic units are the block structural elements of the earth crust: mega blocks, blocks of different classes.

The validation of the boundaries between the mega blocks due to the **gravity field** occupies a significant place as it contains information about the peculiarities of blocks and their boundaries. The anomalous gravitation field of the territory of RA with the Bouguer's correction clarifies itself by negative values and represents a part of great gravity minimum of Alpine-Mediterranean zone. The axis of the minimum has north-west direction and coincides with main peaks of Armenian highland. The mentioned gravitation minimum within the bounds of RA by the level of Δg is divided into big marzes (fig.1): South-West, Central, North-East and South-East. Thus the presented region in general is determined by mosaic gravity field. These areas stretch in North-West direction and coincide with the main geological structures. The North-West and South-East marzes are determined by comparable increased values of Δg and coincides with tectonic zones of Virahayots- Kharabakh and Araks (by A. Aslanyan). The Central region is determined by gravitation minimum and coincides with the Armenian region with folded plate construction(A. Gabrielyan).The boundaries of gravitation field of the territory are presented by stretching zones of horizontal gradients with 3-5 mol/km values those greatly coincides with the faults [3,5,7-9,11]. The first three regions are parallel to each other and stretch like an arch from South–East to North–West and the region of the minimum of South-East like a wedge enters into the Central minimum and North–East maximum. The widths of above mentioned anomaly regions make 70-100 kms and their lengths more then some hundred kms (on the territory of RA 300kms and more). The differences of levels of Δg between the regions make about 60-80mGl. Ordinary the appearance of such anomalies is connected with the surfaces of Konrad and Mohorovich, thus the separated gravitation fields have depth character and reveal the depth inhomogeneous state of the earth crust of the territory of Armenia.

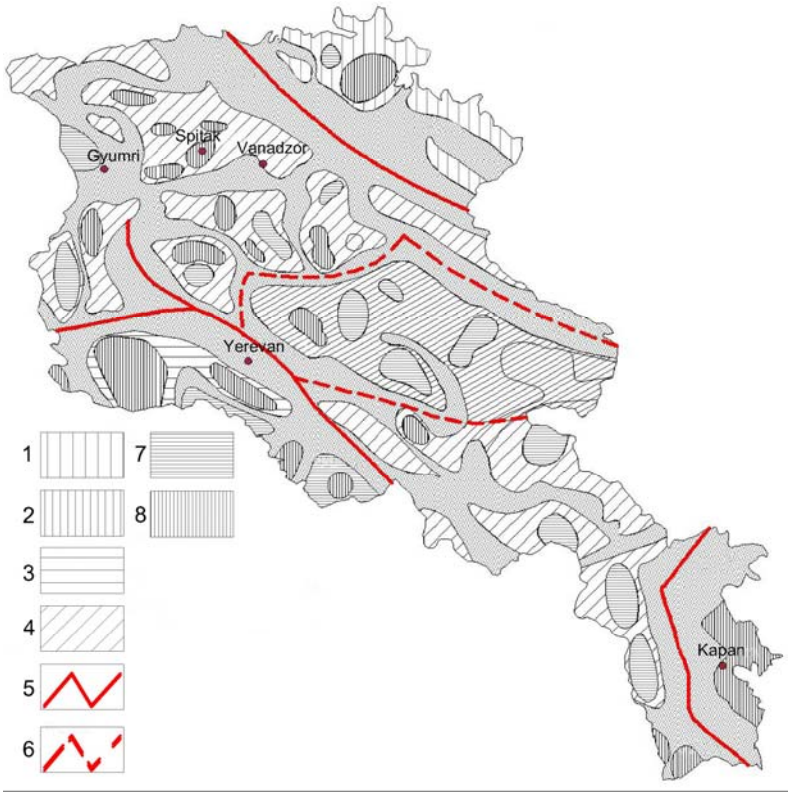

Fig.1. The schematic map of gravity anomalies of the territory RA. Zones with different values of field of the territory: 1-high; 2-not so high; 3-average; 4-low; 5- regional zones stretched by high gradients of field; 6- their axes (by dotted lines are brought the supposed axes). Anomalies of local character: 7-maximums; 8- minimums.

A definite place occupies the determination of boundaries between the mega blocks coming out from the peculiarities of the **magnetic field** of the territory. It is known that on the territory of RA the specialists have separated two severely different zones depend on the strength of anomalous magnetic field, character of changes, sign and morphology: Araks and Sevan [2,8]. By Ts. Hakobyan the boundary between them stretches like an arch in the direction of Hoktemberyan-Yerevan-Vayk-Ordubad line. The application of 1:50 000 scale aero-magnetic maps (the height of the survey makes 80m**)** and the investigations of Z_a by profiles makes possible to correct the boundaries between that zones [8].By this data the boundary mentioned in the South-East stretches in the direction of Nakhichevan- Djugha.

1. The Araks zone includes Ararart and Nakhichevan plains and it is determined by its quiet, near to zero values, without gradient of anomalous magnetic field, where the anomalies with positive sign predominate. The comparable strong, small size anomalies with negative and positive signs were registered in the North–West, where the main structures are covered by volcanic sediment of upper Oligocene–anthropogenic age.

2. The zone nearer to Yerevan includes the all highland of the Lesser Caucasus and by the character of magnetic field is the opposite of the Araks zone. Here strong anomalies of different sizes and signs the values of which reach to some thousand gamms are predominate. But in spite of the complicate character of the Sevan zone it can be divided into three sub-zones that are more precisely separated on aero-magnetic maps, as here the influences of lava sheet and “magnetic relief” is weakened. The sub-zones of magnetic field have total Caucasian stretching and coincide with the main directions of tectonic complexes [2].

The separation of mega blocks by the gradient of geothermal field and values of thermal flow has a definite productivity. The geothermal zonation scheme of the territory of RA built by

R. Mirijanyan is separated into 3 zones [8], those and the zones of gravitation and magnetic fields have a unit Caucasian stretching and coincide with the main tectonic constructions. The coincidence gives us a basis

to consider that there is a connection among the sources of the all fields that makes the block structure. Exclusion makes only the zone of thermal gradient and average values of thermal flow that in main coincides with Kapan Anticlinorium. For the construction of the final scheme of boundaries of blocks the data of movements of the fragments of depth faults divided by seismic waves and by this the movements in vertical direction of the layers of the earth crust[8] and the maps of regional faults constructed on the results of field observations are used [4,8]. To understand on which data the boundaries of blocks were separated in the fig. 2 on corresponding fault in Latin letters are noted the methods and criteria for separation of the blocks. These criteria are known and are presented in the works [8]. It is important to note that the faults are separated by a few groups of criteria.

The following important condition for separating of the blocks concerns to considerable homogeniousity of the blocks of the earth crust, it means that the blocks must have similar structure at the first approach: rocks of the same class, the same considerable depth of layers and crystal basement, strength, etc, by which it generally differs from neighboring blocks. As the depth construction of the territory of RA is investigated in main by the MEWE, gravitation and magnetic, geological methods and the method of upper layers also, so the depth elements located in the depths of 20-30kms are more reliable. More reliable are the location elements of crystal basement of the surface. During the **classification of the blocks** in the first place as the basis were taken more or less accepted schemes of regional plate tectonics of Anatolia-Caucasus-Iran region and attention was paid to the two main parameters: classes of faults, location of the blocks in known tectonic zonation schemes of the territory of RA. The territory of the Republic is located in the collision zone, it means that the mega block can be a high class unit of block structure on the territory of RA, thus the existence of plates, sub-plates and segments is excluded. The mega blocks can be formed of blocks of different classes, as the zones of crash of plates usually are crashed and the amount of separated faults are many and their classes are different [5, 7-8, 10, 12]. The elements of block structure of the earth crust of the territory of RA have definite peculiarities, for example a grate amount of blocks of different class, depth, complex structure of blocks, their movements both vertical and horizontal directions, stiffness of the rocks forming the blocks till the depths of 20-30kms that corresponds to the strength of seismic layer, the differenced parameters of the earthquakes: strength, depth, source mechanism, etc. The separated 3 mega blocks correspond to tectonic zones that are to regional zones of gravitation or magnetic fields (fig.2). For the classification of the blocks of lower classes preference is given to the data expressing the depth construction of the earth crust, particularly to seismic, gravity data and faults and regions bounded by them and we can persist that the blocks of the first class must correspond to the tectonic sub zones or to geological elements: anticlinorium or synclinorium, segment, etc.. In the fig. 2 five blocks of the first class are separated: the three in the second mega block and the two in the third. There isn't an obvious basis for separation of the first class blocks in the first mega block by geological and geophysical data, but it doesn’t mean that the blocks of the first class are absolutely absent here.

The blocks of second class are separated in the all maga blocks. Their amount is 19 blocks. By these data the first mega block is more crashed then the second one.

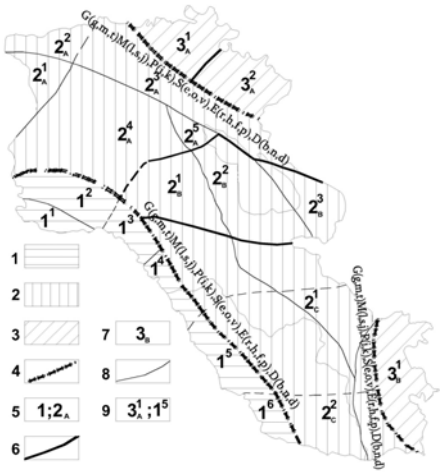

Fig.1 . The scheme of the mega, first and second class blocks of the earth crust of the territory of RA due to complex geological, geophysical data: 1-3 mega blocks; 4- boundaries of mega blocks; 5- numeric display of mega blocks; 6- boundaries of the blocks of first class; 7- numeric display of the blocks of first class; 8- boundaries of the blocks of second class; 9- numeric display of the blocks of second class. On the picture the supposed boundaries of blocks and mega blocks are presented by dotted lines. The criteria of separation of mega blocks, G-gravitation data (g-linear zones of high gradients, m-changes of values of levels of the field, t-changes of directions, shapes, sizes and strengths of local anomalies);M-magnetic data (I- linear zones of high gradients, s-changes of signs of anomalies, t-changes of directions, shapes, sizes and strengths of stretched anomalies); P-geothermal data (i-changes of values of geothermal gradient and thermal flow, k-presence of local anomalies of geothermal gradient and thermal flow);S-Seismological data(e-linear location of the epicenters of strong earthquakes, o-probable faults of the mechanism of source, v–sharp changes of velocities of seismic waves in the earth crust and upper mantle); E- geological data (r-faults nearer to the earth surface, h-linear location of volcanic con, f-sharp changes of formations, p-sharp changes of geo morphological elements);D-data of depth construction (b-sharp changes of the depth of crystal basement, n-gradual changes of depth boundaries of the earth crust, d- changes of strengths of different layers of the earth crust).

Reflection of block construction in the lower levels of the earth crust

During the comparison of the maps of the territory of RA constructed by Mohorovich's surface (built by MEWE data **)** and block structure maps it becomes visible that there is a definite coincidence among the mega blocks, boundaries of the first class and elements of the relief. Those boundaries sometimes coincide to the stretching zones of horizontal gradient of Mohorovich's surface. The data of velocities of seismic waves, which don't include in details the depths of lower earth crust [17] and upper [16] mantle are more or less reliable for investigation of more deep layers of the earth crust of RA. There is a definite coincidence between the mega and first class blocks and anomalies of P waves.

Horizontal movements of the blocks

For this aim the results of observations realized by GPS on the territory of RA and directions of pressing strains defined by different specialists in different time periods in the source zones of the earthquakes with M≥4 are used (fig.3).

By GPS data the all observation points located on different mega blocks and blocks by a very little difference move to North- North- East direction. The velocities of horizontal movements annually make 10-20mms, the velocities of adjacent points those are nearer to the Arabian plate exceed the velocities of the points located in the Northern part of the Republic. If we consider this question for bigger regions, then this regularity in the scale of the Southern Caucasus is more obvious. The directions and velocities of movements of the points during 10 years by GPS observations are stable [14].

The parameters of source mechanisms of the earthquakes with M≥4 for the territory of RA are stable enough. If we take only the directions of pressing axes during those earthquakes, then they also will have an average North – South direction (fig. 3). It is true, that sometimes the pressing vectors of the source deviate from this regularity, but those deviations are not significant, that is obvious from the diagram of pressing axes (fig. 3B). By these data we can't speak about the twist, rise and fall of the blocks. The faults formed during the earthquake of an average strength faults**,** have fall nearer to the vertical direction, and the pressing and stretching vectors have fall in 50-70^0 [15, 18, and 19]. This gives us a basis to suppose that the blocks can move both in vertical and in horizontal directions during the strong earthquakes. It means that the main type of the faults formed during the strong earthquake is strike-slip**,** about which indicate the geological data and the parameters of the mechanisms of strong earthquakes [4, 5-6, 8, 12-13, 15]. The definition of the width of the zone of crash of the fault is more complicated. The specialists think that in this question the data of width of aftershock zone of strong earthquakes are more reliable [6, 11, 18, 19], which directly show the width of the zone of crash. Due to those data the maximal width of the crash zone is 5-8kms.

Conclusions

1. A new scheme for block structure of the territory of RA on which the mega blocks, and the blocks of first and second classes are separated coming out of the geological and geophysical complex data. An attempt to give the general scheme of movements of the blocks and to make conclusions about their dynamics is done. The concept done by different authors that the earth crust of the territory of RA is crashed is confirmed. The widths of mega blocks makes about 80kms and they stretch in general Caucasian direction, and the blocks of first and second classes have limitation in stretching and they are more isometric.
2. The boundaries among the mega blocks: regional faults in main are separated by the all geological–geophysical data and are reliable enough. With some admissions the separated boundaries of blocks of first and second classes are also reliable. The significant part of the boundaries of third class must be corrected by new initial data, in spite of the fact that they were separated by the same approaches and complex data.

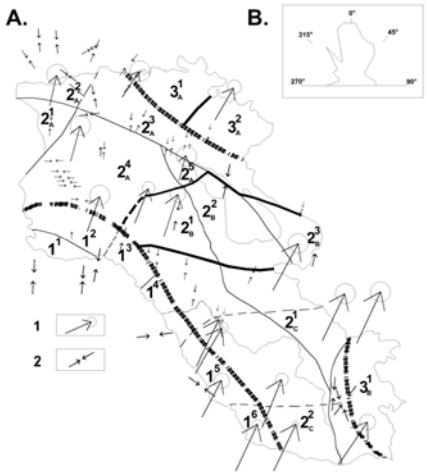

Fig. 3.*Map of block construction of the earth crust of the territory of RA* ***(A)*** *added with some geodynamical data.1- velocity vectors of GSP, the lengths of which correspond to the values of the velocities [18].2- the directions of the pressing strains of the earthquakes sources with M≥4 [12], the separation diagram is presented in the fig.* ***B.***

3. The dominating horizontal movement of the blocks of the territory of RA is in the North-Northeast direction and the pressing strains of the earthquake sources with M=4, 5 in main have North- South stretching. The faults formed during the earthquakes of average strengths have inclination nearer to the vertical direction, and the pressing and tension vectors have inclination of 50-70^0. During the strong earthquakes the blocks can move as in vertical and horizontal directions and the main type of the activated fault is strike-slip. Twisting, damping or other movements haven't been mentioned factually.

4. The data expressing the block structure of the territory have depths nearer to the surface or are located in the depths of 20-30kms, so the above mentioned regularities in the best case concern only to those depths or as it is accepted in seismology to the seismic layers.
5. The earth crust of the territory of RA is crashed very much, and the existing data about the movements and strains give us a basis to suppose that the specialist excluding the possibility of the earthquakes with M>7.5 on the territory of RA are true [5, 11, 15], as in such geological conditions the accumulation of tectonic strains corresponding to that is impossible.

References

[1] Shahbekyan T. About the block structure of the territory of RA. Bulletin of Yerevan State uniwersity, №3, 2013. pp. 12-19(in Armenian).

[2] Akopyan Ts.G. Geological interpretation of the abnormal magnetic field, Geology of Armenian SSR. Geology of Armenian SSR, v. "Geophysics", Publ. NAS PA 1972, 460p. (in Russian).

[3] Aslanyan A.T. Regional geology of Armenia. Publ. Hajpethrat, Yerevan, 1959. 340c. (in Russian).

[4] Badalyan M. S., Kirakosyan A.A., Osipova I.B. Boundaries of the section in crust of Armenia according to seismic data. Proceedings of the NAS RA, Earth Sciences, 1986, I, pp. 42-52 (in Russian).

[5] Gabrielyan A.A. Sargsyan O. A. Simonyan G. P. Seismotectonics of Armenian Soviet Socialist Republic. Publ. In Yerevan State University, Yerevan, 1981, 284p. (in Russian).

[6] Kazaryan A.E. Analysis of seismic condition of the territory of Armenia, as one of the factors for assessment of the current seismic hazard. Proceedings of the NAS RA, Earth Sciences, #2, 2011, pp.29-42 (in Russian).

[7] Meliksetyan B. M., Arkhipov B. K., Kapralo G.P., Meshcheryakov V. B. Features of tectonic-magmatic development and regularities of placement of magmatism and minings in the Southern part of Lesser Caucasus (the messages 1 and 2), Proceedings of the AS Armenian SSR, Earth Sciences, # 6, 1975, pp. 52-66 (in Russian).

[8] Nazaretyan S.N. Deep faults of the territory of Armenian SSR (by geophysical data), Yerevan, Publ. AS Armenian SSR, 1984. p.134(in Russian).

[9] Sargsyan O. A, Volchanskaya N. K., About the block structure of the territory Armenian SSR and the adjacent regions of the Small Caucasus. Publ. AS Armenian SSR, Earth Sciences, #4, 1973, pp. 6-17, (in Russian).

[10] Sargsyan O. A. Paleo tectonic maps of Armenian SSR and adjacent parts of the Small Caucasus for the Alpine stage of development. Pub AS Armenian SSR, Earth Sciences, 1971, #3, pp. 3-22 (in Russian).

[11] Balassanian S., **Nazaretian S., et. al.** The new seismic zonation map for the territory Armenia, Natural Hazards. 15.1997, pp. 231-249

[12] Davtyan V., Doerflinger E., Karakhanyan A., et al. Fault slip rates in Armenia by the GPS data.Publ. NAS RA,Earth sciences, № 2. 2006,

[13] Karakhanyan A., Vernant P., Doerflinger E. etc., GPS constraints on continental deformation in the Armenian region and the Small Caucasus. Tectonophysics, 592 (2013). pp. 39–45.

[14] Robert Reilinger et al. GPS constraints on continental deformation in the Africa-Arabia-Eurasia continental collision zone and implications for the dynamics of plate interactions. Journal of geophysical researches,vol. 111, 2006.pp. 115-134

[15] Nazaretyan S. N., Kirakosyan A.A., Gasparyan V. S., Mikaelyan E.M. The directions of regional sptains in the upper crust of the territory of Armenia and probable active deep faults. Pub. "The geodynamics of the Caucasus", Moscow, "Science", 1989, pp. 165-170 (in Russian).

[16]. **Zakaryan K.A.** About the features of the structure of upper mantle of the Caucasus according to seismological researches. IPE of Academy of Sciences of the USSR, reprinted # 12, 1983. p.14 (in Russian).

[17] Mkrtchyan M. B. Velocities of longitudinal waves in the lower parts of crust of the Small Caucasus according to observations of seismic stations, pub. AS Armenian SSR, Earth Sciences, #.3, 1984, pp. 57-66, (in Russian).

[18] Arefyev S. S. Epicenter seismological researches. Publ.Academical book, 2003, p. 375 (in Russian).

[19] Dorbath L., Dorbath C., Rivera L., Fuenzalida A., Cisternas A., Tatevossian R., Aptekman J. Arefiev S. Geometry, segmentationn and stress regime of the Spitak (Armenia) earthquake from the analysis of the aftershock sequence. Geophys., 108, 1992. pp. 309-328,

Блоковое строение земной коры территории Армении

С.Назаретян, Т.Шахбекян

Резюме

На основе анализа результатов изучения блокового строения земной коры территории Армени разными исследователями геологическими и геофизическими методамы в работе были сформулированы основные нерешенные задачи. Затем, опираясь на комплекс геолого-геофизических данных была составлена новая схема блокового строения, дана классификация блоков. На схеме блокового строения Армении выделены три мегаблока и 19 блоков разного порядка. Границами между мегаблоками были приняты региональные(глубинные) разломы, которые традиционно считаются границами между тектоническими зонами. Эти разломы достаточно надежно выделяются почти всеми фактическими даннымы. С некоторыми допущениями достаточно надежно выделяется также большая часть блоков первого порядка. Границы блоков наинизкого(второго) порядка нуждаються уточнению.

Из рисунка 2 видно, что земная кора территории Армении сильно раздроблена на блоки разного порядка, что характерно зонам колизии тектонических плит. Большинство блоков двигаются на северо-восток со средней горизонтальной скоротью 1-2мм/год. Основной тип подвижок по границам блоков(по разломам) при сильных землетрясениях-взбросо-сдвиг.

Block structure of the earth crust of the territory of Armenia

Sergey Nazaretyan, Tigran Shahbekyan

Abstract

On the base of previous studies analysis of block structure of the territory of Armenia by different researchers the main unsolved problems were formulated. Then according to complex geological-geophysical data the new scheme for block structure was built and the classification of those blocks was done. On the scheme of block structure of Armenia three mega blocks and 19 blocks of different classes are separated. As the boundaries of the mega blocks were accepted the regional (deep) faults that traditionally are considered as the boundaries among the tectonic zones. These faults more reliable are separated almost by the all factual data. The great part of the blocks of first class, with some admissions, are separated more reliable. The boundaries of lower classes (second) must be corrected. From the figures it is visible that the earth crust of the territory of Armenia is crashed into blocks of different classes strongly that corresponds to the zones of collision tectonic plates. The great part of the blocks move to the North- East with average horizontal velocity of 1-2mm/year. The main type of movements by the boundaries of blocks (faults) during the strong earthquakes is strike-slip.

დედამიწის ქერქის ბლოკური აგებულება სომხეთის ტერიტორიაზე

ს. ნაზარეტიანი, ტ. შახბეკიანი

სომხეთის სეისმური დაცვის ეროვნული სამსახური

ერევნის სახელმწიფო უნივერსიტეტი

Journal of Georgian Geophysical Society,
Issue (A), Physics of Solid Earth, v.15a, 2011-2012, pp. 77-87

The Map of Expected Earthquakes Algorithm: Results of 30 Years of Testing and Latest Findings

A.D. Zavyalov
Institute of Physics of the Earth, Russian Academy of Sciences,
Moscow, Russia, zavyalov@ifz.ru

Summary

The Map of Expected Earthquakes (MEE) algorithm was suggested in the mid-1980s by G.A. Sobolev, T.L. Chelidze, L.B. Slavina, and A.D. Zavyalov, the most active members of a special informal team called QCSA (Quick-Look Comparative Seismic Analysis). Over the last 30 years, the algorithm has been tested in a variety of seismically active regions all over the world, including the Caucasus, Kamchatka, the Kopet Dag, the Kyrgyz Republic, Southern California, Northeast and Southwest China, Greece, West Turkey, the Kuril Islands, and New Zealand. The average predictive effectiveness for these regions was J_{MEE}=2.56 and 3.82, with conditional probability value $P(D_1|K)$=70% and 90%, respectively, selected as an alarm level. This being the case, 68% and 41% of predicted earthquakes occurred in the zones with these levels of conditional probability; the area of alarm zones was 30% and 14% of the total area of observations, respectively.

The most recent paper was the first to use the MEE (Map of Expected Earthquakes) medium-term earthquake prediction algorithm to develop maps of expected earthquakes in a classical area with a transient seismic regime, namely the Koyna-Warna reservoir site (India).

The local earthquake catalogue for this area, covering the period of time from 1996 to 2012 (approximately 17 years) and including 4,500 earthquakes with M_L=0-6.5 magnitudes that occurred in the depth range of *H*=0-20 km, was used as the database for this work. Linear dimensions of the seismic area are 40×60 km. Approximately half of all earthquakes included in the catalogue are the aftershocks of earthquakes with $M_L \geq 4$. They were not excluded from the catalogue when calculating time and space distributions of predictor parameters and expected earthquake map values. Magnitude M_c=2.1 selected as a representative magnitude, all subsequent calculations of seismic parameters used all earthquakes with $M_L \geq 2.1$ magnitudes registered continuously starting from 1996 over the entire Koyna-Warna area.

A standard set of seismic predictor parameters (dynamic characteristics) used for expected earthquake mapping of seismically active regions with pronounced tectonic activity was used for the Koyna-Warna area: *b*-value of the magnitude-frequency relationship, number of earthquakes in the form of relative seismic quiescences *Nq* and in the form of seismicity activations *Na*, released seismic energy in the form of energy quiescences *Eq* and in the form of energy activations *Ea*, and density of seismogenic ruptures K_{sf}. Time and space distributions of seismic parameters were calculated in half-overlapping rectangular grid cells ΔX×ΔY. As the base case scenario, we selected the dimensions of a spatial cell equal to 10×10 km. When calculating K_{sf} parameter distributions, the cell dimensions were 5×5 km. The sliding time window value ΔT_c for calculation of current predictive characteristics was selected as ΔT_c=3 years with the shift Δt =3 months.

Earthquakes with $M_L \geq 4.0$ were selected as targets for prediction since they are of interest not only from a scientific point of view, but also from a social and economic point of view. In 1996-2012, 26 such earthquakes and their groups occurred in the area under study. This was enough to obtain retrospective statistical estimates for each precursor used. Among these earthquakes, four groups of events that include earthquakes with $5.0 \leq M_L < 5.5$ were the largest. Seven groups include earthquakes with $4.5 \leq M_L < 5.0$. Unconditional probability of a major earthquake in the grid cell was estimated as $P(D_1)$=0.1698.

Effectiveness of most predictive characteristics *J* for the selected alarm levels turned out to be more than 3, i.e. these characteristics can be regarded as *"quite useful"*. For just one characteristic (*Ea*), effectiveness was about half as much and equal to *J* =1.58, which is classified as *"useful"*.

A series of 42 expected earthquake maps was developed for the Koyna-Warna area, from 1 July 2002 till 1 October 2012, with 3-month step and 2-year prediction periods for each map. The findings of using the

MEE algorithm in a classical area with a transient seismic regime for the first time were very encouraging. They showed that its prediction reliability was quite high and equal to J_{MEE}=2.76. Zones with conditional probability levels $P(D_1|K)$≥90% experienced 56.3% of all earthquakes with M_L ≥4.0. The alarm area was 20.4±8.4% of the total area of observations. The MEE algorithm was particularly efficient in predicting the largest earthquakes in the Koyna-Warna area that occurred during the retrospective prediction period. At a later stage, more accurate adjustment of algorithm parameters may improve the overall prediction reliability.

The prediction can be verified in real time using the most recent expected earthquake map in the series for the period from 1 October 2012 to 30 September 2014.

Therefore, integral predictive reliability estimates obtained when the MEE algorithm was used for the Koyna-Warna reservoir site are close to the average values of these parameters for all previous seismically active regions. These findings may be considered proof of the flexibility of the proposed algorithm.

Introduction

In the mid-1980s, an informal research team called the Quick-Look Comparative Seismic Analysis (QCSA) Team was formed at the Institute of Physics of the Earth (IPE) in the USSR Academy of Sciences. The team was headed by G.A. Sobolev and had no permanent members. At different times, the members of the team were:

From IPE of the Russian Academy of Sciences (RAS): *Gennady A. Sobolev, Lidia B. Slavina, Alexey D. Zavyalov, Elizaveta N. Sedova, Evgeny A. Rogozhin, Andrey A. Nikonov, Timur T. Tagizade.*

From the Institute of Geophysics (Georgia): *Tamaz L. Chelidze, Tamaz Pilishvili, Rusiko Khelashvili, Vano E. Nikoladze, Lali Kakhiani, Lali Labadze, Yury M. Kolesnikov.*

The task of the team was to develop methodology for mapping areas where major earthquakes are most likely to occur, using time and space distributions of various geological and geophysical data. After several years of work, the team developed an algorithm that was later called the Map of Expected Earthquakes (MEE).

By the earthquake prediction algorithm we shall mean a sequence of actions to distinguish unique characteristics or abnormal changes in various geological and geophysical fields, and study and analyze them all to determine the location, intensity, and time of an earthquake.

The MEE algorithm is based on the concept of destruction of the geological environment as a self-similar and self-organized system of different-scale rock blocks. Based on the kinetic concept of strength in solids, the authors developed images of abnormal behaviour for different seismological parameters (precursors) before major (M≥5.5) earthquakes. The MEE algorithm uses the principle of space-time scanning of the earthquake catalogue within the seismically active region under study. Using the Bayesian approach, maps of conditional probability distribution $P(D_1|K)$ for a potential major earthquake in each space-time cell were calculated. These maps were called the Maps of Expected Earthquakes.

Over the last 30 years, the algorithm has been tested in a variety of seismically active regions all over the world, including the Caucasus, Kamchatka, the Kopet Dag, the Kyrgyz Republic, Southern California, Northeast and Southwest China, Greece, West Turkey, the Kuril Islands, and New Zealand. The average predictive effectiveness for these regions was J_{MEE}=2.56 and 3.82, with conditional probability value $P(D_1|K)$=70% and 90%, respectively, selected as an alarm level. This being the case, 68% and 41% of predicted earthquakes occurred in the zones with these levels of conditional probability; the area of alarm zones was 30% and 14% of the total area of observations, respectively.

This paper also presents the results of developing maps of expected earthquakes for the Koyna-Warna reservoir site. The site is interesting for the reason that it was considered aseismic prior to the construction of the Koyna Dam in the north (Fig. 4) and reservoir filling (started in 1961); therefore, no instrumental seismic observations were conducted in the area. However, on 10 December 1967 a devastating earthquake with M_L=6.5 hit the area. The earthquake later named the Koyna Earthquake was a classic example of an earthquake triggered by human activity. The same happened again when the Warna Dam was constructed (to the south of the Koyna Dam) and its reservoir was filled (filling started in 1985). Therefore, seismic activity has been observed in the region for almost 50 years and seismic observations have been underway.

The Koyna-Warna area has a transient seismic regime, with such important features as short duration of the observation period, a small area under study and, therefore, a small number of seismic events in the catalogue. During our work, we managed to overcome the challenges associated with a relatively short period of instrumental observations and a small number of earthquakes in the catalogue. This work was done for the first time. Before that, maps of expected earthquakes were developed only for seismically active regions with pronounced tectonic activity, such as continental margins, island arcs, subduction zones, etc.

Examples of MEE Algorithm Applications in Various Regions

Kamchatka. The regional earthquake catalogue for 1962-2012, prepared by the Kamchatka Branch of the Geophysical Survey of RAS was used to compile maps of expected earthquakes in Kamchatka. The catalogue includes almost 180 thousand earthquakes with energy classes K =0-16.1 that occurred in the depth range of H=0-701 km. K_{rep} =9.5 is the representative energy class of earthquakes. H=0-100 km was selected as the hypocenter depth range for earthquakes included in MEE calculations. Approximately 16,300 events were included in the working catalogue of representative earthquakes with $K_{rep} \geq 9.5$ that occurred in the depth range of H=0-100 km during 1962-2012. The energy class of major earthquakes, i.e. prediction targets, was selected equal to $K_{pr} \geq 13.5$ ($M_{pr} \geq 6.0$).

Fig. 1 shows one of the maps of expected earthquakes in Kamchatka with the prediction period from 1 January 1997 to 31 December 2002. All earthquakes with $K_{pr} \geq 13.5$ that occurred during this time interval are plotted on the map. Most of these earthquakes originated in zones where levels of conditional probability were higher than 50%. The results of the retrospective prediction for Kamchatka for the entire period of observations are summarized in Table 1. The total number of earthquakes with the corresponding energy range is given in brackets.

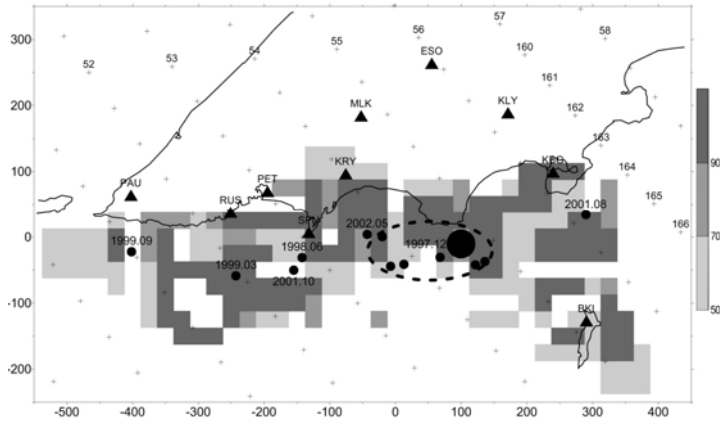

Fig. 1. Map of expected earthquakes (map of conditional probability distribution) in Kamchatka for the period from 1 January 1997 to 31 December 2002. The map shows epicenters of earthquakes and their groups with $K_{pr} \geq 13.5$ that occurred during the MEE validity period (6 years). The size of circles is proportional to the length of rupture in the earthquake source on the map scale. The dashed ellipse indicates a group of earthquakes that occurred on 5-7 December 1997. The legend in conditional probability terms is shown on the right. The dimensions of a square elementary cell are 25×25 km.

Table 1. Retrospective Prediction Results for the MEE Algorithm in Kamchatka

Energy class range	Conditional probability level, $P(D_1 \mid K)$		
	50 %	**70 %**	**90%**
$K \geq 15.5$	1 (2)	1 (2)	**1 (2)**
$14.5 \leq K < 15.5$	5 (7)	4 (7)	**2 (7)**
$13.5 \leq K < 14.5$	38 (46)	35 (46)	**26 (46)**
Total:	44 (55)	40 (55)	**29 (55)**
J_{MEE}	2.30	3.17	**3.27**

The Kuril Islands. Fig. 2 shows an example of a map of expected earthquakes for the Kuril Islands area with the prediction period from 1 October 2006 to 30 September 2010 covering the series of Simushir earthquakes in November 2006 (M=8.3) and January 2007 (M=8.2). In this case,

we used the data from the regional earthquake catalogue for 1962-2009, prepared by the Sakhalin Branch of the Geophysical Survey of RAS for calculation purposes. K_{rep} =9.5 is the representative energy class of earthquakes. *H*=0-100 km was selected as the hypocenter depth range for earthquakes included in MEE calculations. Approximately 18 thousand events were included in the working catalogue of 1962-2009. The energy class of major earthquakes, i.e. prediction targets, was also selected equal to K_{pr} ≥13.5 (M_{pr} ≥6.0). As can be seen from Fig. 2, most of the earthquakes K_{pr} ≥13.5 originated in the zones where levels of conditional probability were higher than 50%.

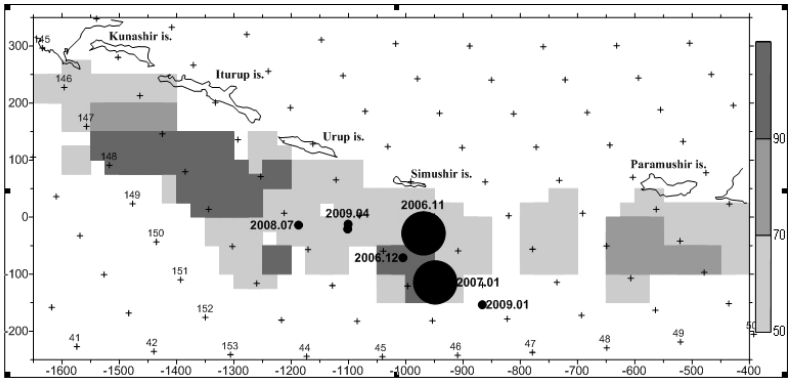

Fig. 2. Map of expected earthquakes in the Kuril Islands for the period from 1 October 2006 to 30 September 2010. The map shows epicenters of earthquakes and their groups with K_{pr} ≥13.5 that occurred during the MEE validity period (4 years). The other symbols are the same as in Fig. 1.

New Zealand. The regional earthquake catalogue for 1980-2010, compiled by GeoNet Project (http://www.geonet.org.nz/), with a total of some 400 thousand seismic events, was used for MEE calculations. According to preliminary analysis, the representative magnitude for this catalogue is M_{rep} =3.5 for the entire period of observations and for the most part of the seismically active region. *H*=0-50 km was selected as the depth interval. The working catalogue included almost 20 thousand representative earthquakes. Earthquakes with magnitudes M_{pr} ≥5.5 were the prediction target. Fig. 3 shows one of the maps of expected earthquakes in New Zealand with a prediction period from 1 January 2006 to 31 December 2010. Table 2 contains retrospective prediction data for New Zealand for the whole series of maps of expected earthquakes.

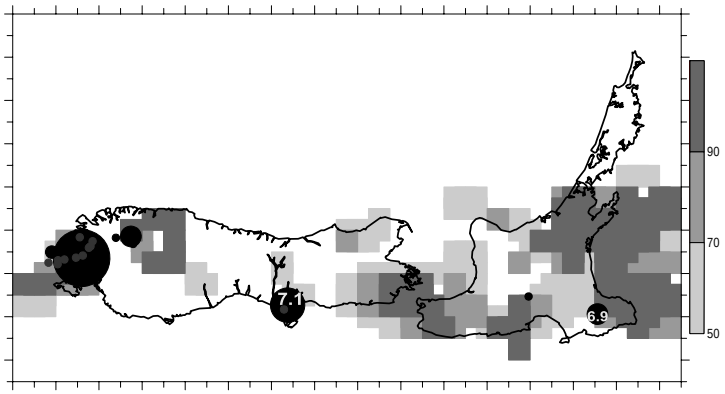

Fig. 3. Map of expected earthquakes in New Zealand for the period from 1 January 2006 to 31 December 2010. The map shows epicenters of earthquakes and their groups with M_{pr} ≥5.5 that occurred during the MEE validity period (5 years). The dimensions of a square elementary cell are 50×50 km. The other symbols are the same as in Fig. 1.

Table 2. Retrospective Prediction Results for the MEE Algorithm in New Zealand

Magnitude range	Conditional probability level, $P(D_1\|K)$		
	50 %	**70 %**	**90%**
$M \geq 7.0$	5 (5)	4 (5)	**4 (5)**
$6.5 \leq M < 7.0$	4 (4)	4 (4)	**4 (4)**
$6.0 \leq M < 6.5$	10 (11)	10 (11)	**8 (11)**
$5.5 \leq M < 6.0$	16 (20)	16 (20)	**13 (20)**
Total	35 (40)	34 (40)	**29 (40)**
J_{MEE}	1.40	1.79	**2.76**

Koyna-Warna reservoir site. Let us discuss in detail how maps of expected earthquakes for this region are compiled and analysed.

Input Data and Selection of Parameters

The local earthquake catalogue for the Koyna-Warna area covering the period from 1996 to 2012 (approximately 17 years) and including 4,500 earthquakes with M_L=0-6.5 magnitudes that occurred in the depth range of H=0-20 km was used as the database for this work. Linear dimensions of the seismic area are 40×60 km. Approximately half of all earthquakes included in the catalogue are the aftershocks of earthquakes with $M_L \geq 4$. These aftershocks were not excluded from the catalogue when calculating time and space distributions of precursor parameters and expected earthquake map values. With M_c=2.1 selected as a representative magnitude, all subsequent calculations of seismic parameters used all earthquakes with $M_L \geq 2.1$ magnitudes registered continuously starting from 1996 over the entire Koyna-Warna area. Average location errors were approximately 1 km for epicenters and 3 km for hypocenters.

A standard set of seismic predictor parameters (dynamic characteristics) used for expected earthquake mapping of seismically active regions with pronounced tectonic activity was used for the Koyna-Warna area: *b-value* of the magnitude-frequency relationship, number of earthquakes in the form of relative seismic quiescences *Nq*, number of earthquakes in the form of seismicity activations *Na*, released seismic energy in the form of energy quiescences *Eq*, released seismic energy in the form of energy activations *Ea*, and density of seismogenic ruptures K_{sf}. Each of these parameters and their mathematical definitions are described in detail in [2]. All dynamic predictor characteristics, excluding concentration of seismogenic ruptures K_{sf}, which has a cumulative nature and is a threshold value, were represented as time and space distributions of abnormal deviations from the respective long-term (background) levels scaled to the root-mean-square error of its definition (the so-called ξ-parameter). Time and space distributions of seismic parameters were calculated in half-overlapping rectangular grid cells ΔX×ΔY. As the base case scenario, we have selected the dimensions of a spatial cell equal to 10×10 km. When calculating parameter distributions of K_{sf}, the basic cell dimensions were 5×5 km. The sliding time window value ΔT_c for calculation of current predictive characteristics was selected as ΔT_c=3 years with a shift Δt =3 months.

Since there were no data on static predictor characteristics (that vary very little during the seismic cycle) for the Koyna-Warna area, they were not used for this paper. The MEE calculation methodology allows for such an approach.

In 1996-2012, 26 earthquakes and their groups with magnitudes $M_L \geq 4.0$ occurred in the area under study (Table 3). Prediction of earthquakes in this magnitude range is of interest both from a social and economic point of view and a scientific point of view and their number is large enough to draw statistical conclusions. Among these earthquakes, four groups of events that include earthquakes with $5.0 \leq M_L < 5.5$ were the largest. Seven groups include earthquakes with

4.5≤M_L<5.0.

Calculation of Retrospective Statistical Characteristics for Seismic Regime Parameters

Retrospective statistical characteristics for precursor parameters were calculated for different alarm levels set by the researcher; after that, experts selected the values at which prediction reliability (i.e. the ratio of the average density of major earthquake flow during alarms (or in the alarm area) to their average density during the period of observations (or in the area of observations) for a specific precursor best matched the objective: either the largest number of predicted earthquakes over quite a long alarm time or the smaller number of predicted major earthquakes over a short alarm time (strategy by G.M. Molchan). The calculations were performed as described in [2]. Table 4 shows retrospective statistical characteristics for precursors with alarm levels selected by the expert for use in subsequent calculations. Note that reliability of most predictive characteristics *J* for the selected alarm levels proved to be more than 3, i.e. these characteristics can be regarded as *"quite useful"* (see Table 3.2 in [2]). For just one characteristic ξ_{ea}, reliability was about half as much and equal to *J*=1.58, which is classified as "*useful*".

The results of using each characteristic to predict earthquakes with M_L ≥4.0 at the Koyna-Warna reservoir site are summarized in Table 3.

Table 3. Retrospective Prediction Results for Earthquakes with M_L ≥4.0 that occurred in the Koyna-Warna Area from 1 January 1996 to 30 November 2012

No.	Date	Time	Geographic coordinates, grad.		Depth, km	Magnitude	Prognostic feature					
			Lat.	Lon.	*H*	M_L	*b*	*Nq*	*Na*	*Eq*	*Ea*	K_{sf}
1	1996.04.26	12:19:32	17.17	73.71	7	4.4						
2	1997.04.25	16:22:53	17.35	73.76	3	4.4						
3	1998.02.11	01:08:47	17.17	73.77	6	4.3						+
	1998.02.14	00:59:49	17.15	73.73	10	4.2						+
4	1999.06.07	15:45:01	17.27	73.76	2	4.7			+			+
5	**2000.03.12**	**18:03:54**	**17.20**	**73.72**	**12**	**5.2**		+	+		+	+
6	2000.04.06	22:30:12	17.14	73.67	2	4.8						
7	**2000.09.05**	**00:32:43**	**17.20**	**73.77**	**14**	**5.3**		+				+
8	2000.12.08	13:23:05	17.11	73.74	7	4.1		+	+	+		+
9	2001.05.17	16:04:27	17.19	73.74	8	4.0			+		+	
10	2001.08.02	04:08:52	17.13	73.76	5	4.0		+	+	+		+
11	2003.03.27	06:18:23	17.34	73.79	8	4.1			+		+	
12	**2005.03.14**	**09:43:48**	**17.14**	**73.76**	**3**	**5.0**	+	+	+	+	+	+
	2005.03.15	**02:07:07**	**17.18**	**73.76**	**10**	**4.2**	+	+	+		+	+
	2005.03.26	**00:56:36**	**17.16**	**73.77**	**2**	**4.0**						
13	2005.06.07	21:32:06	17.24	73.72	14	4.2	+	+	+		+	+
14	2005.08.30	08:53:17	17.19	73.79	5	4.5						+
15	2005.11.20	18:50:41	17.20	73.76	5	4.0						+
16	2005.12.26	10:46:05	17.16	73.76	12	4.2						+
17	2006.04.17	16:39:59	17.16	73.77	8	4.6			+			+
18	2007.08.20	19:15:53	17.18	73.78	2	4.0			+		+	+
19	2007.11.24	10:57:48	17.14	73.79	9	4.3	+		+		+	+
20	2007.11.24	11:35:45	17.12	73.7	5	4.0		+			+	+
21	2008.07.29	19:10:51	17.31	73.74	4	4.2						+
22	2008.09.16	21:47:13	17.31	73.72	14	4.8						
23	2009.11.14	13:03:34	17.14	73.79	4	4.7	+	+	+		+	+
	2009.11.14	13:34:35	17.12	73.78	3	4.0						+
24	**2009.12.12**	**11:51:25**	**17.13**	**73.78**	**5**	**5.1**			+			+
	2009.12.12	**16:25:41**	**17.16**	**73.8**	**12**	**4.3**	+				+	+
25	2009.12.23	03:49:29	17.12	73.78	3	4.0						
26	2012.04.14	05:27:41	17.33	73.74	12	4.8		+		+		+
Total number of predicted earthquakes, *N*pr							**6 (23)**	**10 (23)**	**14 (23)**	**4 (23)**	**11 (23)**	**23 (26)**
Total number of predicted earthquakes in %%							**26.1**	**43.5**	**60.9**	**17.4**	**47.8**	**88.5**
M_L≥5.0							**2 (4)**	**3 (4)**	**3 (4)**	**1 (4)**	**3 (4)**	**4 (4)**

4.5≤M_L<5.0	**1 (7)**	**2 (7)**	**2 (7)**	**1 (7)**	**1 (7)**	**4 (7)**
4.0≤M_L<4.5	**2 (12)**	**4 (12)**	**7 (12)**	**2 (12)**	**6 (12)**	**11 (15)**

Note: The total number of earthquakes with the corresponding magnitudes is given in brackets.

The analysis of the table suggests the following conclusions:

1. Only one group of earthquakes (No. 12), which consisted of 3 events with the largest one having a magnitude of M_L=5.0, was preceded by abnormal, statistically significant values of all six predictive characteristics.
2. Of the total number of earthquakes, only 5 earthquakes (No. 1, 2, 6, 22, and 25) were not preceded by any anomalies in any of the characteristics.
3. All four groups of earthquakes with the largest events with M_L≥5.0 were preceded by anomalies in a number of characteristics.
4. Of all predictive characteristics, density of seismogenic ruptures K_{sf} is the most successful in terms of the number of predicted earthquakes. Using this characteristic, 88.5% of earthquakes with M_L≥4.0 were predicted.

Validity of a map of expected earthquakes obtained by averaging expectation times for all 6 characteristics ξ_b, ξ_{nq}, ξ_{na}, ξ_{eq}, ξ_{ea}, K_{sf}, with the selected alarm levels, is ΔT_{MEE} =2.13□0.94 years, whereas the expectation area for an earthquake with M_L≥4.0 is S_{1exp} =152□17 km^2 (Table 4).

Table 4. Retrospective statistical characteristics for predictive characteristics before earthquakes with M_L≥4.0 that occurred in the Koyna-Warna area from 1 January 1996 to 30 September 2012

Parameter K_i	Alarm level	Probability of detection $P(K_i\|D_1)$	Probability of false alarm $P(K_i\|D_2)$	Average expectation time, year $T_{exp} \pm \sigma_t$	Average expectation square, km^2 $S_{exp} \pm \sigma_t$	Real number of predicted earthquakes	Number of false alarm / Number of missed targets	Effectiveness of prediction in time J_t
ξ_b	+2.0σ	0.1190	0.0211	1.5±1.1	133±26	6	10/71	3.84
ξ_{nq}	-2.0σ	0.2024	0.0227	1.8±2.2	133±47	10	2/66	5.39
ξ_{na}	+2.0σ	0.3929	0.0100	2.6±2.5	164±40	14	0/45	4.78
ξ_{eq}	-1.2σ	0.1310	0.0358	1.9±1.7	175±61	4	3/71	3.41
ξ_{ea}	+1.5σ	0.2500	0.1431	3.8±3.0	145±42	11	13/59	1.58
K_{sf}	11.7	0.5684	0.1508	1.2±1.1	161±50	23	35/41	2.92

Note: Grid size: 10×10 km for ξ_b, ξ_{nq}, ξ_{na}, ξ_{eq}, ξ_{ea} parameters and 5×5 km for K_{sf} parameter.

Calculation of Unconditional Probability of a Major Earthquake

To calculate the unconditional probability of a major earthquake in a spatial cell with the selected dimensions, data on major earthquakes (and their groups) that occurred in the area under study during the period of observations are used (Table 3). In this case, spatial cells must not be ***overlapped*** (they must be ***independent***). Each seismic event (or a group of events) is represented by a certain nucleation area where typical changes in geophysical fields are observed, rather than by a single point corresponding to the hypocenter. The average major earthquake expectation area can be taken in a first approximation for a set of predictive characteristics as an estimated area of earthquake nucleation. Then the average number of major earthquakes and their groups that occur in the expectation area during the expectation time (period of MEE validity) will be equal to

$= (S_1 \exp^{\uparrow}\kappa)/S_1 obs \cdot (\Delta T_1 \mathrm{MEE})/T_1 obs \cdot N_1 tot$, where N_{tot} is the total number of major earthquakes and their groups; T_{obs} is the period of observations during which N_{tot} events occurred; S_{obs} is the area of observations where N_{tot} events occurred. We will call λ the major earthquake flow intensity.

If we assume that the flow of major earthquakes obeys the Poisson distribution (and this is enough in a first approximation), then the unconditional probability of ***one*** major earthquake occurring in the expectation area during the expectation time will be equal to $P(D_1) = \lambda \exp(-\lambda)$ [1]. Therefore, $P(D_2) = 1 - P(D_1)$ is the probability of an earthquake not occurring. The resultant unconditional probability of a major earthquake $P(D_1)$ is assigned to each spatial grid cell. In our case, if we substitute the required parameter values, we obtain $P(D_1)$=0.1698. Then $P(D_2)$=0.8302. $P(D_1)$ values were assigned to each rectangular cell of the grid covering the area under study.

Calculation and Initial Analysis of Maps of Expected Earthquakes for the Koyna-Warna Area

All conditional probability values $P(D_1|K)$ for all spatial grid cells was called the Map of Expected Earthquakes for a period of time $[t_0, t_0+\Delta T_{\mathrm{MEE}}]$, where ΔT_{MEE} is the MEE validity. It is assumed that the occurrence of a major earthquake in this time interval is equally probable. However, it is appropriate to mention here the work by M.O. Kutsenko and A.D. Zavyalov [3] which shows that the occurrence of earthquakes in different one-year expectation time intervals is not equally probable. As it turned out, major earthquakes are most likely to occur during the first years after the precursor appears. The possibility of a major event was 25% during the first year and more than 70% during the first 5 years for almost all precursors. Please note that this work was based on data from tectonic earthquake catalogues from different seismically active regions of the world.

A series of 42 expected earthquake maps was developed for the Koyna-Warna area, from 1 July 2002 to 1 October 2012, with 3-month shift and 2-year prediction periods for each map. The period from 1 January 1996 to 30 June 2002 (6.5 years) was used to train the algorithm; therefore, the earthquakes that occurred during this period were not included in the assessment of retrospective prediction results and MEE algorithm effectiveness. The prediction can be verified in real time using the most recent map in the series with the prediction period from 1 October 2012 to 30 September 2014 (Fig. 4). As can be seen from Fig. 4, two areas are the most hazardous: one of them is located to the south of the Koyna Dam and the other, which is larger, is located to the north of the Warna Dam. At present, we do have no data available on earthquakes with $M_L \geq 4.0$ that occurred in the area under study.

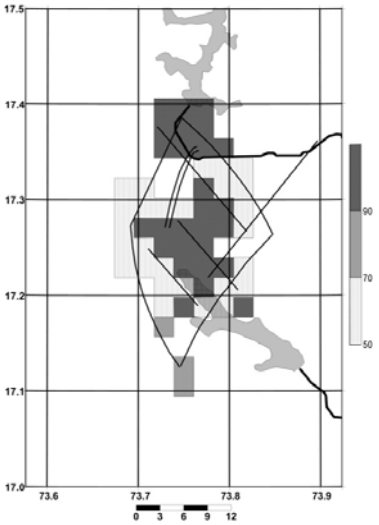

Fig. 4. Map of expected earthquakes for the Koyna-Warna reservoir site (India) for the period from 1 October 2012 to 30 September 2014 (real-time prediction target). The dimensions of a square elementary cell are 5×5 km.

All earthquakes with $M_L \geq 4.0$ that occurred during the prediction period of the map were plotted on each map of expected earthquakes; then the area of alarm zones with different conditional probability levels $P(D_1|K)$ was calculated. Fig. 5a shows a typical map of expected earthquakes for the Koyna-Warna area for the two-year period from 1 October 2003 to 30 September 2005. Another MEE with a different prediction period is shown in Fig. 5b. As can be seen on both maps, major earthquakes occurred in the zones with the conditional probability level $P(D_1|K) \geq 90\%$ during the prediction period.

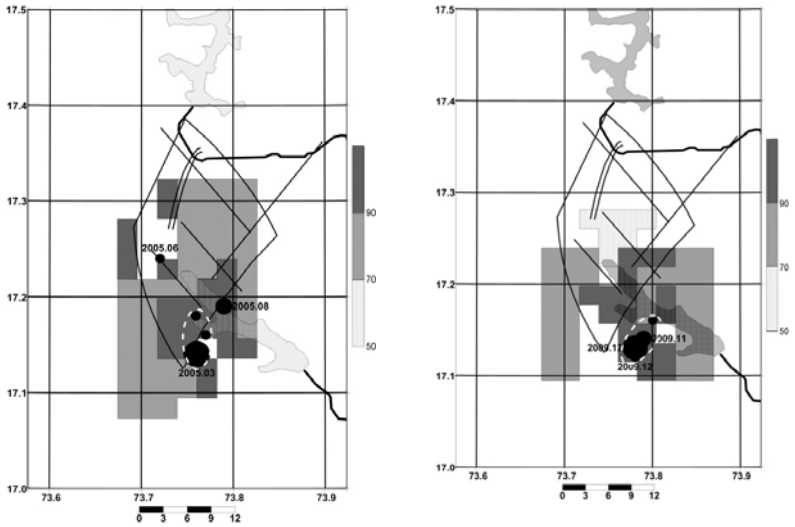

Fig. 5. Map of expected earthquakes for the period from 1 October 2003 to 30 September 2005 (a) and from 1 January 2009 to 31 December 2010 (b). The map shows epicenters of earthquakes and their groups with $M_L \geq 4.0$ that occurred during the MEE validity period (2 years). The size of circles is proportional to the length of rupture in the earthquake focus on the map scale. The dashed ellipse indicates a group of earthquakes that occurred on 14-26 March 2005 (a) and 12-23 December 2009 (b). The dimensions of a square elementary cell are 5×5 km.

The results of the analysis of the whole MEE series are summarized in Table 5. As can be seen from the table, during the retrospective prediction period from 1 January 2003 to 30 September 2012 at the

conditional probability level $P(D_1|K)$≥90%, which is more than 5 times higher than the level of unconditional probability, both largest earthquakes with M_L≥5.0 (No. 12 and 24), 3 earthquakes out of 5 in the 4.5≤M_L <5.0 range (No. 14, 23, and 26), and 5 out of 9 earthquakes with 4.0≤M_L <4.5 (No. 13, 15, 19, and 25) were predicted. Out of 16 major earthquakes, a total of 9 earthquakes (56.3%) occurred in the zone with $P(D_1|K)$≥90%. In this case, the area of observations S_{obs} with the seismic activity level of 0.1 events per year falling within the zone with the conditional probability level of 90% was 20.4±8.4%. The integral prediction effectiveness of the MEE algorithm at this level of conditional probability was 2.76. Table 5 also shows similar data for other levels of conditional probability (50% and 70%).

Table 5. Retrospective prediction results for earthquakes with M_L≥4.0 that occurred in the Koyna-Warna area from 1 July 2002 to 30 November 2012, using MEE algorithm.

Magnitude range	Conditional probability level, $P(D_1|K)$		
	50 %	**70 %**	**90%**
$M_L \geq 5.0$	2/2	2/2	**2/2**
4.5≤ M_L < 5.0	4/5	3/5	**3/5**
5.0≤ M_L < 4.5	7/9	6/9	**4/9**
Total number of predicted earthquakes, *N*pr	13	11	**9**
Number of predicted earthquakes in %%	81.3	68.8	**56.3**
Total number of strong earthquakes that occurred in the area, N_{tot}	16		
Average alarm square S_{al}/S_{obs} in %%	40.5±7.6	36.6±8.8	**20.4±8.4**
MEE effectiveness J_{MEE}	2.01	1.88	**2.76**

Conclusions

The paper contains examples of MEE for a variety of seismically active regions all over the world and retrospective prediction results for each of them.

The paper also provides a detailed description of MEE calculations for the Koyna−Warna area and initial analysis of the results. A retrospective analysis of prediction effectiveness has been made for each of the seismic precursors used in the MEE algorithm. It transpired that the density of seismogenic ruptures is the most successful characteristic of all predictive characteristics in terms of the number of predicted earthquakes. The resultant unconditional probability of a major earthquake in grid cells is $P(D_1)$=0.1698.

The findings of using the MEE algorithm in a classical area with a transient seismic regime for the first time were very encouraging. They showed that its prediction effectiveness equal to 2.76 was quite high. Zones with conditional probability levels $P(D_1|K)$≥90% experienced 56.3% of all earthquakes with M_L≥4.0. The alarm area was 20.4±8.4% of the total area of observations. The MEE algorithm was particularly efficient in predicting the largest earthquakes in the Koyna-Warna area that occurred during the retrospective prediction period. At a later stage, more accurate adjustment of algorithm parameters may improve the overall prediction effectiveness. Integral predictive effectiveness estimates obtained when the MEE algorithm was used for the Koyna-Warna reservoir site are close to the average values of these parameters for all previous seismically active regions. These findings may be considered proof of the flexibility of the proposed algorithm.

The prediction can be verified in real time using the map of expected earthquakes for the period from 1 October 2012 to 30 September 2014.

References

1. E.S. Ventsel. Probability Theory. M.: Nauka. 1969, 576 p. (*in Russian*).

2. A.D. Zavyalov. Medium-Term Earthquake Prediction: Fundamentals, Methodology, Implementation // M.: Nauka. 2006, 254 p. (*in Russian*).

3. M.O. Kutsenko, A.D. Zavyalov. Probability of an Earthquake in the Expectation Time Interval Based on a Set of Predictive Characteristics // Proceedings of the 12th Urals Youth Scientific School for Geophysics. Perm, 21-25 March 2011, p. 131-136. (*in Russian*).

Алгоритм Карты Ожидаемых Землетрясений: результаты 30-летних испытаний и последние достижения

А. Д. Завьялов

Резюме

Алгоритм КОЗ – Карта Ожидаемых Землетрясений был предложен в середине 1980-ых годов Г.А.Соболевым, Т.Л.Челидзе, А.Д.Славиной и А.Д.Завьяловым, являвшимися наиболее активными членами неформальной тематической группы ОСАС – оперативного сравнительного анализа сейсмичности. За прошедшие 30 лет алгоритм был протестирован в различных сейсмоактивных регионах мира: Кавказ, Камчатка, Копет-Даг, Киргизия, Южная Калифорния, Северо-Восточный и Юго-Западный Китай, Греция, Западная Турция, Курильские о-ва, Новая Зеландия. Средняя прогностическая эффективность по этим регионам составила *J*коз=2.56 и 3.82 при выборе в качестве уровня тревоги величины условной вероятности $P(D_1|K)$=70% и 90% соответственно. При этом в зонах с этими уровнями условной вероятности произошло 68% и 41% прогнозируемых землетрясений, а площадь зон тревоги составила 30% и 14% от общей площади наблюдений.

В последней работе впервые предпринята попытка использовать алгоритм среднесрочного прогноза землетрясений КОЗ для построения карт ожидаемых землетрясений в классическом районе с переходным режимом сейсмичности – район водохранилищ Койна-Варна, Индия.

Величины интегральных оценок прогностической эффективности, полученные при использовании алгоритма КОЗ в районе водохранилищ Койна-Варна, близки к средним величинам этих параметров по всем предыдущим сейсмоактивным регионам. Этот результат можно рассматривать в качестве свидетельства универсальности предложенного алгоритма.

მოსალოდნელი მიწისძვრების რუკის ალგორითმი: 30 წლიანი გამოცდების შედეგები და უახლესი მიღწევები

ა. ზავიალოვი

რუსეთის მეცნიერებათა აკადემიის დედამიწის ფიზიკის ინსტიტუტი

Journal of Georgian Geophysical Society,
Issue (A), Physics of Solid Earth, v.16a, 2013, pp. 88-95

Boreholes Water Level and Earthquake's Prediction (2011-2013)

A.Sborshchikovi[1,2], G.Kobzev[1,2], S.Cht.Mavrodiev[2], G.Melikadze[1]

1. M.Nodia Institute of Geophysics, Georgia
2. Institute for Nuclear Research and Nuclear Energy, Bulgarian Academy of Sciences

Abstract

Studies of precursors and events that occur before an earthquake is one of the most important problem that arose in todays' seismology. Earthquake prediction has become the issue that needs to be solved, it will help us to forecast destructive earthquake. In this article we will discuss water level daily monitoring in several boreholes located in different parts of Georgia.

Keywords: water level, precursors, earthquake prediction, geoelectromagnetism

Introduction

The main reason of this research was to find the answer to the question is the change of water level in the boreholes the same effect on the incoming earthquake appearance as the variations of magnetic fields or not.

The hypothesis for possible correlations between the earthquakes and the variations of magnetic fields, Earth's horizontal and vertical currents in the atmosphere, was born when in the when the historical data on the Black Sea was systemized. The achievement in the Earth surface tidal potential modeling, with the ocean and atmosphere tidal influences being included, makes an essential part of the research. In this sense, the comparison of the Earth tides analysis codes [1] was very useful. The possible tidal triggering of earthquakes has been investigated for a long period of time [2].

The earthquake-related part of the models has to be infinitely repeated in the "theory–experiment–theory" process, using nonlinear inverse problem methods in looking for correlations between the different fields in dynamically changing space and time scales. Each approximate model supported by some experimental evidence should be included in the analysis. The adequate physical understanding of the correlations among electromagnetic precursors, tidal extremes and a impendant earthquake is related to the progress of an adequate Earth magnetism theory and electrical currents distribution, as well as to the quantum mechanical understanding of the processes in the earthquake source volume before and during the earthquake.

Simultaneous analysis of more accurate space and time measuring sets for the Earth crust condition parameters, including the monitoring data of the electromagnetic field under and over the Earth surface, as well as the temperature distribution and other possible geophysical precursors, would be the basis of nonlinear inverse problem methods. It could be promising for studying and solving the "when, where and how" earthquake prediction problem.

The discovery of geomagnetic quake as reliable precursor for increasing of regional seismicity

In December 1989, a continuous measurement of a projection of the Earth's magnetic field (F) with a magnetometer (know-how of JINR, Dubna, Boris Vasiliev) with absolute precision less than one nano-Tesla at a sampling rate of 2.5 samples per second was started. The minute's mean value of F, its error mean value, the minute's standard deviation *SDF*, and its error were calculated, i.e., every 24 hours, 1440 quartets of data were recorded.

Minute standard deviation of F is defined as:

$$SDF_m = \left(\left(\frac{1}{N} \right) \sum_{i=1}^{N_m} \left(F_i - F_{mean} \right)^2 \right)^{\frac{1}{2}} \qquad (1)$$

where m is the chosen time interval and n is the number of simples during the period,

$$F_{mean} = \left(\frac{1}{N}\right)\sum_{i=1}^{N_m} F_i \qquad (2)$$

with N_m the number of samples per minute.

The connection between variations of local geomagnetic field and the Earth currents was established in INRNE, BAS, Sofia, 2001 seminar [3]. The statistic of earthquakes that occurred in the region (1989-2001), confirmed the Tamrazyan notes [4,5], that the extremes of tides are the earthquake's trigger. The Venedikov's code [6,7] for calculating the regional tide force was used [8].

The signal for imminent increasing regional seismic activity (incoming earthquakes) is the "geomagnetic quake" (Gq), which is defined as a jump (positive derivative) of daily averaged SDF_{mean}, devoted to half sum of middle geomagnetic field indices. Such approach permits to compare by numbers the daily behavior of the geomagnetic field with those in other days.

Among the earthquakes occurred on the territory under consideration in certain time period, the "predicted" one is the earthquake with magnitude M and distance between epicenter and monitoring point $Dist_p$, which is identified by the maximum value of the function:

$$S_{ChtM} = 10^{1.5M+4.8} / \left(D + Depth_p + Dist_p\right)^2 \left[energy / km^2\right] \qquad (3)$$

where D=40 km is a fit parameter.

The physical meaning of the function S_{ChtM} is a surface density of earthquake's energy in the point of measurement. It is important to stress out that the first consideration of the earthquake magnitude M and epicenter distance dependence was obtained using nonlinear inverse problem methods. Obviously, the close distance strong earthquake (with relatively high value of S_{ChtM}) will bear more local Earth currents variations, which will generate more power geomagnetic quake.

It is very important to note that in the time scale of one minute, the correlation between the time period of increasing regional seismic activity (incoming earthquake), and tide extrema, recognized of predicted earthquake was established using the Alexandrov's code REGN for solving the over - determined nonlinear systems [8,9]. The very big worthiness of Alexandrov's theory and its code is possibility to choose between two functions, which describe the experimental data with the same *hi*-squared, the better one.

Day-Difference analysis

The role of the electromagnetic variations as earthquake's precursor can be explained in general by the hypothesis: the strain accumulation in the Earth Crust during the earthquake preparation causes medium's density change, within which a chemical phase ("dehydration") shift and a corresponding electrical charges shift appears. The Earth tides extreme as earthquake's trigger could be based on the hypothesis of "convergence of tidal surface waves" in the region (territory with prominent tectonic activity as consequences of chemical phase shift) of impending seismic activity.

For every occurred earthquake was calculated "day-difference"; the smaller absolute time difference between the hypocenter time and the daily times of pre and post tide's extreme time at that site on the Earth surface (the earthquake epicenter). This procedure was provided on all reported earthquakes in ISC catalogue (http://www.isc.ac.uk/) for the time period 1981-2011 and $M \geq 3.5$. The program for calculating of daily averaged module of vector movement *Tmean* is based on Dennis Milbert TIDE program (solid.for), by which Tide data could be calculated only for the time period after 1981. The DailyTide time of the Tide extremes *Tmean* were calculated by analogy of center mass calculation.

The statistic of day-differences for the earthquakes that occurred worldwide (1981-2011) and the Gaussian fitted curve (Fig.4), confirmed the Tamrazyan notes [5,6] from 1960-th, that the extrems of tides play a role of earthquake's trigger.

Data and stations

The main reason of this research was to find the answer to the question has changing water level in the boreholes the same effect on the earthquake appearance as the variations of magnetic fields or not.

The hypothesis for possible correlations between the earthquakes, the variations of magnetic fields, Earth's horizontal and vertical currents in the atmosphere, was born when in early 1988, the historical data on the Black Sea was systemized. The achievement in the Earth surface tidal potential modeling, with the

ocean and atmosphere tidal influences being included, makes an essential part of the research. In this sense, the comparison of the Earth tides analysis codes [6] is very useful. The possible tidal triggering of earthquakes has been investigated for a long period of time [7].

After studying this fact a hypothesis was born may be we can forecast earthquake using the same methodology.

Before discussing our methodology let stop our attention on the boreholes, which are located in different parts of Georgia.We have Ajameti borehole (depth 1300 m); Axalkalaki (1400 m); Borjomi-70 (1300 m); Kobuleti (2000 m); Lagodehi (800m) and Marneuli (3500m).

The location of these boreholes is shown in Fig.1a.

Fig.1a Map of boreholes in Georgia

Here is the detail description of the boreholes:

Borehole	Depth, meters	Filter interval, meters	Lithology	Geological intervals, meters	Water level, meters
Ajameti	1330	520-740	Litostone	520-740	-6
Ahalkalaki	1400	1000	Tuff, andezit, basalt, dolomite	580-1000	-0.2
Borjomi-70	1330	1260-1300	Clay	0-12	-22
Kobuleti	2000	187-640	Tuff, andezit, bazalt	0-150 150-2000	-0.5
Lagodehi	800	255-367	Sand+gravel	0-24	-15.8
Marneuli	3500	1235-1600	Gravel	0-50	-5

Methodology of analysis

We have selected earthquakes with magnitude $M \geq 3.5$ at distance $D \leq 500$km from boreholes for 2011,2012 and 2013 years. After format conversion of water level data we calculate the daily standard deviation (daily level signal). When we have the jump of today and yesterday signals we say that we have a precursor for incoming regional seismicity. After this we analyze the day difference between occurred earthquakes and next extreme of the tide, calculated using Dennis Milbert Fortran code for local tidal behavior, http://home.comcast.net/~dmilbert/softs/solid.htm.

For precursors calculation we used one hour water level data. The statistic evidence that water level precursors can be used for estimation of incoming regional seismic situation is illustrated in the figures 2,3 and 4,5.

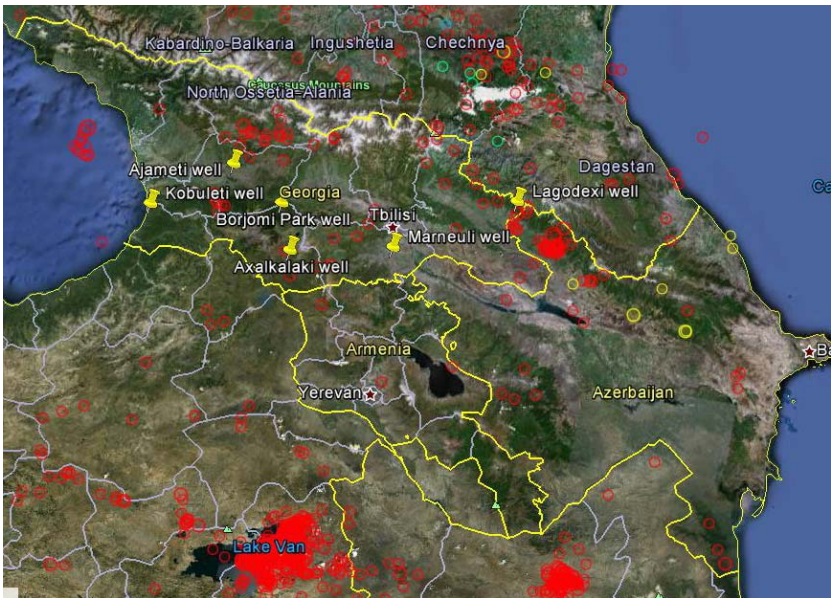

Fig.1b The map of earthquakes during 2011-2012

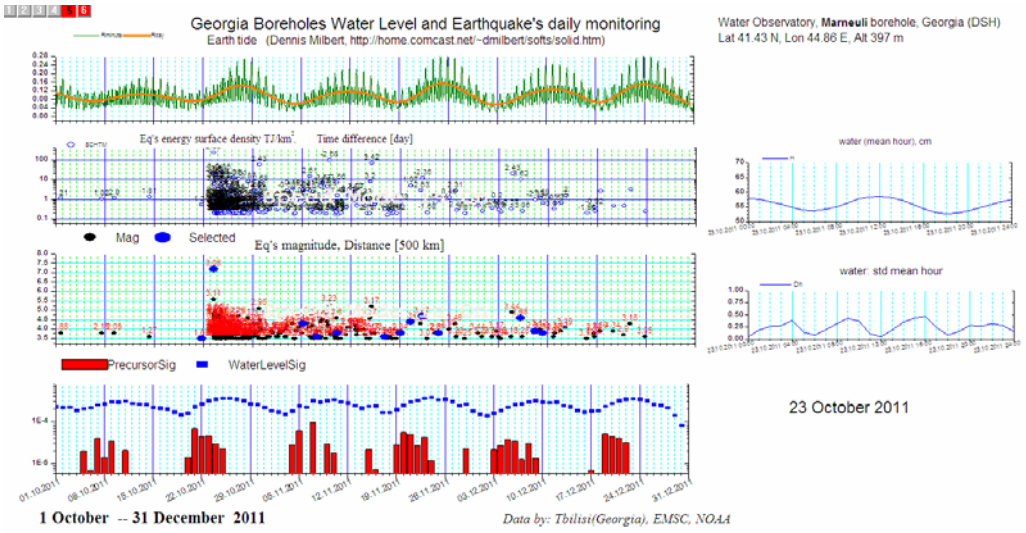

Fig.2 Marneuli borehole daily monitoring including period of great earthquake in Turkey (2011)

As we see in figure 2 the first graph in the left corner is the picture of tidal behavior [m], the next shows the energy (J/km ^{2}), the next – magnitude, and the last describes precursors (red columns) and water level signals (blue points). The blue points has been count using normal standard deviation and the red columns so called precursors were obtain by subtraction of the daily standard deviation of today and the previous day [10,11]. The first graph in the right corner is water mean during 23 October the period of great Turkey earthquake and the next describes standard deviation of water level [12].

The same emplacement is shown for another period in the figure 3.

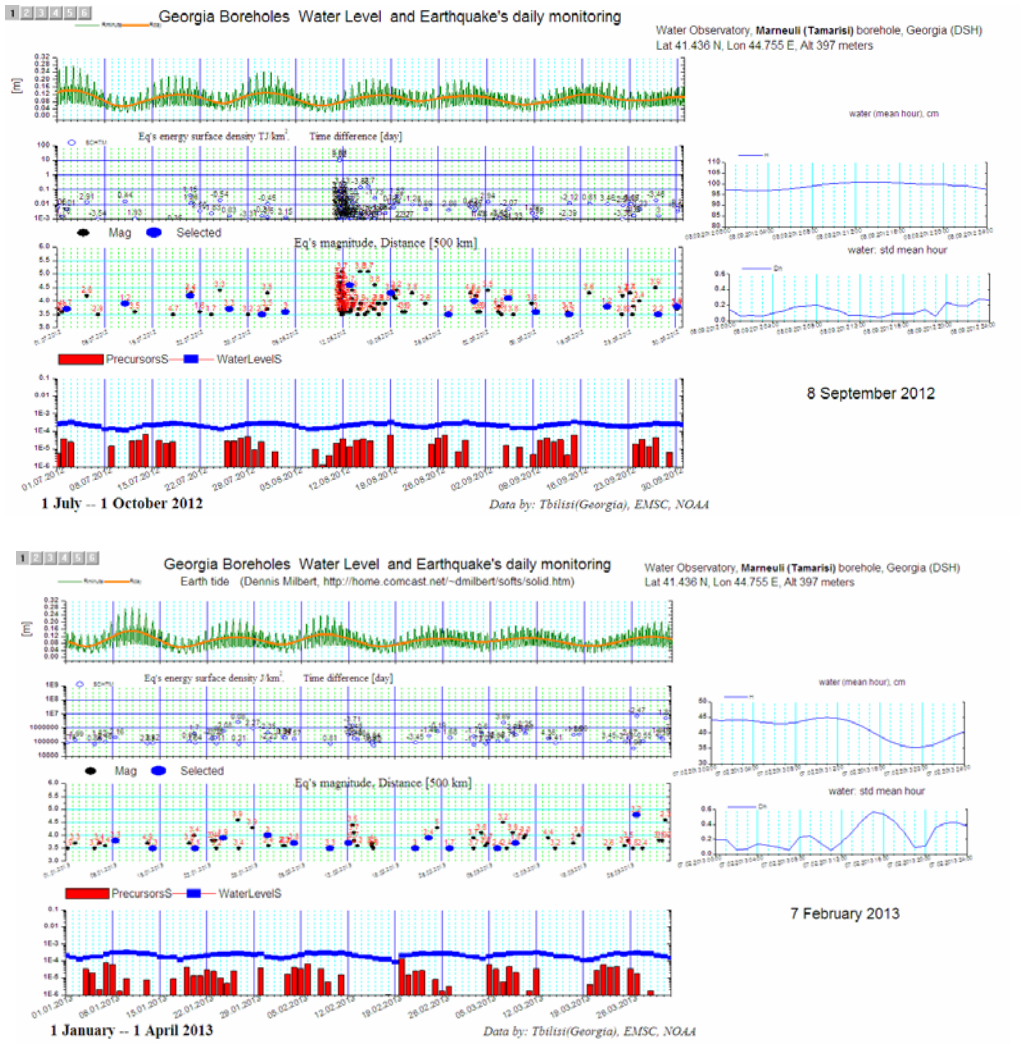

Fig.3 Marneuli borehole daily monitoring (2012,2013)

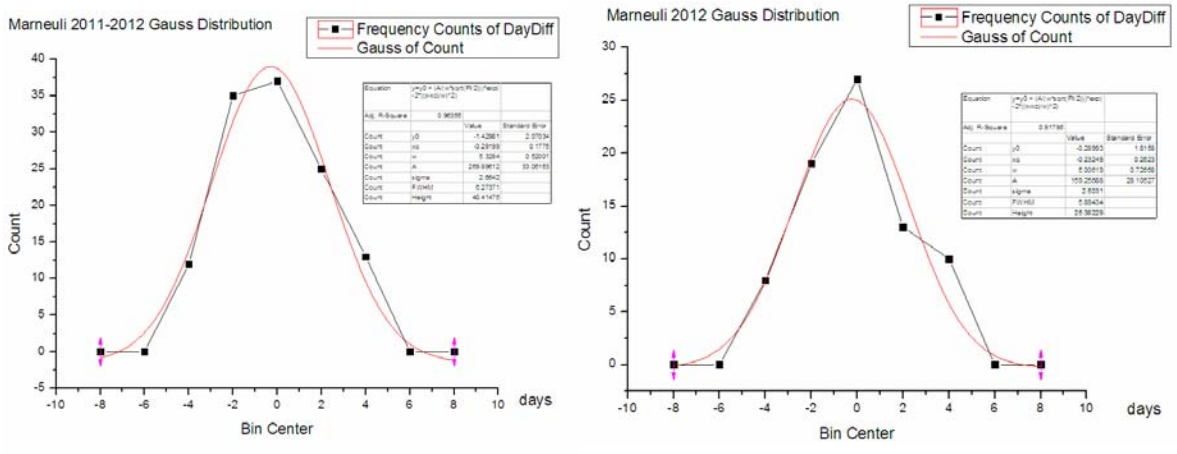

Fig.4 Marneuli borehole Gauss Distribution for day difference (2011-2012,2012)

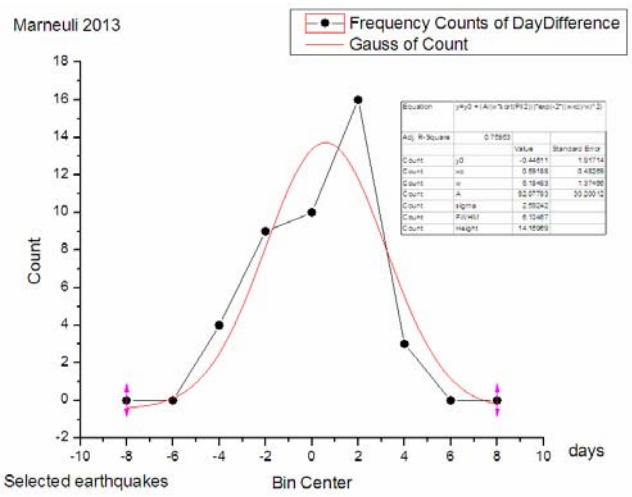

Fig.5 Marneuli borehole Gauss Distribution for day difference (2013)

From the figures 4 and 5 we see that the day difference distribution from 2011 until 2013 are described well by Gaussian curve with the R-square not less than 0.90.

The figure 6 presents frequency count for the distance of the selected by precursors earthquakes with maximal energy density in monitoring point with increment 10 km.

The highest number of the earthquakes is at the distance 300-350 km (Turkey earthquakes), the earthquake at distance 350-450 km are Iran earthquakes and the other one that are at distance less than 300 km are regional local earthquakes.

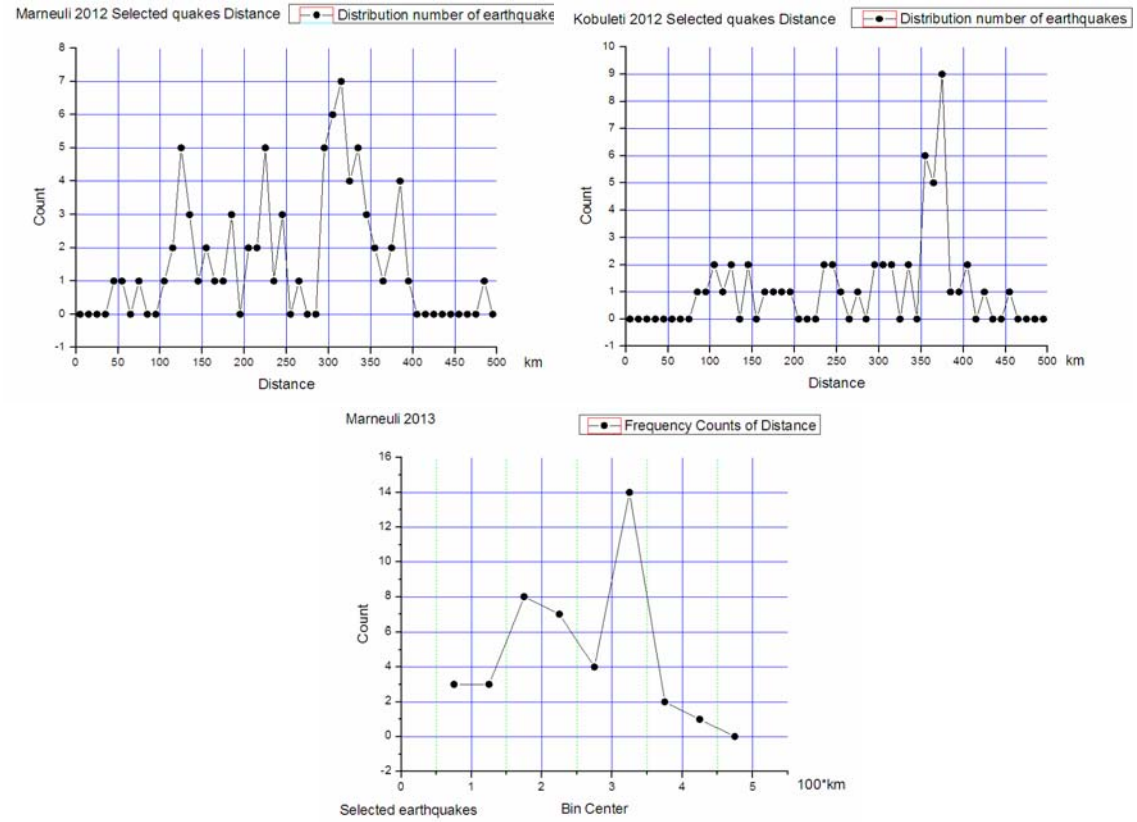

Fig.6 Two boreholes frequency counts for distance of selected by precursors quakes and frequency count of distance on Marneuli borehole 2013

Conclusion

As conclusion we can say that the using in analogy of geomagnetic quake approach of daily boreholes water data level analysis can serve as precursor of increasing regional seismic activity.

References

1. Venedikov A. P., Arnoso R., and Vieira R.: A program for tidaldata processing, Computer & Geosciences, 29, 4, 487–502,2003.
2. Tamrazyan G.P., Tide-forming forces and earthquakes, ICARUS, Vol.7, pp.59-65, 1967.
3. Mavrodiev S.Cht., Thanassoulas C., "Possible correlation between electromagnetic earth fields and future earthquakes", ISBN 954-9820-05-X, Seminar proceedings, 23-27 July, 2001, INRNE-BAS, Sofia, Bulgaria, 2001.
4. Knopoff L., Earth tides as a triggering mechanism for earthquakes, Bull. Seism. Soc. Am. 54:1865–1870, 1964.
5. Tamrazyan G.P., Tide-forming forces and earthquakes, ICARUS, Vol.7, pp.59-65, 1967.
6. Tamrazyan G.P., Principal ragularities in the distribution of major earthquakes relative to Solar and Lubar tades and other Cosmic forces, ICARUS, Vol.9, pp.574-592, 1968,15.
7. Venedikov A. and Arnoso R.: Program VAV/2000 for Tidal Analysis of Unevenly Spaced Data with Irregular Drift and Colored Noise, J. Geodetic Society of Japan, 47, 1, 281–286, 2001.
8. Venedikov A. P., Arnoso R., and Vieira R.: A program for tidal data processing, Computer & Geosciences, 29, 4, 487–502, 2003.
9. Alexandrov L., Program code REGN, PSR 165 RSIK ORNL, Oak Ridge, Tennessee, USA,1983.
10. Mavrodiev S.Cht., On the reliability of the geomagnetic quake as a short time earthquake's precursor for the Sofia region, Natural Hazards and Earth System Sciences (2004) 4: 433–447, SRef-ID: 1684-9981/nhess/2004-4-433.
11. Mavrodiev S.Cht., and Pekevski L., Complex Regional Network for Earthquake Researching and Imminent Prediction, Electromagnetic phenomena related to earthquakes and volcanoes, Editor: Birbal Singh, Publ., Narosa Pub. House, New Delhi, pp.135−146, 2008.
12. T. Chelidze, T. Matcharashvili, and G. Melikadze, Earthquakes' Signatures in Dynamics of Water Level Variations in Boreholes, In: Synchronization and Triggering: from Fracture to Earthquake Processes, Eds.V.de Rubeis, Z. Czechowski, R. Teisseyre, Geoplanet: Earth and Planetary Sciences, 2010, Vol. 1, Part 3, 287-304, DOI: 10.1007/978-3-642-12300-9_20, Springer.
13. G. Kobzev, G. Melikadze, T. Jimsheladze., New method of hydrodynamical data analyse, Workshop-ceminarmateraials "BlackSeaHazNet Series, Vol. 25-72, 2011, Tbilisi, Georgia.
14. T. Jimsheladze, G. Melikadze, G. Kikuashvili, S. Mavrodiev, L. Pekevski, M. Chkhitunidze, Study of Geomagnetic Variations in Georgia and establishment the Anomaly Nature of Earthquake Precursors, Workshop-ceminarmateraials "BlackSeaHazNet Series, Volume 2, 205-214, 2011, Tbilisi, Georgia
15. A.Sborshchikovi, G.Kobzev, S.Cht.Mavrodiev, G. Melikadze BOREHOLES WATER LEVEL AND EARTHQUAKE'S DAILY MONITORING, Nano Studies 2013 8 203-212
16. Mavrodiev S.Cht., Pekevski L., and Jimseladze T. Geomagnetic-Quake as Imminent Reliable Earthquake's Precursor: Starring Point for Future Complex Regional Network, Electromagnetic phenomena related to earthquakes and volcanoes, Editor: Birbal Singh, Publ., Narosa Pub. House, New Delhi, pp.116−134, 2008.

ჭაბურღილებში წყლის დონის ყოველდღიური მონიტორინგი და მიწისძვრების პროგნოზი

ა. სბორშიკოვი, გ. კობზევი, ს. მავროდიევი, გ. მელიქაძე

რეზიუმე

პრეკურსორების და სხვა მოვლენების შესწავლა არის თანამედროვე მეცნიერების ერთ-ერთი უმნიშნელოვანესი საკითხი. მიწისძვრების წინასწარმეტყველება გახდა ერთ-ერთი იმ პრობლემებიდან, რომლებიც აუცილებლად უნდა გადაიჭრას და ამ ამოცანის

ამოხსნა დაგვეხმარება მომავალში შევამციროთ დამანგრეველი მიწისძვრების ეფექტი. ამ სტატიაში ჩვენ შევეხებით საქართველოს ტერიტორიაზე განლაგებულ სხვადასხვა ჭაბურღილების წყლის დონის მონიტორინგის საკითხს.

Мониторинг уровня воды в скважинах и метод предсказания землетрясений

А. Сборщиков, Г. Кобзев, С. Мавродиев, Г. Меликадзе

Резюме

Изучения прекурсоров и некоторых других процессов предшествующих землетрясению является одной из важнейших проблем современной науки. Предсказание землетрясений стало чуть ли не вопросом номер один, который нуждается в решении, для того чтобы смягчить последствия разрушительных землетрясений. В этой статье мы рассмотрим изменения уровня воды в скважинах и метод предсказания землетрясений.

Journal of Georgian Geophysical Society,
Issue (A), Physics of Solid Earth, v.16a, 2013, pp. 96-103

Time variation of the seismicity related with the Enguri high dam reservoir-field and laboratory data analysis

A. Sborshchikov, E. Mepharidze, D. Tephnadze, N. Javakhishvili, I. Petriashvili

M. Nodia Institute of Geophysics, 1, Alexidze str. 0171, Tbilisi, Georgia,
e-mail: ekamep@gmail.com

Abstract

In present research we investigated the fractal and multifractal properties of the earthquake time series occurred around the Enguri dam. We used field and laboratory data sets. Different data analysis methods including the methods of detrended fluctuation analysis (DFA) has been used. Exactly, we analysed the interevent time series in two periods: i) 1960-1980, in which the investigated area was characterized by the natural seismicity; ii) 1981-2012, in which quasi-periodic change of the reservoir water level affected the earthquake generation. Additionally stick-slip acoustic emission data sets have been used.

Our findings in both field and laboratory data sets show that the water level variation may influence the dynamical properties of earthquake temporal distribution in the local area around the Enguri dam.

Introduction

As it follows from many literature data large reservoirs may influence local seismic activity. Reservoir-induced seismicity has been reported in many cases worldwide in last two decades (e.g. Simpson et al., 1988; Talwani, 1997; Telesca, 2010; Telesca, 2011; Telesca et al., 2012a; Telesca et al., 2012b; Telesca et al., 2012c; Telesca et al., 2012d; Telesca et al., 2012e). Proposed mechanisms are change of strain in the earth's crust caused by the weight of water, or increased groundwater pore pressure which decreases the effective strength of the rocks around the reservoir (Simpson et al., 1988; Talwani, 1997; Trifu, 2002). This mechanism seems may work at the first stage of influence of large amount of water increasing to the maximal level. Later, for the period when the change becomes periodic, like for electric hydro power stations, it was proposed mechanism of reservoir induced synchronization of seismic process (Peinke et al. 2006; Matcharashvili et al., 2008).

Although several aspects related with reservoir-induced seismicity are well-know, some other issues related with the changes of local seismic activity caused by water level still remain poorly investigated. One of these is related to the dynamical characterization of time distribution of seismicity in the area around large dams and water reservoirs.

In this paper, we investigate, dynamical properties of the time distribution of the earthquake series with and without the influence of reservoir water level variation in the Enguri area. Laboratory data of stick slip acoustic emission also have been analised.

Methods

In present research we used the detrended fluctuation analysis (DFA) (Peng, et al. 1993, 1995) and phase synchronization quantification methods for our data sets. DFA is method for detrending local variability in a time series, providing insight into its long-term variation features. This technique provides a quantitative parameter (DFA scaling exponent) that gives information about the correlation properties of the time series. The reason why the DFA is so useful is that it allows to detect scaling behavior in nonstationary time series, along with its really simple implementation; these characteristics feature the DFA as a very effective method in gaining information about an observational time series.

The DFA works as follows (Peng et al., 1993). The time series $x(k)$ (of length N), is firstly integrated and the so-called "profile" $Y(i)$ is determined . Then $Y(i)$ is divided into boxes of size n, and in each box of length n, the polynomial local trend $Y_n(i)$ is calculated and removed from the profile. The root mean square fluctuation of the integrated and detrended series is, then, calculated:

$$F(n) = \sqrt{\frac{1}{N}\sum_{i=1}^{N}\left[Y(i) - Y_n(i)\right]^2}$$

This process is repeated for all the available scales (box sizes n). If the relationship between $F(n)$ and n is a power-law, the signal is fractal:

$$F(n) \sim n^{\alpha}$$

The scaling exponent α gives the information about the long-range power law correlation properties of the signal. Scaling exponent $a = 0.5$ corresponds to white noise (noncorrelated signal), when $a < 0.5$ the correlation in the signal is anti-persistent, if $a > 0.5$ the correlation in the signal is persistent. $a = 1$ means uniform power law behavior of 1/*f* noise and $a = 1.5$ represents a Brownian motion (Peng et al., 1993,1995). The value $a > 1.5$ corresponds to long-range correlations that may be related to both stochastic and deterministic correlations **(**Peng et al., 1995; Rodriguez et al., 2007**).**

Besides the field data, as an appropriate laboratory model we investigated acoustic emission data collected during the stick-slip experiments with superimposed weak periodical forcing. The experimental set up consists of a system of two roughly finished basalt plates. A constant dragging force of about 10 N was applied to the upper (sliding) plate weighting 0.7 kg. During the first series of experiments, the upper plate was subjected to periodic electric (48 Hz) perturbations with variable amplitude (from 0 to 1000 V) superimposed on the constant dragging force. During second series of experiments the periodic perturbations were of the constant amplitudes, correspondingly 7.5 V and 975 V. Slip events were recorded as acoustic emission bursts. Acoustic emission waveforms as well as the sinusoidal electro magnetic signal (f = 48 Hz) were digitized at 44 kHz. Details of the setup and technique are given in (Chelidze and Lursmanashvili, 2003; Chelidze et al., 2005).

From these acoustic emission data sets the time series (catalogues) of the emitted acoustic power during consecutive 2π cycles of the external 48 Hz periodic forcing were calculated as a ratio of the area between the acoustic signal curve and x-axis for 2π periods of superimposed sinusoidal signal to the time duration of this 2π periods.

In experiments without or with small external periodic forcing the same duration of the mentioned 2π cycles was used as a time scale. In Fig. 5 a typical time series of the emitted acoustic power at increasing external forcing is presented. The data were normalized to zero mean and unit of standard deviation. As in the case of seismic energy analysis, the probability of emitted acoustic power P, exceeding the given threshold value was calculated for laboratory stick-slip data.

For the investigation of possible synchronization effects, the instantaneous phases of mentioned data sets were calculated based on the Hilbert transform and analytic signal concept (Pikovsky et al., 2003).

Results and discussions

We analyzed the earthquake catalogue of the Enguri area (west Georgia) within 90km from the location of the dam. The construction of the dam started in 1970. The filling period ended in 1980 and after that, the water level variation became quasi-periodic. Therefore, we investigated the fractal properties of the interevent times (in minutes) in two time periods, 1960-1980 and 1981-2012 (Fig. 1). We considered both the whole and the declustered (Reasenberg, 1985) catalogues for a threshold magnitude of 2.0.

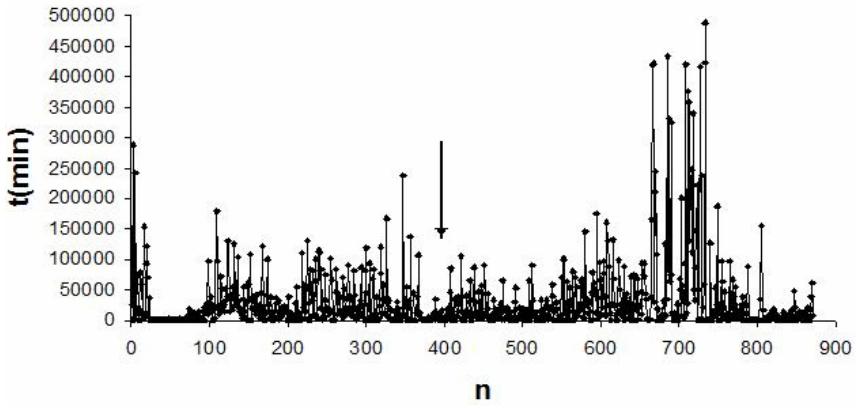

Fig. 1. Interevent time intervals from the whole catalogue of Enguri area in 1960-2012. The arrow indicates the separation in the two periods: before the arrow, 1960-1980; after the arrow 1981-2012.

Fig. 2 shows the DFA fluctuation curves in the two investigation periods. We calculated the fluctuation curves for p=2,..,5 where p indicates the degree of the fitting polynomial. Table 1 shows the scaling exponents with varying p.

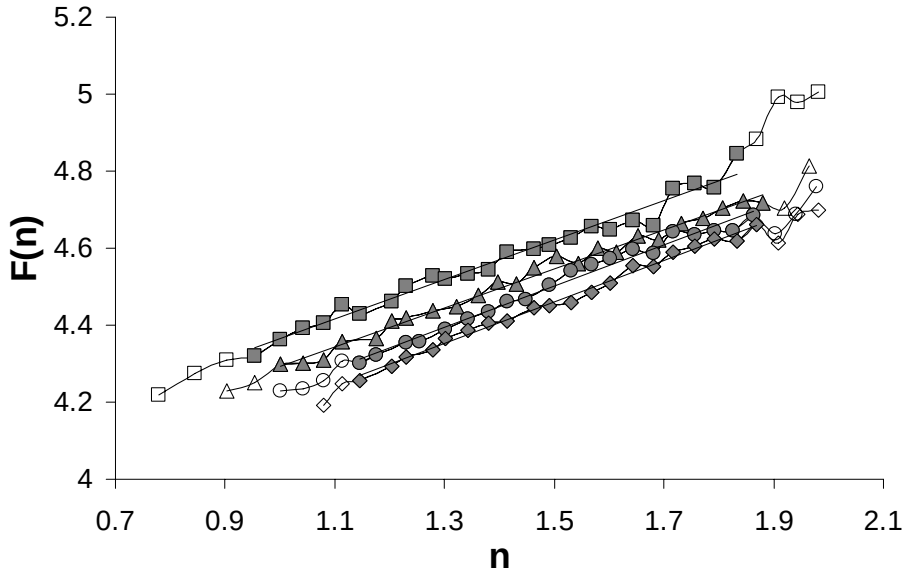

a.

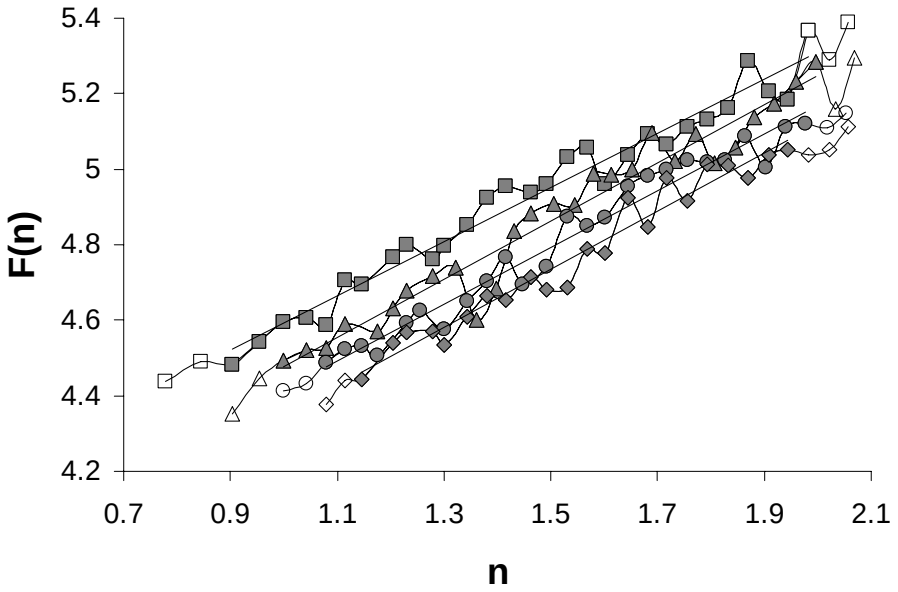

b.

Fig. 2. DFA fluctuation curves for interevent time series from earthquake catalogue in 90km area around Enguri dam in a)1960-1980 and b)1981-2012. Order of polynomial fitting p=2 (squares), 3 (triangles), 4 (circles), 5 (diamonds).

Table 1. DFA scaling exponent α of interevent time series.

Order of fitting polynomial, p	Before influence of water level variation, (1960-1980)	During influence of water level variation in reservoir, (1981-2012)
2	0.54 ± 0.02	0.72 ± 0.03
3	0.50 ± 0.01	0.77 ± 0.03
4	0.51 ± 0.02	0.75 ± 0.03
5	0.54 ± 0.02	0.77 ± 0.04

It is striking that the scaling exponent is approximately unchanged with varying of the detrending polynomial degree. In particular, the period during the effect of the water level quasi-periodic variation is characterized by a more persistent interevent time series than the period before, with exponent around 0.7, significantly larger than 0.5, which characterizes the seismicity in the first period (Fig 3).

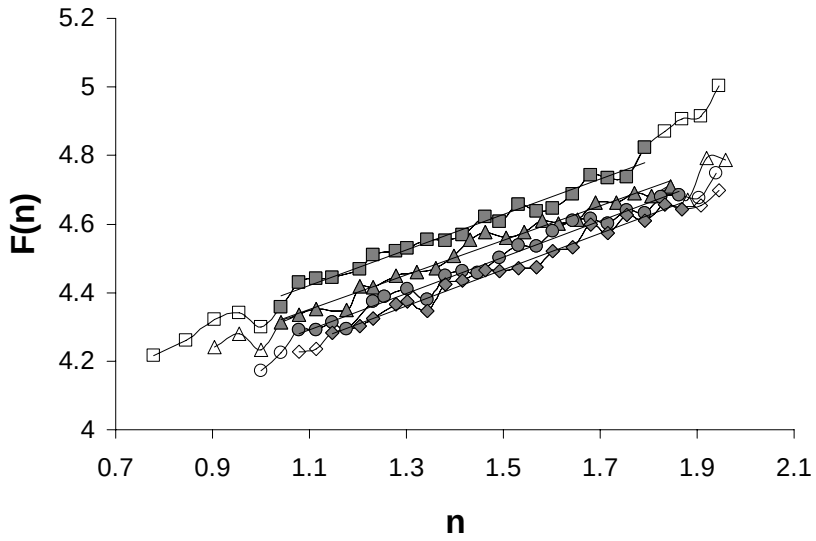

a.

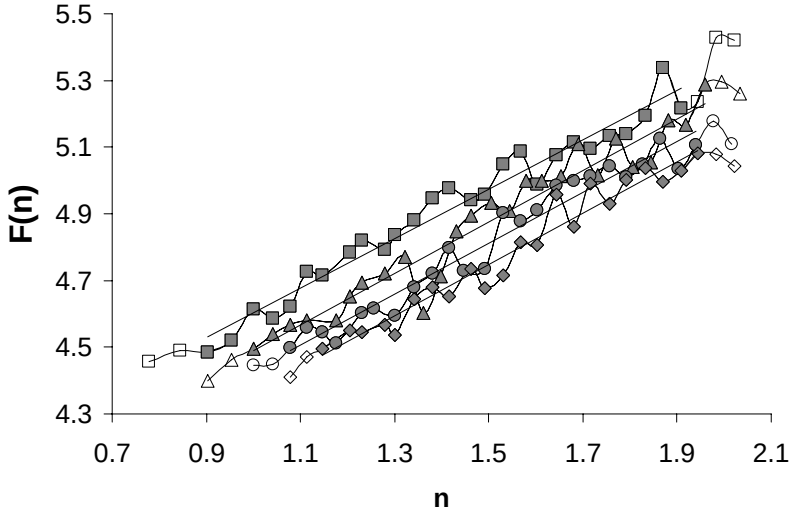

b.

Fig. 3. DFA fluctuation curves for interevent time series from declustered earthquake catalogue in 90km area around Enguri dam in a)1960-1980 and b)1981-2012. Order of polynomial fitting p=2 (squares), 3 (triangles), 4 (circles), 5 (diamonds).

Table 2. DFA scaling exponent α of interevent time series from declustered catalogue.

Order of fitting polynomial, p	Before influence of water level variation, (1960-1980)	During influence of water level variation in reservoir, (1981-2012)
2	0.52 ± 0.02	0.77 ± 0.03
3	0.50 ± 0.02	0.77 ± 0.04
4	0.53 ± 0.02	0.74 ± 0.03
5	0.53 ± 0.02	0.73 ± 0.03

Next in order to have longer data sets we analysed acoustic emission data from stick-slip experiments which is laboratory model of seismicity. Results of stick-slip (acoustic emission)

experiments with external periodic forcing confirm the hypothesis that the dynamics of process was changed under water level periodic influence.

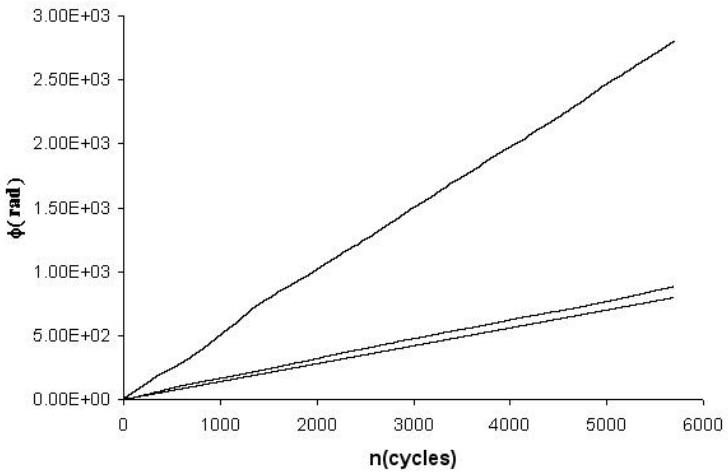

Fig. 4. Phase increase of power of emitted acoustic energy time series. Upper line –lower, and mid line –larger, external periodic forcings. Bottom line corresponds to phase increase of periodic influence.

Such changes connected with synchronization confirmed above results on field data.

Indeed, in order to test the results on longer time series and at constant amplitude of external forcing the data on the acoustic emission experiments with stable external influence were analysed from the synchronisation point of view. Namely, the time series of power of emitted acoustic energy obtained in two series of experiments with different external periodic forcing (Fig. 4).

Thus, comparing field seismic and experimental acoustic energy emission data, the conclusion can be drawn that the during periodic variation of water level in reservoir dynamical changes in local seismic process are detectable both by DFA as well as synchronization testing analysis.

Conclusions

We investigated properties of the earthquake temporal distribution around Enguri dam located in West Georgia during two periods: 1960-1980 and 1981-2012. The first period is characterized by natural seismicity, because occurred before the construction and the filling of the dam; the second period is characterized by reservoir-induced seismicity affected by the quasi-periodic water level fluctuation.

It was found that, water level variation may influence the dynamical properties of the temporal distribution of the seismicity of the Enguri area. In particular, the temporal dynamics of the seismic process under the effect of the quasi-periodic water level oscillation is more persistent and more homogenous than that governing the natural seismicity typical of the area before the filling of the dam.

Acknowledgements

This research wouldn't have been possible without the kind support and overall help of member of Georgian National Academy of Sciences Prof. T.Chelidze as well as Prof. T.Matcharashvili who influenced the creation of this article both directly and indirectly, without whose knowledge and assistance this study would not have been successful.

References

1. Chelidze, T., Lursmanashvili, O., 2003. Electromagnetic and mechanical control of slip: laboratory experiments with slider system, Nonlinear Processes in Geophysics, 20, 1–8.
2. Chelidze, T, Matcharashvili, T., Gogiashvili, J., Lursmanashvili, O., Devidze, M., 2005. Phase Synchronization of Slip in Laboratory Slider System, Nonlinear Processes in Geophysics, 12, 1-8.
3. Matcharashvili, T., Chelidze,T., Peinke, J., 2008. Increase of order in seismic processes around large reservoir induced by water level periodic variation, Nonlinear Dynamics, 51, 399-407.
4. Peinke, J., Matcharashvili, T., Chelidze, T., Gogiashvili, J., Nawroth, A., Lursmanashvili, O., Javakhishvili, Z., 2006. Influence of Periodic Variations in Water Level on Regional Seismic Activity Around a Large Reservoir: Field and Laboratory Model, Physics of the Earth and Planetary Interiors, 156/1-2, 130-142.
5. Peng, C. K., Mietus, J., Hausdorff, J., Havlin, S., Stanley, H. E., Goldberger, A. L., 1993. Long-Range Anticorrelations and Non-Gaussian Behavior of the Heartbeat, Phys. Rev. Lett. 70, 1343-1346.
6. Peng, C. K., Havlin, S., Stanley, H. E., Goldberger, A. L., 1995. Quantification of scaling exponents and crossover phenomena in nonstationary heartbeat time series, Chaos. 5, 82–87.
7. Pikovsky, A., Rosenblum, M.G., Kurth. J., 2003. Synchronization: Universal Concept in Nonlinear Science, Cambridge University Press, Cambridge, 411.
8. Reasenberg, P., 1985. Second-order moment of central California seismicity, 1969–1982, J. Geophys. Res., 90, 5479–5495.
9. Rodriguez, E., Echeverria, J. C., Alvarez-Ramirez, J., 2007. Detrended fluctuation analysis of heart intrabeat dynamics, Physica A: Statistical Mechanics and its Applications. 384, 2, 429-438.
10. Simpson, D.W., Leith,W.S., Scholz, C., 1988. Two types of reservoirinduced seismicity. Bull. Seism. Soc. Am. 78, 2025–2040.
11. Telesca, L., 2010. Analysis of the cross-correlation between seismicity and water level in Koyna area (India), Bull. Seismol. Soc. Am., 100, 2317-2321.
12. Telesca, L., 2011. Investigating the temporal variations of the time-clustering behavior of the Koyna-Warna (India) reservoir-triggered seismicity, Chaos Solit. & Fractals, 44, 108-113.
13. Telesca, L., Mohamed, A. E.-E. A., ElGabry, M., El-hady, S., Abou Elenean, K. M., 2012a. Time dynamics in the point process modelling of seismicity of Aswan area (Egypt), Chaos Solitons & Fractals, 45, 47-55.
14. Telesca, L., Lovallo, M., Amin Mohamed, A. E.-E., ElGabry, M., El-hady, S., Abou Elenean, K. M., ElShafey Fat ElBary, R., 2012b. Investigating the time-scaling behavior of the 2004–2010 seismicity of Aswan area (Egypt) by means of the Allan factor statistics and the detrended fluctuation analysis, Nat. Hazards Earth Syst. Sci., 12, 1267–1276.
15. Telesca, L., do Nascimento, A. F., Bezerra, F. H. R., Ferreira, J. M., 2012c. Analyzing the temporal fluctuations of the reservoir-triggered seismicity observed at Açu (Brazil), Nat. Hazards Earth Syst. Sci., 12, 805–811.
16. Telesca, L., ElShafey Fat ElBary, R., Amin Mohamed, A. E.-E., ElGabry, M., 2012d. Analysis of the cross-correlation between seismicity and water level in the Aswan area (Egypt) from 1982 to 2010, Nat. Hazards Earth Syst. Sci., 12, 2203–2207.
17. Telesca, L., Matcharasvili, T., Chelidze, T., Zhukova, N., 2012e. Relationship between seismicity and water level in the Enguri high dam area (Georgia) using the singular spectrum analysis, Nat. Hazards Earth Syst. Sci., 12, 2479–2485.
18. Talwani, P., 1997. On nature of reservoir-induced seismicity. Pure Appl. Geophys. 150, 473–492.
19. Trifu, C.I. (Ed.), 2002. Special Volume Pure & Applied Geophysics, vol. 159.

Временные вариации сейсмичности, связаные с водохранилищем Ингури - анализ полевых и лабораторных данных

А. Сборщиков, Е. Мепаридзе, Д. Тепнадзе, Н. Джавахишвили, И. Петриашвили

Резюме

В данной работе были исследованы фрактальные и мультифрактальные свойства временные серии землетрясений, произошедших вокруг водохранилища Ингури. Использовались полевые и лабораторные данные. Были использованы различные методы анализа, включая детрендированный флуктуационный анализ. Также были проанализированы две временные серии: 1) 1960-1980 этот

период был охарактеризован естественной сейсмичностью; 2) 1981-2012 в этот период квази-периодичная изменения уровня воды в резервуаре влияла на генерирование землетресений. В работе была использована аккустическая эмиссия вида стик-слип.

Исследование полевых и лабораторных данных показали, что вариация уровня воды может влиять на динамическую характеристику распределения землетресений в окрестностях водохранилища Ингури.

ენგურის მაღლივი კაშხალთან დაკავშირებული სეისმურობის დროითი ვარიაციები -საველე და ლაბორატორიული მონაცემების ანალიზი

ა. სბორშჩიკოვი, ე. მეფარიძე, დ. ტეფნაძე, ნ. ჯავახიშვილი, ი. პეტრიაშვილი

რეზიუმე

წარმოდგენილ ნაშრომში ჩატარდა ენგურის კაშხლის ირგვლივ წარმოქმნილი მიწისძვრების დროითი ვარიაციების ფრაქტალური და მულტიფრაცტალური თვისებების გამოკვლევა. კვლევებისათვის გამოყენებული იყო საველე და ლაბორატორიული მონაცემები. მონაცემები დამუშავდა სხვადასხვა მეტოდებით მათ შორის დეტრენდირებული ფლუკტუარული ანალიზის მეთოდით. მონაცემები დაიყო ორ დროით მონაკვეთად: 1)1960-1980 ეს მონაკვეთი ხასიათება ბუნებრივი სეისმურობით; 1) 1981-2012 ამ პერიოდისთვის მისაღებია წყალსაცავებში წყლის დონის კვაზი-პერიოდული ცვლილება, რომელიც გავლენას ახდენს მიწისძვრების გენერირებაზე. ნაშრომში გამოყენებული იყო სტიკ-სლიპის აკუსტიკური ემისია.

საველე და ლაბორატორიული შედეგებიდან ნათლად ჩანს, რომ ენგურის წყალსაცავის ირგვლივ წყლის დონის ვარიაცია გავლენას ახდენს მიწისძვების განაწილების დინამიურ თვისებებზე.

Journal of Georgian Geophysical Society,
Issue (A), Physics of Solid Earth, v.16a, 2013, pp.104-107

ECOLOGICAL RISK OF TERRITORY AFFECTED BY MINING INDUSTRY IN CONDITIONS OF HIGH SEISMIC HAZARD

Zaalishvili V., Burdzieva O.

CENTER OF GEOPHYSICAL INVESTIGATIONS
of Vladikavkaz Scientific Center of Russian Academy of Sciences and the Government of the Republic of North Ossetia-Alania, e-mail:cgi_ras@mail.ru

In connection with the growing anthropogenic impact the protection of environment became the global issue. The portion to the environmental pollution made by the mining industry is significant.

In conditions of mountainous relief the problem is aggravated even more because of limitedness and closure of space. The factors, which influence the state of environment, under the conditions of highland region bear priority nature because of the special signs of topographical, territorial and geographical plan [1, 6, 7].

It is also necessary to note that practically all forms of natural phenomena and processes of geological, hydrogeological and meteorological nature are the sources of risks. Earthquakes are some of the most dangerous natural phenomena under the conditions of mountainous relief. From the point of view of spreading on the territories the earthquakes are the most dangerous natural phenomena in Russia (about 20% of the territory potentially is subjected to the impact of earthquakes with the intensity of 7 points on MSK scale and more).

Besides its direct destructive impact in the territories, where industrial enterprises generating or processing dangerous chemical substances are located, the earthquake can cause ecological catastrophes.

The estimations of losses from the earthquakes, made according to world data of the insurance company Munich Re, show that the number of events with the severe consequences in the entire world in the period of 1986-1995 is more than three times increased in comparison with 1960, and the volume of losses grew almost 15 times. The analysis of causes for an increase in the losses shows that these are the irreversible consequences of the rapid population and industry growth, increase of the infrastructure, commercial and economic activity in the large cities and the industrial centers, located in seismically active regions.

The wastes of output and processing placed in confined area create the ecologically tense situation in the regions and they contribute to the degradation of environment. The ecological capacity of the biosphere of mining systems in comparison with the plains territories is limited; therefore the technogenic interference on the system of mountain landscapes requires balanced approach [2].

The territory of North Osetia is located in the zone of high seismicity and it is characterized by the greatest seismic risk, since in conditions of high seismic hazard there is the greatest density of population in North Caucasus [4].

In 2007 on the basis of accounting of possible seismic sources (PSS) zones (Rogozhin E.A.) the probabilistic maps of seismic hazard of the RNO-A were constructed by the specialists of Center in collaboration with the Georgian scientists.

According to the maps of seismic hazard in the territory of republic for the important objects, such as the tailings dumps, entire southern part of the republic is located in the limits of 9 MSK intensity (Fig. 1). [4, 5].

In the case of earthquakes with intensity of 5 points the site, folded by some type of soil and occupied by tailings dump (wastes of mining industry), will be under active impact. The natural volume of the waste, which contains heavy metals and their salts, frequently irrigated deformed by waves, will obviously noticeably change under the moderate seismic influences, accelerating the leaching of minerals. This will increase the volume of toxic substances penetration into the soil, which will enlarge the area of pollution. Toxic substances temporarily “preserved” in the bottom deposits, for example river Ardon, will increase the pollution of territory more even though the river flow will take away large part of waste in the estuary.

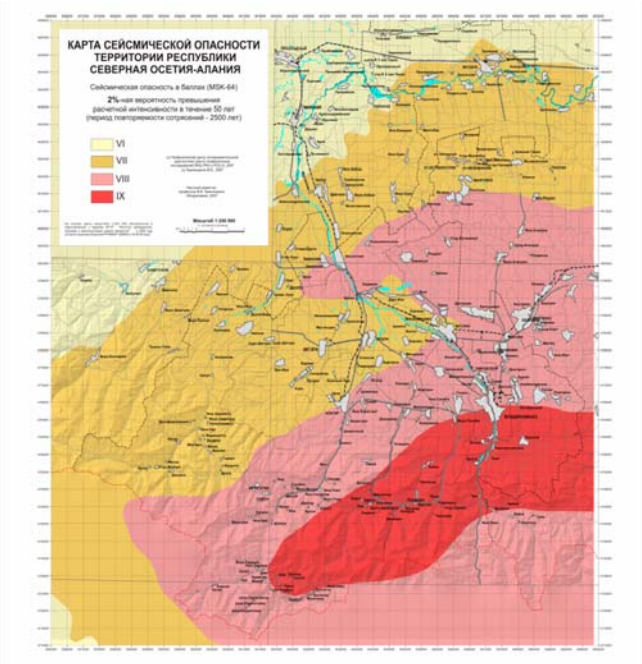

Fig. 1. The seismic hazard map of the RNO-A territory

It is known that even in the case of moderate earthquakes so-called second hazards (for example, landslides or fires) can exceed many times the seismic risk from the earthquake. The leaching process of the mining industry wastes will considerably increase in the case of strong earthquakes, and the consequences, formed by such a second hazard, can, exceed many times losses from the primary sources without any doubt.

To assess the pollution of the territory as closely related parameter, the development of neoplasm among the inhabitants of the urbanized mountain territory on the example of Vladikavkaz city was investigated. Morbidity was studied depending on the distance from the metallurgical enterprises and tailings dumps, located in the northeastern part of the city. The dispersion halo of heavy metals from the enterprises is revealed over the area of approximately 40 km^2, where the content of metals by an order exceeds the mean concentration.

For the processing and the subsequent analysis of the obtained data about the neoplasm morbidity the special database was developed [3]. We also studied the wind rose to investigate the influence of the air flow on the spreading of pollutants and their possible influence on cancer morbidity of population. Investigating the dependence of the number of diseases from the distance to the sources of pollution, makes it is possible to conclude that the number of cases per unit of area decreases with an increase of the distance from the industrial objects and the tailings dump (Fig. 2) [3].

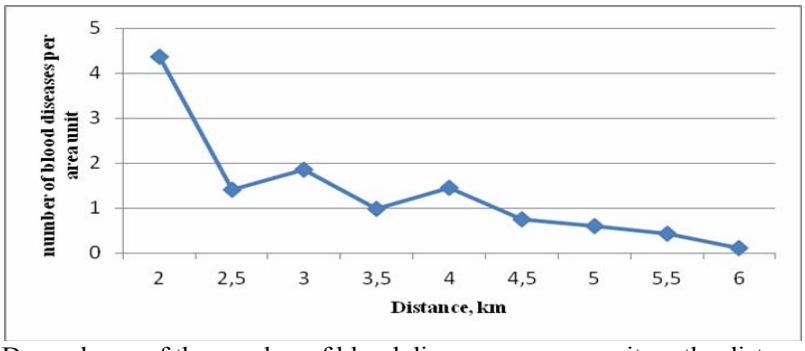

Fig 2. Dependence of the number of blood diseases per area unit on the distance from the industrial objects

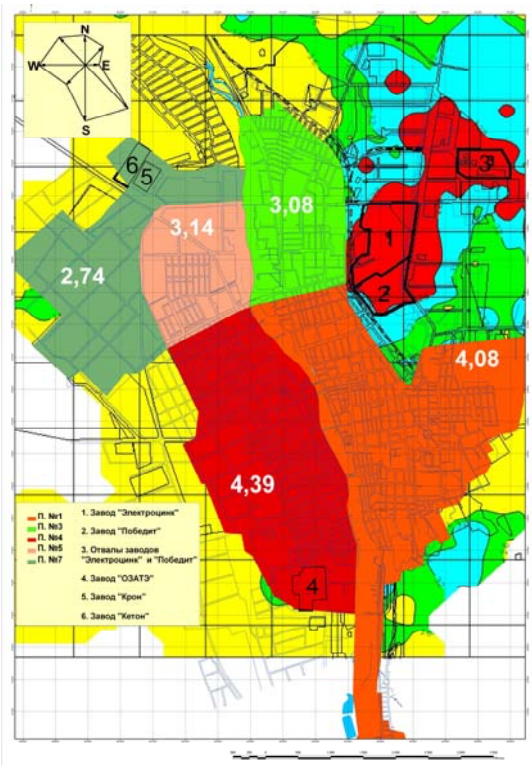

Fig 3. Neoplasm morbidity on data of city polyclinics

The analysis of the constructed maps for different age groups, and also forms of localizations, makes it possible to conclude that the special features of air flow directions and the immediate vicinity of buildings and construction of industrial enterprises “Electrozinc” and "Pobedit”, including tailings dumps form the maximum negative contribution (fig.3).

Conclusions

The map of neoplasm morbidity for the territory of Vladikavkaz city is constructed.

The closest correlation of the air flow motion the special features of which penetrate on the tailings dump and expanding the region of pollution by toxic substances in the territory of city, is observed on cancer morbidity of age class of up to 20 years and on cancer morbidity in some locations for all age classes.

In the case of sufficiently strong earthquake the emission into the environment of harmful wastes and substances, which will affect ruinously the health of population and environment, can occur.

References

1. Beriev O.G., Zaalishvili V.B., Zaks T.V. Medical-ecological-geophysical monitoring of the urbanized mountain territory. Proceedings of VII of international scientific conference “Sustainable Development of Mountain Territories in Conditions of Global Changes”, Vladikavkaz, 2010
2. Burdzieva O.G., Shevchenko E.V. The ecological-economic aspects of mining waste storage. // *Mining information-analytical bulletin*. # 8, 2010.
3. Zaalishvili V.B., Burdzieva O.G., Beriev O.G., Zaks T.V., Kanukov A.S. About the ecological aspects of the modern urbanized territory in case of the strong earthquakes // Earthquake engineering. Safety of constructions. - M.: VNIINTPI, # 3. 2012. p.52-67.
4. Zaalishvili V.B., Arakelyan A.R., Makiev V.D., Melkov D.A., Burdzieva O.G., Dzeranov B.V., Gabeeva I.L., Kharebov A.K. Development of the general seismic zoning (GSZ) map of the territory of republic North Osetia - Alania M 1:200 000 // Proceedings of CGI RAS and RNO-A, Vladikavkaz, 2007. V. 2. 38s.
5. Zaalishvili V. Assessment of seismic hazard of territory // Earthquake Engineering. Published by InTech. Edited Halil Sezen, 2012, P. 25-64
6. Zaalishvili V.B., Beriev O.G., Burdzieva O.G., Kanukov A.S., Zaks T.V. Correlation between distribution of heavy metals in the urbanized area of the mining region and oncological morbidity of population // Geology and geophysics of South of Russia # 3 (in press)

7. Zaalishvili V.B., Burdzieva O.G., Kanukov A.S., Zaks T.V. Geoinformational monitoring of distribution of physical fields within the urbanized territory // Geology and geophysics of South of Russia # 4 (in press)

ЭКОЛОГИЧЕСКИЙ РИСК ТЕРРИТОРИИ ПОДВЕРГАЮЩЕЙСЯ ВОЗДЕЙСТВИЮ ГОРНЫХ ПРЕДПРИЯТИЙ В УСЛОВИЯХ ВЫСОКОЙ СЕЙСМИЧЕСКОЙ ОПАСНОСТИ

Заалишвили В.Б., Бурдзиева О.Г.

Для оценки загрязнения территории тяжелыми металлами было изучено развитие новообразований на территории г. Владикавказа. Было установлено, что их распределение находится в корреляция с особенностями движения воздушных потоков (Роза ветров).

Территория Северной Осетии расположена в зоне высокой сейсмической опасности. Согласно карте детального сейсмического районирования для ответственных объектов, хвостохранилища расположены в пределах зоны 9-балльной интенсивности.

Известно, что даже при умеренных землетрясениях т.н. вторичные опасности могут многократно превысить сейсмический риск от собственно землетрясения. При сильных землетрясениях процесс выщелачивания отходов горнодобывающей промышленности значительно увеличится, а последствия, формируемые подобной вторичной опасностью, могут безо всякого сомнения, во много раз превысить потери от первичных источников.

При достаточно сильном землетрясении может произойти выброс в окружающую среду вредных отходов и веществ, которые пагубно отразятся на здоровье населения и окружающей среде в целом.

სამთო საწარმოების ზემოქმედების ქვეშ მყოფი ტერიტორიების ეკოლოგიური რისკი მაღალი სეისმური საშიშროების პირობებში

ვ. ზაალიშვილი, ო. ბურძიევა
რუსეთის მეცნიერებათა აკადემია, გეოფიზიკური კვლევების ცენტრი, ვლადიკავკაზი

Journal of Georgian Geophysical Society,
Issue (A), Physics of Solid Earth, v.16a, 2013, pp. 108-110

ANALYSIS OF GLACIER KOLKA FALL ON 20-th SEPTEMBER 2002 ON THE BASIS OF INSTRUMENTAL DATA OF THE SEISMOLOGICAL NETWORK OF GEORGIA

Zaalishvili V., Makiev V., Melkov D.
CENTER OF GEOPHYSICAL INVESTIGATIONS
of Vladikavkaz Scientific Center of Russian Academy of Sciences and the Government of the Republic of North Ossetia-Alania, e-mail:cgi_ras@mail.ru

On 20-th September of 2002 the tragic event occurred, which took aback the entire population of the Republic of North Ossetia-Alania – sudden fall of the glacier Kolka. As a result the village Nizhniy Karmadon disappeared. The bigger part of houses in village Gornaya Saniba, built in recent years in the river Genaldon floodlands, turned out to be under water. People were buried by the flow, there were children among them. The group of Sergey Bodrov, that participated in filmingwas also buried.

The instrumental records obtained by the local network of the Center of Geophysical Investigations (at that time – the Geophysical Center of Experimental Diagnostics (GCED)), due to the trigger start mechanism of the seismic stations, the preceding event and the large part of the glacier Kolka fall process were registered only partially. This caused the need for the comparison of the obtained records with the data of other stations. The absence of complete information often led to different and sometimes to reinforced in no way hypotheses [Berger, 2013].

The analysis of available instrumental data shows the correspondence of the basic stages, obtained on the different stations of the local network of the seismological observations of RNO-A [Zaalishvili, Nevskaya, 2003; Zaalishvili et.al., 2004, Zaalishvili et.al., 2005, Zaalishvili, Kharebov, 2008; Zaalishvili, Melkov, 2008, 2012].

For the purpose of the more detailed investigation of the glacier Kolka fall process data of the seismic stations (Abastumani, Ambrolauri, Akhalkalaki, Akhaltsikhe, Oni, Tbilisi) given by Georgian colleagues civilly in 2004 year, were investigated. These analog records completely cover the period of twenty-four hours from 19-th to 20-th September of 2002. The most complete and qualitative is the data of Tbilisi station (geophysical observatory) (Fig. 1-2).

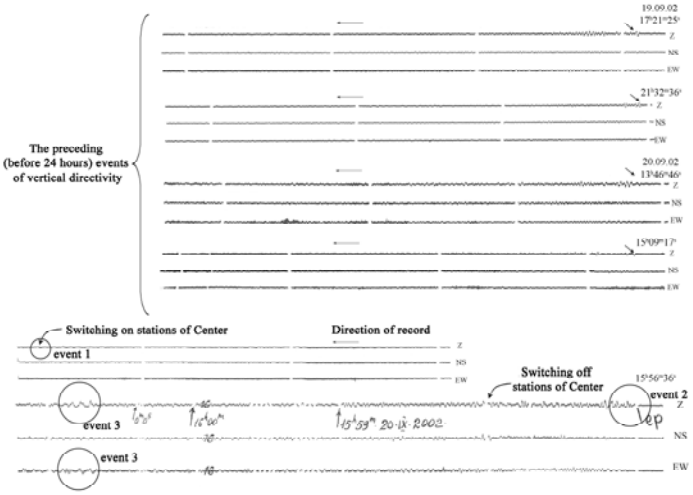

Fig. 1. Records of the preceding events (time of the beginning of events is indicated in the absolute corrected values)

The analysis of the earthquake catalog showed that on 20-th September of 2002 before the catastrophic fall of the glacier Kolka the earthquake occurred. Thus on 15:43:50,3 in region of West Irian (1,68° N 134,23° E) the earthquake with magnitude M_s=6,2 and the depth of the epicenter of h=33 km occurred. This

distance longitudinal P-waves pass in time of approximately 13 min., and shear S-waves in time of approximately 26 min. It is necessary to note that the arrival of P-wave in this case will occur in 15 h 56 m 50 s, and S-wave 16 h 09 m 50 s. The attention is immediately drawn to the good correspondence of the times of the basic phases of waves with the stages of the glacier fall.

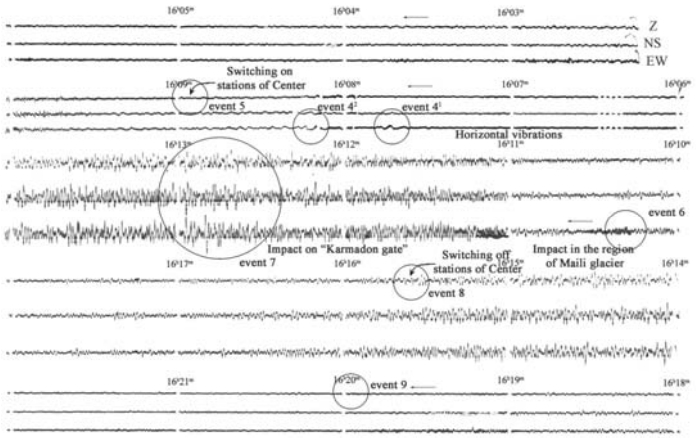

Fig. 2. The glacier Kolka fall process on 20-th September 2002.

The registration of such remote signals by the indicated type of observations is quite possible. Moreover, even less sensitive local network of the observations of CGI RAS & RNO-A repeatedly recorded the remote earthquakes (China, Japan, etc) [Zaalishvili et al., 2012]. In connection with this, it can be assumed that the "trigger" for the glacier fall was the indicated earthquake. In our opinion, precisely, it caused the trigger recording of the most sensitive stations: Chikola, Vladikavkaz 31 and stations of Geodynamic Observation Center in the Energy Sector (GOCES) located in Zaramag hydroplant construction site [Zaalishvili et.al., 2004].

Vertical component attenuates with the distance considerably more rapidly than the horizontal component. In connection with this the records of the remote earthquakes, as a rule, are characterized by relativly weak vertical component. After attenuation of the indicated vibrations it is possible to observe the long-period pulse on the vertical component (events 4^1, 4^2 in Fig. 2). The horizontal component of pulse (EW) is quite significant.

On 16 h 09 m 29 s low-amplitude high-frequency vibrations (in our opinion the beginning of the glacier fall!) are observed, through 80-82 s end by large high-frequency pulse (impact on the rocks of the starboard of river Genaldon valleylower the ice tongue of the Mayli glacier) and further continues nearly the same high-frequency process, but characterized by the considerably large, distinctly expressed vibrations. According to the data of different stations, the amplitude of horizontal vibrations in this case exceeds the amplitude of vertical not less than in 2.5 times. Strictly the process of the glacier Kolkafall before the achievement of microseismic disturbance level continued for 10 m 31 s. In this case the monotonic reduction of the amplitude of vibrations is observed already after 16 h 14 m 31 s.

The maximum duration of the process of the glacier Kolka fall, which was controlled by GCED stations, covers, as noted above, 7 m 40 s and, undoubtedly, includes the major part of the fall process according to its amplitude contribution (event 5, event 8, Fig. 2).

Thus, the analysis of obtained data gives grounds to assert that in the region of glacier Kolkaon 15 h 56 m the echoes of the remote earthquake appeared, which was "the trigger"of the glacier Kolka fall.

Conclusions

1. On the basis of instrumental records, the basic stages of the process of the glacier Kolka fall are established.
2. According to the results of analysis, undoubtedly different nature of the preceding event and basic process of the glacier Kolkafallon 20-th September 2002 is established.
3. In the region of glacier Kolkaon 15 h 56 m the echoes of the remote earthquake appeared, which was "the trigger" of the glacier Kolka fall.

References

1. Berger M.G. About some marks remained in glacier Kolka place as characteristics of nature of Kolka catasthrope in 2002 Alania // Geology and Geophysics of the South of Russia. 2012. # 4. p. 75-85.

2. Zaalishvili V.B., Nevskaya N.I. Fall of the glacier Kolka on September 20, 2002 and the problems of the information technologies of the natural systems investigation// Proceedings of International Conference “Information Technologies and Systems: Science and Practice. V. 2. Vladikavkaz, 2003. p. 175-180.
3. Zaalishvili V.B., Nevskaya N.I., Kharebov A.K. Analysis of the instrumental records of the glacier Kolkafallaccording to the data of the local network of seismic observations // Herald of Vladikavkaz Scientific Center. 2004, T. 4, # 3. p. 58–64.
4. Zaalishvili V.B., Nevskaya N.I., Makiev V.D., Melkov D.A. Interpretation of instrumental data of the process of the glacier Kolkafallon 20-th September 2002 // Herald of Vladikavkaz Scientific Center. 2005, V. 5, # 3. p. 43-54.
5. Zaalishvili V.B., Kharebov K.S. Investigation of the process of the glacier Kolkafallon 20-th September 2002 according to the dynamic characteristics of instrumental records // Proceedings of International Practical-Scientific Conference “Dangerous Natural and Technogenic Geological Processes in the Mountain and Foothill Territories of the North Caucasus”. Vladikavkaz: VSC RAS, 2008. - p. 202-221.
6. Zaalishvili V.B., Melkov D.A. Features of the ice-rock mass motion on 20-th September 2002 according to seismological and geomorphological data // Proceedings of International Practical-Scientific Conference “Dangerous Natural and Technogenic Geological Processes in the Mountain and Foothill Territories of the North Caucasus”. Vladikavkaz: CGI VSC RAS and RNO-A, 2008. p. 185-195.
7. Zaalishvili V.B., Melkov D.A. Features of process and macroseismic evidenceof glacier Kolka fall 20 September 2002 on instrumental data of modern observation systems // Geology and Geophysics of the South of Russia. 2012. # 3. p. 29-44.
8. Zaalishvili V.B., Nevskaya N.I., Nevsky L.N., Melkov D.A., Shempelev A.G. Monitoring of hazordous geological processess in zone of supposed Ardon fault and in part of gas pipeline from Dzuarikau to the borderof RNO-Alania // Geology and Geophysics of the South of Russia. 2012. # 4. p. 25-32.

АНАЛИЗ СХОДА ЛЕДНИКА КОЛКА 20 СЕНТЯБРЯ 2002 Г. ПО ДАННЫМ ЗАПИСЕЙ СЕЙСМОЛОГИЧЕСКОЙ СЕТИ ГРУЗИИ

Заалишвили В.Б., Макиев В.Д., Мельков Д.А.,
Центр геофизических исследований ВНЦ РАН и РСО-А, Владикавказ, Россия

20 сентября 2002 г. произошел внезапный сход ледника Колка. В результате указанного схода исчез пос. Нижний Кармадон. Оказалась под водой большая часть домов с. Горная Саниба, построенных в последние годы, в пойме р. Геналдон. Погибли люди, в том числе, дети.

Полученные с помощью локальной сети Центра геофизических исследований инструментальные записи, в силу триггерности включения сейсмических станций, лишь частично зарегистрировали предшествующее событие и большую часть процесса схода ледника Колка.

С целью более детального изучения процесса схода ледника были изучены записи сети сейсмических станций (Они, Амбролаури, Тбилиси, Абастумани и др.), любезно переданные грузинскими коллегами в 2004 году.

На основе обработки инструментальных записей станции Тбилиси были выделены события с 19 по 20 сентября 2002 г. и были установлены основные этапы процесса схода ледника Колка. В частности была доказана различная природа предшествующего события и основного процесса схода. Было показано, что на записях выделены продольные и поперечные волны от удаленного землетрясения.

საქართველოს სეისმოლოგიური ქსელის მონაცემების მიხედვით კოლკას მყინვარის 2002 წ. 20 სექტემბრის ჩამოშლის ანალიზი

ვ. ზაალიშვილი, ვ. მაკიევი, დ. მელკოვი

რუსეთის მეცნიერებათა აკადემია, გეოფიზიკური კვლევების ცენტრი, ვლადიკავკაზი

Journal of Georgian Geophysical Society,
Issue (A), Physics of Solid Earth, v.16a, 2013, pp. 111-114

CAPABILITIES OF POLARIZATION ANALYSIS IN SEISMIC RECORDS PROCESSING

Zaalishvili V., Melkov D.

CENTER OF GEOPHYSICAL INVESTIGATIONS
of Vladikavkaz Scientific Center of Russian Academy of Sciences and the Government of the Republic of North Ossetia-Alania, e-mail:cgi_ras@mail.ru

Polarization analysis opens great possibilities in processing of different data, in particular, algorithm developing by the Center of Geophysical Investigations makes it possible to locate epicenter of earthquake (with a certain accuracy) in "real time", using data even of one seismic station (in the absence of connection with the remaining observation points). The task of localization consists in detection of arrivals of p- and s-waves, azimuth and incidence angles, and evaluation of epicenter coordinates and depth using hodograph.

The possibilities of using the polarization analysis for the identification of seismic waves [Alkaz and other, 1977], in practice we have approved for the first time in 2008 for operational processing of the Kirov earthquakes records took place on the territory of North Ossetia [Zaalishvili et al., 2008].

On May 11, 2008 in 14:57 of local time (MSK) in the territory of North Ossetia occurred the earthquake, felt in Vladikavkaz city with intensity of 2–3. In the first hours after earthquake, on the request of EMERCOM of RNO-A, we have processed the record of the SGI VSC RAS station and by means of polarization analysis the azimuth was estimated and suppositional region of the earthquake epicenter was determined.

The determination of the coordinates of epicenter according to the data of one station was conducted on epicentral distance, determined according to the difference in the time of the first entrances p- and s-waves and the azimuth to the epicenter, which was determined by the parameters of the ellipsoid of the wave form of the first arrivals of the longitudinal wave. According to the preliminary data the epicenter was found in 30 km to the West-NorthWest from Vladikavkaz city. Macroseismic survey of the territory of epicentral region (Ardon and Alagir regions) was carried out.

Special features of seismic impact were taken into account. Earthquake affect was described by all the respondents in the form of the push, remarkable by to the reaction of household articles (table, sofa, bed, etc). The special features of vibrations during the earthquake are well visible on the instrumental records, where the entrance of share wave has the form of short-term pulse (Fig. 1).

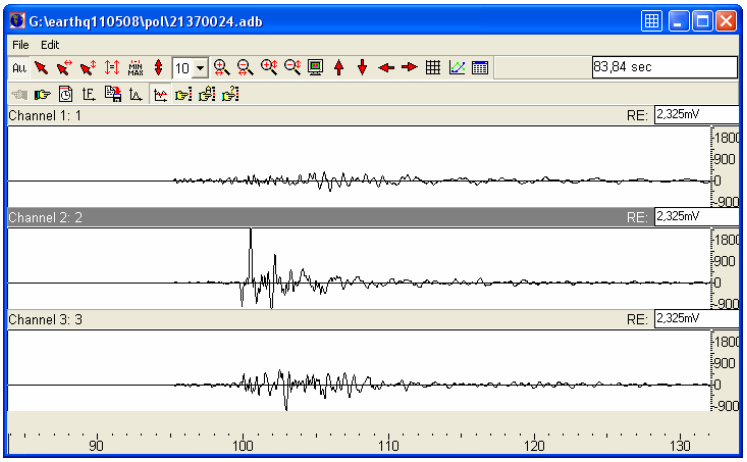

Fig. 1. The record of earthquake 11 May 2008, station Geocenter (Vladikavkaz).

Assuming duration of vibrations as the interval, in which the amplitude exceeds half of its maximum value, one can obtain it equal to 1.6 seconds. In connection with this, even under the conditions of the relatively high impact amplitude, the facts of the rattle of dishes (seismic scale) and, all the more, windows and doors, will be absent because of the short duration of action. On the basis of the survey results map of seismic of intensity on the territory of the Republic was composed (Fig. 3). The macroseismic epicenter of earthquake was located in the region of Kirov village in the Ardon region. Since in ss.villages Nogkau and Michurin intensity was also more significant than in the remaining territory, and given populated areas were assigned the zone of three-point intensity.

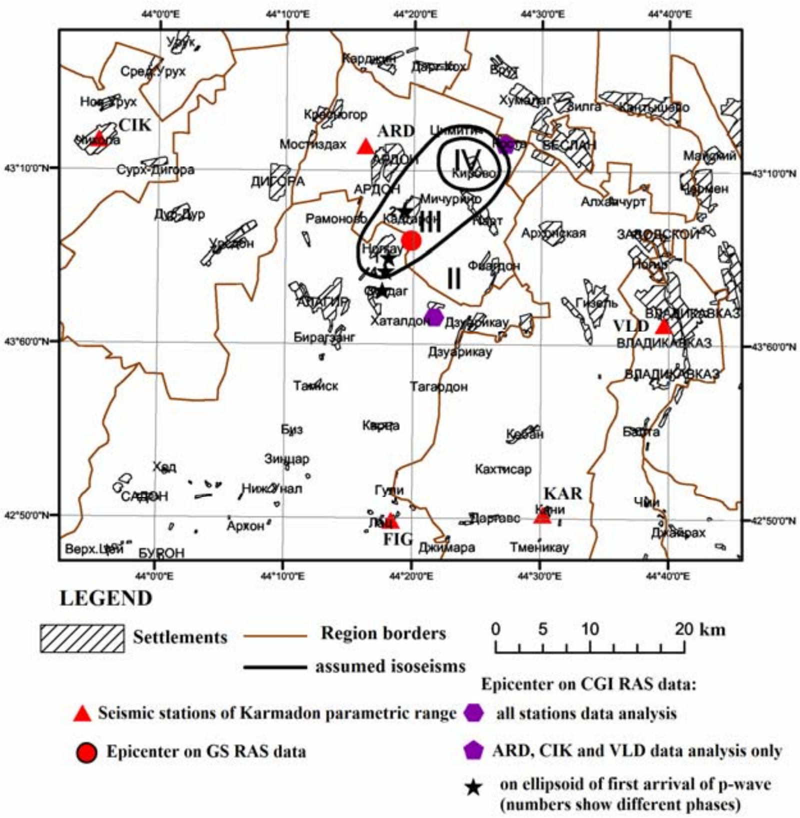

Fig. 2 Map-diagrams of the manifestation of the earthquake of 11.05.08 in the RNO-A territory

After detection of arrivals of p-wave the azimuth to epicenter and incidence angle of seismic ray are determined directly by eigenvectors e_n^j and eigenvalues λ_n of the matrix a_j^i :

$$\left(a_j^i - \lambda_n \cdot \delta_j^i\right) e_n^j = 0,$$

$$a_j^i = \sum_t u_i(t) \cdot u_j(t),$$

where i, j = x, y, z, sum is accomplished on the chosen time fragment.

The results of calculating the azimuths are represented in Table 1, epicenters are designated by the asterisks in Fig. 2: number 1 corresponds to the assumed epicenter, determined according to the first entrance, and 2-4 on the following phases of the fluctuations of p-wave (Fig. 3).

Table 1.

# of fragment	incidence angle	azimuth
1	68°	284°
2	71°	294°
3	60°	277°
4	49°	281°

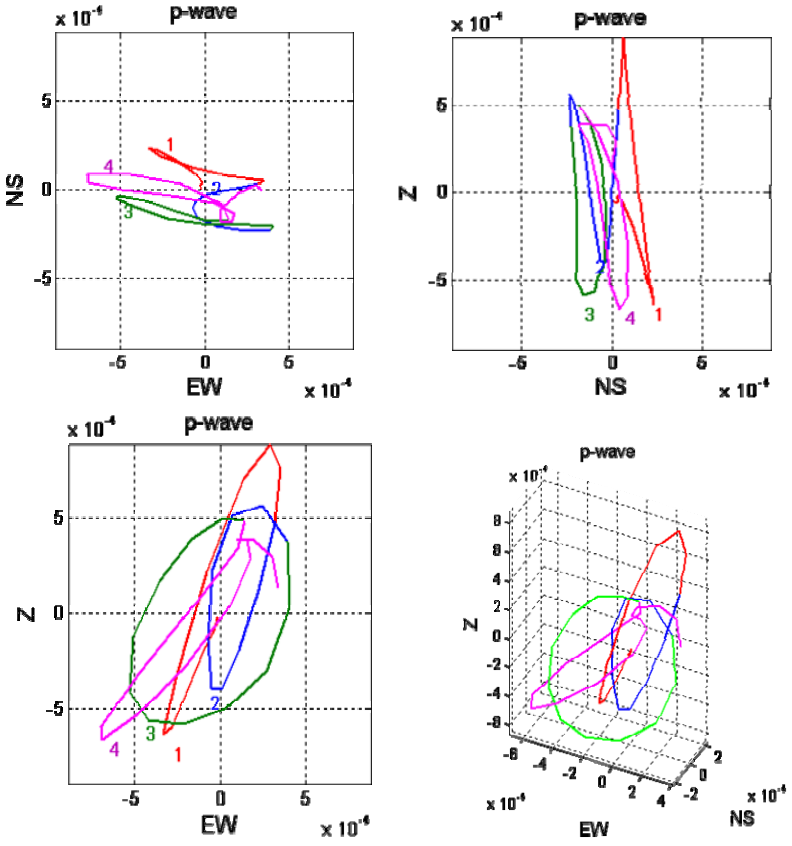

Fig. 3. The analyzed fragments of the record of p-wave

For determination of p- and s-waves arrivals STA/LTA algorithm is used, i.e., the ratio of energy of signal in the sliding windows, for the background (LTA) and the useful signal (STA). The results of the algorithm application presented in Fig. 4. The values of the parameters are LTA = 5 s; STA = 0,5 s. For s-wave allocation preliminary projection of record to the direction, perpendicular to azimuth to the source was performed, which makes it possible to unambiguously identify it on the seismogram.

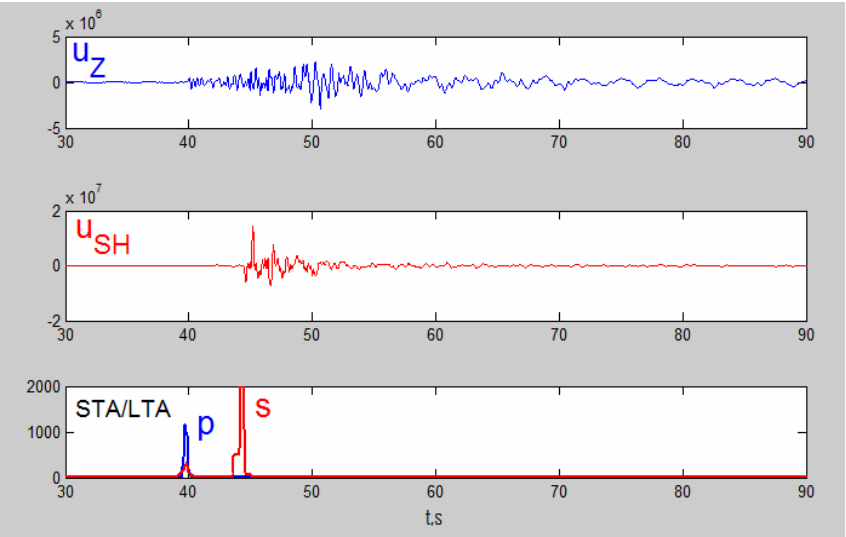

Fig. 4. Results of the isolation of the entrances of longitudinal and transverse waves.

The examined event was also localized with the use of a package of standart programs (HYPOELLIPSE, etc.) [Zaalishvili and others, 2008]. As a result difference between the instrument and macroseismic epicenters was noted. However, such differences are well known. Thus, for Racha earthquake (Georgia,

1991) the difference between instrument and macroseismic epicenters was significant. Such facts of intensity distribution are, obviously, caused by a whole series of the factors: the special feature of the geological structure of the structures formation - source (fault), the depth, the way of the propagation of seismic waves, by directional effect, and finally by the influence of local conditions.

Conclusions

1. The use of polarization analysis with the algorithms of automatic pick-up of seismic waves makes it possible to produce operational preliminary localization of seismic events according even on the basis of data of single seismic station.
2. Proposed algorithm can be used together with other procedures of data processing, in particular its use improves the accuracy of detection of s-waves.
3. The work of algorithms is demonstrated on the example to postprocessing, at the same time there is a possibility of their use in the data processing systems in real time regime.

References

1. Alkaz V.G., Onofrash N.I., Perelberg A.I. Polarization analysis of seismic fluctuations. - Kishinev: Shtiintsa, 1977. - 110 p.
2. Zaalishvili V.B., Nevskaia N.I., Zabirchenko D.N., Melkov D.A., Dzeranov B.V. To a question of the creation of local network “Karmadonskiy parametric poligon” // Dangerous natural and technogenic geological processes in the mountain and foothill territories of the North Caucasus. Vladikavkaz: VSC RAS RNO-A, 2008. p. 359-366.

ВОЗМОЖНОСТИ ПОЛЯРИЗАЦИОННОГО АНАЛИЗА В ОБРАБОТКЕ СЕЙСМОЛОГИЧЕСКИХ ДАННЫХ

Заалишвили В.Б., Мельков Д.А.

Центр геофизических исследований ВНЦ РАН и РСО-А, Владикавказ, Россия

Использование поляризационного анализа совместно с алгоритмами автоматического выделения сейсмических волн позволяет производить оперативную предварительную автоматизированную локализацию очагов землетрясений в режиме реального времени.

Оценка координат эпицентра может быть выполнена по эпицентральному расстоянию, вычисленному по времени первых вступлений P и S волн азимуту на эпицентр и углу выхода сейсмического луча, которые определялся по параметрам эллипсоида волновой формы первых вступлений продольной волны.

Показаны возможности использования алгоритма на примере землетрясения11 мая 2008 г. на территории Северной Осетии.

პოლარიზაციული ანალიზის შესაძლებლობანი სეისმოლოგიური მონაცემების დამუშავებაში

ვ. ზაალიშვილი, დ. მელკოვი

რუსეთის მეცნიერებათა აკადემია, გეოფიზიკური კვლევების ცენტრი, ვლადიკავკაზი

Journal of Georgian Geophysical Society,
Issue (A), Physics of Solid Earth, v.16a, 2013, pp. 115-119

Automatic onset time picking of acoustic signals

N. Zhukova, T. Chelidze, T. Matcharashvili.

M. Nodia Institute of Geophysics of Iv. Javakhishvili Tbilisi State University

Abstract

We present an application of the modified Akaike Information Criterion (AIC) for an automatic determination of the onset time of acoustic emissions (AE). Instead of analysis of original signal in the modified AIC the Hilbert Transformation of a signal with further implementation of 3 SIGMA signal filtering is suggested .The onset time information is used to derive automatically AE characteristics during laboratory natural and forced stick-slip experiments for dynamical investigations, namely revealing phase synchronization of natural slip events by a weak forcing.

Program description

There are many methods for determination of onsets of seismic and acoustic signals automatically (Grosse et al, 2004; Kurz et al, 2005; Niccolini1et al, 2012). For our task we adapted a well known Akaike Information Criterion (AIC) techniques. Initially developed to predict an optimal order for an autorecursive filter, the criterion can be used to demark the point of two adjacent time series with different underlying statistics.

We modified AIC method like it is shown on the block-scheme bellow:

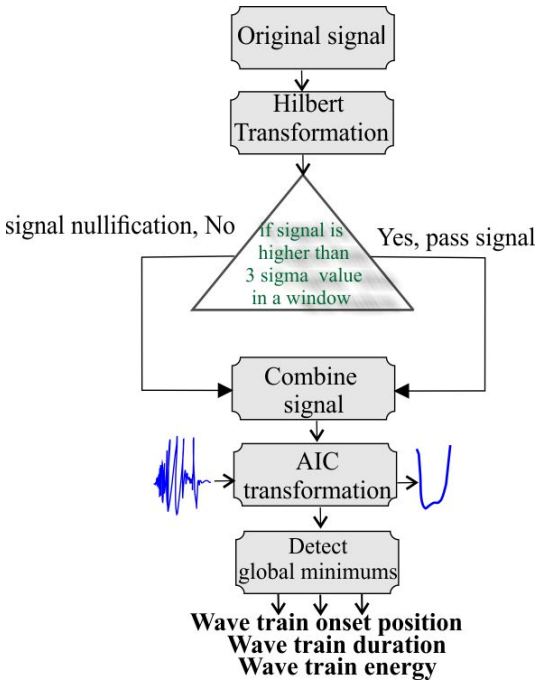

Fig.1. Block-scheme of modified AIC method calculations

In our case we do not apply AIC directly to original acoustic signal. The program package developed at M. Nodia Institute of Geophysics implements the algorithm with underlying block-scheme, shown in (Fig.1).

The program ANBW.exe passes the original acoustic signal (Fig.1a, wav file) through the Hilbert Transform block. As the result of this operation we get envelopes of acoustic signals (Fig.

2b). The construction of envelope of the signal leads to increase of the signal-noise ratio. After this using the second program (filt.exe), we compare each point in acoustic time series with a 3 Sigma value in a predefined window. By this procedure we are able to separate wave trains the from noise background (Fig. 2c).

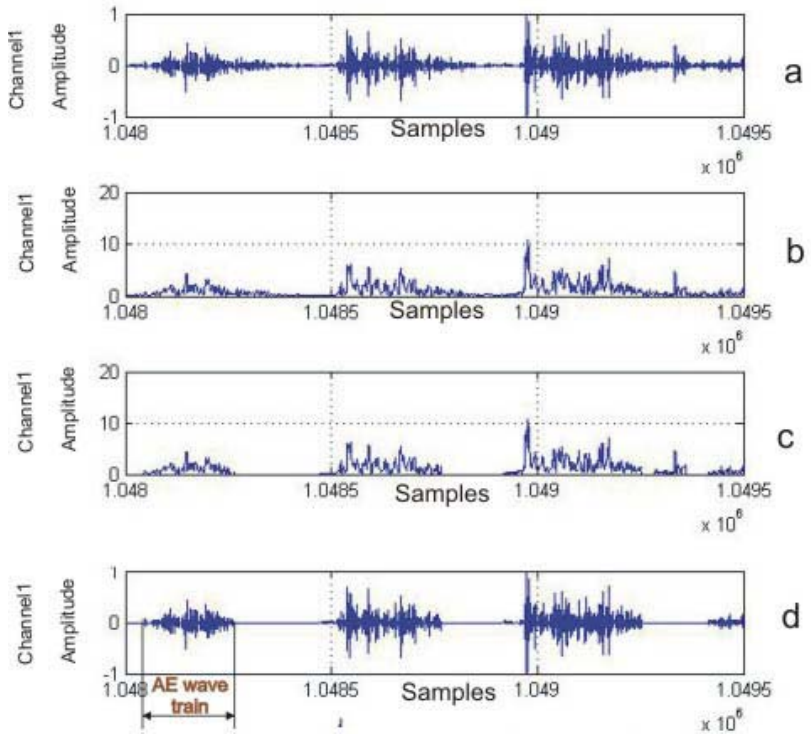

Fig.1. Wave trains processing scheme by the modified AIC method

Lastly we calculate AIC function (by program naicf.exe) for the each wave train (Fig.2d)
AIC value is calculated from the signal by formula:

$$AIC(t) = t \cdot \log\{\mathrm{var}(x[1,t])\} + (N-t-1) \cdot \log\{\mathrm{var}(x[t+1,N]\},$$

where x - time series, N - window, t - current point position in a window,

var is determined as $\sigma^2_{N-1} = \frac{1}{N-1}\sum_i^N (x_i - \bar{x})^2$, $\bar{x}$ – mean value of x.

A time window is chosen on the previous steps. AIC picker finds the onset point as the global minimum, the selected time window includes only the segment of the wave train. If the time window is chosen properly, AIC picker can find the first arrival of the signal very well.

The program was tested on time series of Acoustic Emission (AE) produced during stick-slip motion of a sliding rock plate on the fixed one. These spring-slider experiments were aimed to model dynamic triggering/synchronization of the seismicity by a weak forcing (Chelidze et al, 2010a, 2010b). In our case the segment of interest is the acoustic emission AE signal (wave train) generated by slip events during instable friction movement; precisely, can these slip events be triggered/synchronized by the weak external applied force.

Typical acoustic time series is depicted on Fig.3. During stick-slip experiments acoustic time series with triggered wave trains have been recorded. Experimental setting and detailed description can be found in (Chelidze et al, 2010a, 2010b). We used these time series for adaptation of AIC method and for comparing results of manual and automatic determination of onset time arrivals.

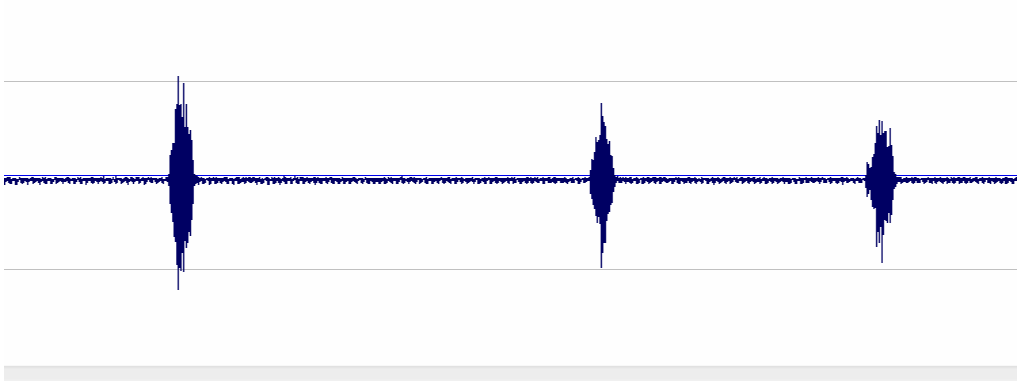

Fig. 3. Acoustic Signal generated during stick-slip motion

Fig. 4 shows the calculated AIC functions for each AE. The min value of AIC is located in the position T, which corresponds to the time of onset arrival.

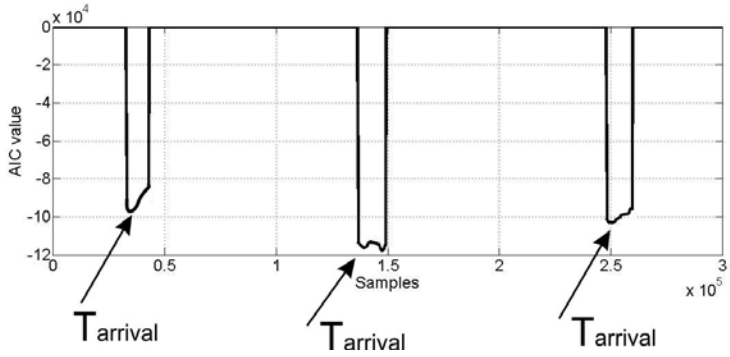

Fig.4. AIC transformation of AE

Our research showed that the automatic picking by AIC gives a good coincidence with manual picking. Fig. 5 shows 2 curves of PDF plotted for waiting times between wave trains, plotted manually and automatically.

As we can see the curves are generally identical.

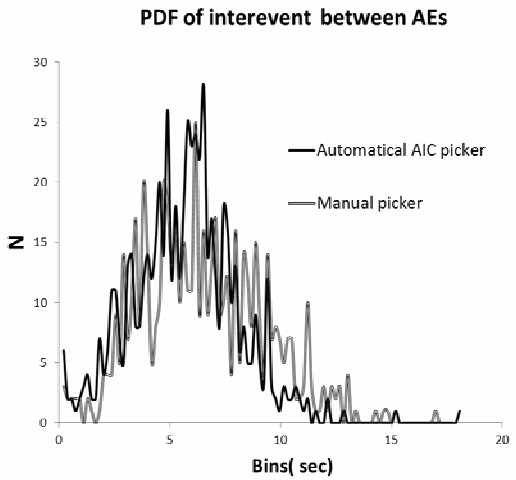

. Fig. 5. Distribution of waiting times between onsets of wave trains: (black line) - onsets are found automatically by AIC method; (grey line) - onsets' are found manually.

The times between onsets we used also to plot the distribution function of phase shifts $\Delta\varphi$ between onsets of AE for natural and mechanically forced stick-slip (Fig. 6). The experiments were carried out in identical conditions except forcing. We can see 2 curves: the first corresponds to a

stick-slip experiment with a weak periodic (20 Hz) mechanical forcing and the second one – to a natural stick slip. The PDF function of $\Delta\varphi$ for forced stick-slip, which shows a strong maximum indicates that the assumption on phase synchronization of stick-slip is correct. The PDF for $\Delta\varphi$ between AE during natural stick-slip and virtual 20 Hz sinusoid shows absence of synchronization as it was expected.

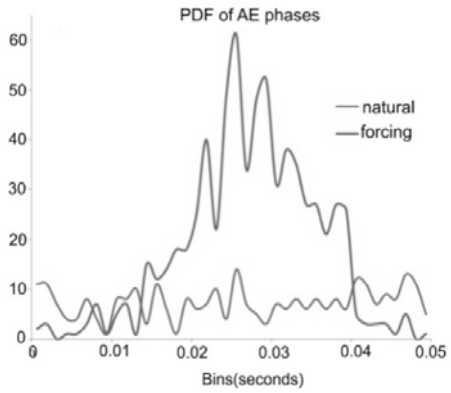

Fig. 6. Distribution of AE phase shifts $\Delta\varphi$ relative to the virtual sinusoid phase for natural (grey line) and forcing sinusiod (black line) stick-slip in seconds.

It should be noted that besides onsets and terminations timing the modified AIC program developed in M. Nodia Institute of Geophysics allows automatic determination of many characteristics of AE wavetrain: position of the maximum of AE signal, magnitude of the absolute maximum in AE signal, duration of the wavetrain, interevent time between maxima of AE busts, time between termination of one AE signal and the onset of the following one, time between successive onsets of AE signals, the energy of the AE signal (as a sum of squares of amplitudes in the wavetrain), sum of modules of amplitudes in the wavetrain.

Conclusion

Modified AIC picker is able to find accurately the onset of acoustic signals against the backgroundnoise as well as several other important characteristics of AE wavetrains. The modified AIC calculation improves the accuracy of acoustic signal filtration.

Literature

1. Chelidze, T., de Rubeis, V., Matcharashvili, T. and Tosi, P. 2010a. Dynamical Changes Induced by Strong Electromagnetic Discharges in Earthquakes' Waiting Time Distribution at the Bishkek Test Area (Central Asia). In: Synchronization and Triggering: from Fracture to Earthquake Processes.(Eds V.de Rubeis, Z. Czechowski and R. Teisseyre), pp.339-360.
2. Chelidze, T., Lursmanashvili, O., Matcharashvili, T., Varamashvili,N., Zhukova, N., Mepharidze, E.2010b. Triggering and Synchronization of Stick-Slip: Experiments on Spring-Slider System. In: Synchronization and Triggering: from Fracture to Earthquake Processes. Eds.V.de Rubeis, Z. Czechowski and R. Teisseyre, pp.123-164.
3. Grosse, C., Finck, F., Kurz, J., Reinhardt, H. 2004. Improvements of AE technique using wavelet algorithms, coherencefunctions and automatic data analysis. Construction and Building Materials. 18, 203–213.
4. Kurz, J., Grosse, C., Reinhardt, H. 2005. Strategies for reliable automatic onset time picking of acoustic emissions and of ultrasound signals in concrete. Ultrasonics, 43, 538–546.

5. Niccolini1, G., Xu, J., Manuello, A., Lacidogna G., and Carpinteri A. 2012. Onset time determination of acoustic and electromagnetic emission during rock fracture. Progress In Electromagnetics Research Letters, 35, 51-62.

Автоматическая система для выделения вступлений акустических сигналов

Н. Жукова, Т. Челидзе, Т. Мачарашвили

Резюме

В работеописан модифицированный нами метод Акаике (AIC) для определения времени вступления волны акустических эмиссий. Инфомация о временах прихода волн очень полезна для анализа динамических характеристик сигнала.

ავტომატური სისტემა აკუსტიკური სიგნალის პირველი შემოსვლის გამოყოფისათვის

ნ. ჟუკოვა, თ. ჭელიძე, თ. მაჭარაშვილი

რეზიუმე

სტატიაში ნაჩვენებია აკაიკე მეთოდის გამოყენება აკუსტიკური ემისიის ტალღების შემოსვლის დროს დადგენისათვის. ეს ინფორმაცია არის დინამიკური მახასიათებლების ანალიზის საფუძველი.

Information for contributors

Papers intended for the Journal should be submitted in two copies to the Editor-in-Chief. Papers from countries that have a member on the Editorial Board should normally be submitted through that member. The address will be found on the inside front cover.

1. Papers should be written in the concise form. Occasionally long papers, particularly those of a review nature (not exceeding 16 printed pages), will be accepted. Short reports should be written in the most concise form not exceeding 6 printed pages. It is desirable to submit a copy of paper on a diskette.
2. A brief, concise abstract in English is required at the beginning of all papers in Russian and in Georgian at the end of them.
3. Line drawings should include all relevant details. All lettering, graph lines and points on graphs should be sufficiently large and bold to permit reproduction when the diagram has been reduced to a size suitable for inclusion in the Journal.
4. Each figure must be provided with an adequate caption.
5. Figure Captions and table headings should be provided on a separate sheet.
6. Page should be 20 x 28 cm. Large or long tables should be typed on continuing sheets.
7. References should be given in the standard form to be found in this Journal.
8. All copy (including tables, references and figure captions) must be double spaced with wide margins, and all pages must be numbered consecutively.
9. Both System of units in GGS and SI are permitted in manuscript
10. Each manuscript should include the components, which should be presented in the order following as follows:
    Title, name, affiliation and complete postal address of each author and dateline.
    The text should be divided into sections, each with a separate heading or numbered consecutively.
    Acknowledgements. Appendix. Reference.
11. The editors will supply the date of receipt of the manuscript.

CONTENTS

სარჩევი

საქართველოს გეოფიზიკური საზოგადოების ჟურნალი

სერია ა. დედამიწის ფიზიკა

ჟურნალი იბეჭდება საქართველოს გეოფიზიკური საზოგადოების პრეზიდიუმის დადგენილების საფუძველზე

ტირაჟი 200 ცალი

ЖУРНАЛ ГРУЗИНСКОГО ГЕОФИЗИЧЕСКОГО ОБЩЕСТВА

Серия А. Физика твердой Земли

Журнал печатается по постановлению президиума Грузинского геофизического общества

Тираж 200 экз

JOURNAL OF THE GEORGIAN GEOPHYSICAL SOCIETY

Issue A. Physics of Solid Earth

Printed by the decision of the Georgian Geophysical Society Board

Circulation 200 copies